## MASTER OF SCIENCE THESIS SIMON WANG

# ADDITION OF THE ANTI-INFLAMMATORY SALSALATE TO STANDARD-OF-CARE THERAPIES OF RADIOTHERAPY AND LENVATINIB FOR THE TREATMENT OF HEPATOCELLULAR CARCINOMA.

By Simon Wang, B.Sc.

A Thesis Submitted to the School of Graduate Studies in Partial Fulfillment of the Requirements for the Degree Master of Science

MASTER OF SCIENCE (2024) McMaster University, Hamilton, Ontario, Canada

Title: Addition of the anti-inflammatory Salsalate to standard-of-care therapies of

radiotherapy and Lenvatinib for the treatment of hepatocellular carcinoma

Author: Simon Wang, B.Sc (McMaster University)

Supervisor: Dr. Theos Tsakiridis

Number of pages: x, 111

## Lay abstract

Radiotherapy is a second-line treatment for HCC despite its effectiveness in killing tumors because of the high incidence of radiation-induced liver disease and more convenient alternatives. Salsalate possesses anti-inflammatory properties that may mitigate radiation-induced liver disease. Further, this drug and its derivative salicylate, the backbone agent of aspirin, was found to inhibit prostate and lung cancer growth. Salicylate-induced radio-sensitization in prostate and lung cancer cell lines. We found that salicylate could inhibit HCC cells and improve the efficacy of radiotherapy by reducing off-target radiation toxicity and increasing HCC radiosensitivity. In this study, we investigated the radioprotection of normal liver by salsalate and its anti-tumor activity in HCC alone and in combination with radiotherapy and Lenvatinib, a current standard of care targeted therapy for HCC.

## Abstract

Radiotherapy (RT) is an effective treatment for hepatocellular carcinoma (HCC), overshadowed by causing radiation-induced liver disease (RILD), which reduces its therapeutic ratio. Therefore, RT is relegated to a second-line or adjuvant treatment for HCC. Salsalate (SAL) is a non-steroidal anti-inflammatory drug (NSAID) used to treat rheumatoid arthritis, but there is evidence that it can also attenuate RT damage. Previous work from our group found that salsalate possesses anti-cancer efficacy and sensitizes prostate and lung cancer to RT. Ongoing studies also showed the anti-cancer activity of salicylate in HCC cell lines worked well with Lenvatinib. Therefore, salsalate could mitigate RILD and improve HCC sensitivity to RT, with the Lenvatinib combination explored to further increase the anti-tumor efficacy. To begin, normal female C57BL/6 mice were pre-treated with salsalate incorporated into the normal chow diet and received whole liver RT. Salsalate pretreated mice exhibited a survival advantage, so another cohort of mice received similar treatments for tissue analysis to understand the mechanisms behind the survival advantage. For the anti-cancer effects of salicylate, in vitro experimentation on human liver cancer cell lines revealed that salicylate inhibited the proliferation and colony formation, with enhanced inhibition in most cell lines combined with RT. In vitro findings on the anti-tumor efficacy of salicylate alone and in combination with RT were reproduced in vivo with Hep3B xenografts. In Hep3B cells, incorporating Lenvatinib to salicylate and RT generated even greater anti-cancer activity. Very early investigation into the mechanisms of action suggests that the mTOR, MAPK, and Hif-1α pathways, as well as cell cycle markers may be modulated. Overall, these findings suggest that salsalate may mitigate RILD and help improve the efficacy of RT and Lenvatinib in HCC. Additional studies are required to consolidate these findings and generate a solid basis to investigate this concept in clinical studies.

## Acknowledgment

I am very fortunate to have the support of so many people during my journey as a master's student. First and foremost, I would like to express my deepest gratitude for the guidance Dr. Theos Tsakiridis has provided me to develop as a scientist. I will forever be grateful for the opportunity to contribute to cancer research. Thanks to you, I have the privilege of conducting research in the crucial fields of cancer metabolism and radiation oncology. Without your support and patience, I would not be where I am today.

I would not have been the person I am today without my mentor, Dr. Elham Ahmadi, when I first began my journey as an undergraduate student. You helped me build up my confidence as a researcher and taught me many of the skills I needed to be successful. Even half a world away, you still answer my questions and provide me with invaluable insights on my project. Your kindness and knowledge made you a great role model to look up to.

To my diligent and supportive lab mates, Olia Biziotis and Amr Ali, I thank you for providing me with all the tools I needed to become a successful researcher. You taught me the skills and mindset required by a graduate student. You were always there to provide sound advice and propose the next steps for my project. You are both the best lab mates I could dream of having.

I would also like to recognize the hard work that Hannah She contributed to my project.

The project achieved goals that would have otherwise been out of reach without your efforts.

Likewise, without the counsel of Dr. Evelyn Tsakiridis, I would not have realized many of the goals I set for my project. Evelyn breathed new life into my project to help elevate my work to its full potential. I am so grateful for the extensive input and time she dedicated to helping me succeed.

Without the help of Dr. Tom Farell, who simulated and developed the radiotherapy treatment plans for cell cultures and animals, the radiotherapy component of my project would not have been possible. Thanks to him, we have radiotherapy models that reflect clinical radiotherapy. By the same token, I would like to thank the Radiation Therapy team at the Juravinski Cancer Centre, who helped deliver radiation sessions, sometimes after hours. I especially would like to thank Gabe Menjolian for organizing every radiation session and delivering many of these sessions. I would also like to thank John, Alfonso, Clarence, Anupa, Cara, Tracy, and Bridgette, among others, for their time and help in delivering radiation sessions.

To my committee members, Dr. Gregory R. Steinberg and Dr. Jonathan Bramson, I thank you for your indispensable guidance throughout the project and appreciate the time you have dedicated to me.

Last but not least, I am eternally thankful that I have the unconditional love and support of my family. There are no words to express the depth of my gratitude for always being there for me and pushing me to be my best self.

## Table of Contents

Lay abstract	iii
Abstract	iv
Acknowledgment	V
Table of Contents	vii
List of figures:	x
List of Tables:	x
List of Abbreviations:	xi
Declaration of Academic Achievement	xv
Chapter 1 – Introduction	1
1.1 The liver and liver cancer	2
1.2 Liver cancer epidemiology	3
1.3 Liver cancer etiology and risk factors	4
1.3.1 Viral HCC	4
1.3.2 MASLD	5
1.3.3 ALD	8
1.3.4 Other	10
1.4 HCC diagnosis	11
1.4.1 Staging of liver cancer	12
1.5 HCC prevention	13
1.6 HCC treatment	14
1.6.1 Local therapies	15
1.6.2 Systemic therapy	21
1.7 Molecular and metabolic signaling in HCC	22
1.7.1 MAPK pathway	24
1.7.2 PI3K/Akt/mTOR pathway	25
1.7.3 mTOR pathway	27
1.7.4 Hif-1α	28
1.7.5 TGF-β pathway	29
1.8 Cell response to radiotherapy	31
1.9 Radiation-induced liver disease	33
1.9.1 Acute phase	34

1.9.2 Chronic phase	34
1.9.3 Modelling chronic RILD in mice	35
1.10 Molecular pathways involved in normal tissue damage by irradiation	37
1.10.1 Transforming growth factor β (TGF-β)	37
1.10.2 Epithelial-to-mesenchymal transition (EMT)	38
1.10.3 Tumor necrosis factor α (TNF-α)	39
1.10.4 Interleukins	39
1.11 Radioprotective drugs	40
1.11.1 Potential radioprotective properties of Salsalate	40
1.11.2 Other potential radioprotective drugs.	43
1.12 Anti-cancer effects of Salsalate/salicylate	44
1.13 Rationale	45
1.14 Hypothesis	47
1.15 Aims	47
Chapter 2 – Methodology	48
2.1 Materials	49
2.1.1 Antibodies	49
2.2 Animal radioprotection experiments	50
2.2.1 Effect of SAL on survival after RILD induction	50
2.2.2 Acute vs chronic RILD / Benefits of SAL	51
2.2.3 Liver radiation delivery	52
2.2.4 Rodent diet	53
2.2.5 Euthanasia & tissue collection	54
2.3 Histology	54
2.4 Digital histological quantification	55
2.5 Cell lines	55
2.5.1 Cell RT	56
2.6 Clonogenic assays	56
2.7 Proliferation assays	56
2.8 Immunoblotting	57
2.9 Mouse xenograft experiments	58
2.10 Statistical analysis	59
Chanter 3 _ Results	61

3.1 Normal tissue protection by Salsalate	62
3.1.1 Animal survival	62
3.1.2. Liver morphology and immune cell infiltration	65
3.1.3. Salsalate regulates fibrosis, immune infiltration, and inflammatory processes in irradiated livers	69
3.2 Anti-tumor and radio-sensitizing effects of salicylate	74
3.2.1 Salicylate drug dose-response.	74
3.2.2 Salicylate inhibits HCC cell clonogenic survival	75
3.2.3 HCC cell response to radiotherapy	76
3.2.4 Salicylate in combination with radiation	76
3.2.5 Salicylate in combination with radiotherapy and Lenvatinib (triple therapy)	78
3.2.6 Anti-tumor activity in-vivo.	83
3.2.7 Modulation of cancer growth pathways by salicylate and combination therapies	84
3.2.8 Regulation of cell cycle and DNA replication markers	87
Chapter 4 – Discussion	89
4.1 Potential protective effects of Salsalate against normal tissue radiation toxicity	90
4.2 Anti-cancer benefits of salicylate and combination with radiotherapy	92
4.3 Combination with Lenvatinib	96
Highlights	98
Limitations	99
Future Directions	100
Conclusion	100
References	102

## List of figures:

- Figure 1. Pathogenesis of HCC from MASLD and ALD.
- Figure 2. Flow chart of HCC treatment options by BCLC staging system.
- Figure 3. mTOR and ERK signaling pathways.
- Figure 4. Pathogenesis of RILD.
- Figure 5. H&E-stained images of 10 Gy irradiated mice liver 6 months later at 20X magnification with preliminary morphological analysis by a trained pathologist.
- Figure 6. Molecular structure of salicylate and salsalate.
- Figure 7. Effects of salsalate therapy on survival of animals receiving whole liver radiotherapy.
- Figure 8. Representative images of macrophage (Kupffer) cells in mouse liver in response to salsalate and radiation.
- Figure 9. Effects of irradiation and salsalate treatment on liver collagen deposition detected by PSR stain.
- Figure 10. Key instigating proteins of RILD, IL-6, Col1A1, CD3, α-SMA, and NF-κB protein expression in mouse liver treated with radiation and salsalate.
- Figure 11. The dose-response curve of Hep3B cells to salicylate.
- Figure 12. Proliferation of Hep3B cells, clonogenic survival of Hep3B, PLC/PRF/5, HepG2, and Sk-Hep-1 cells, and average HAS synergy scores of treatment groups.
- Figure 13. Growth of Hep3B cells xenografted in NRG mice.
- Figure 14. Modulation of signaling pathways.
- Figure 15. Histone H3 phosphorylation, cyclin D1, and p27 expression in Hep3B cells treated with salicylate, Lenvatinib, drug combination, and radiation.

## List of Tables:

- Table 1. BCLC system of categorizing HCC
- Table 2. List of antibodies used for immunoblotting and immunohistochemistry
- Table 3. Animal treatment groups

## List of Abbreviations:

3DCRT – three-dimensional conformal radiotherapy

4E-BP – 4E-binding protein 1

AFP – alpha-fetoprotein

Akt - Ak strain transforming

ALD – alcohol-related liver disease

AMPK – AMP-activated protein kinase

AP-1 – activator protein-1

APS – ammonium persulfate

BAD – B cell lymphoma-2 associated agonist of cell death

BCLC – Barcelona clinic liver cancer

CAR – chimeric antigen receptor

CDK – cyclin-dependent kinase

CIK – cytokine-inducted killer

COX – cyclooxygenase

CPT – charged particle therapy

CT – computed tomography

CTLA4 - cytotoxic T-lymphocyte associated protein 4

DNA – deoxyribonucleic acid

DSB – double-stranded break

EBRT – external beam radiation

ECM – extracellular matrix

EGF - epidermal growth factor

EGFR – epidermal growth factor receptor

eIF04E – eukaryotic translation initiation factor 4E

ELK1 – ETS like-1 protein

EMEM – Eagle's minimum essential medium

EMT – epithelial to mesenchymal transition

ERK – extracellular signal regulated kinase

FFPE – formalin-fixed paraffin-embedded

FGF – fibroblast growth factor

FGFR - fibroblast growth factor receptor

FOLFOX4 – 5-fluorouracil, leucovorin, and oxaliplatin

FOXO – forkhead box O

GEMOX – Gemcitabine-Oxaliplatin

GF – growth factor

GLUT – glucose transporter

GPC3 – glypican-3

GRB2 – growth factor receptor binding protein 2

GSK3 – glycogen synthase kinase 3

GTP – guanosine triphosphate

HAS – highest single agent

HBV – hepatitis B virus

HCC - hepatocellular carcinoma

HCV – hepatitis C virus

HDAC – histone deacetylase

HGF – hepatocyte growth factor

IGF – insulin-like growth factor

IGF-1 – insulin-like growth factor

IGF1R – insulin-like growth factor receptor

IGFR – insulin-like growth factor receptor

IKKβ – inhibitor of nuclear factor kappa-B kinase subunit beta

IL-6 – interleukin-6

IMRT – intensity-modulated radiation therapy

JAK/STAT – Janus kinase/signal transducer and activator of transcription proteins

LAK – lymphokine-activated killer

LINAC – linear accelerator

MAPK – mitogen-activated protein kinase

MASH – metabolic-dysfunction-associated steatohepatitis

MASLD - metabolic-dysfunction associated steatotic liver disease

MDM2 – mouse double minute 2 homolog

MNK – mitogen-activated protein kinase interacting protein kinases

MRI – magnetic resonance imaging

mTOR – mammalian target of rapamycin

MWA – microwave ablation

NF-κB – nuclear factor kappa-B kinase subunit beta

NK – natural killer

NSAID – non-steroidal anti-inflammatory drug

p70S6K – ribosomal protein S6 kinase beta-1

PAMP – pathogen-associated molecular pattern

PDGF - platelet-derived growth factor

PDGFR – platelet-derived growth factor receptor

PD-L1 – programmed death-ligand 1

PEI – percutaneous ethanol injection

PI3K – phosphoinositide 3-kinase

PTEN – phosphatase and tensin homolog

Rb – retinoblastoma

RFA – radiofrequency ablation

RHEB – Ras homolog enriched in brain

RILD – radiation-induced liver disease

RILF – radiation-induced liver fibrosis

ROS – reactive oxygen species

RT – Radiotherapy

RTK – tyrosine kinase receptor

S6rp – S6 ribosomal protein

Sal – Salsalate

SBRT – stereotactic body radiotherapy

SDS – sodium dodecyl sulfate

SIRT – selective internal radiation therapy

SOS – son of sevenless 1

SSB – single-strand break

STAT3 – signal transducer and activator of transcription 3

T2D – type 2 diabetes

TACE – trans-arterial chemoembolization

TBST – tris-buffered saline-tween-20

 $TGF-\beta$  – transforming growth factor beta

TLR – toll-like receptors

TNF- $\alpha$  – tumor necrosis factor-alpha

TSC2 – tuberous sclerosis complex 2

VEGF – vascular endothelial growth factor

VEGFR – vascular endothelial growth factor receptor

α-SMA – alpha-smooth muscle actin

## Declaration of Academic Achievement

Those responsible for the conception and design of these studies are Simon Wang, Elham Ahmadi, Evelyn Tsakiridis, and Theos Tsakiridis. Simon Wang and Elham Ahmadi managed the C57BL/6 mice cohorts that generated figures 7-10. IHC stains were performed and quantified by Simon Wang in Figure 8. The McMaster Immunology Research Center Histology Lab performed the PSR stains on liver sections in Figure 9. PSR stain quantification was done by Simon Wang for Figure 9. Liver tissue homogenization and immunoblotting were conducted by Simon Wang in figure 10. Simon Wang and Hannah She performed the proliferation and clonogenic assays used to generate Figure 12. NRG mice model Hep3B xenografts were initiated with the help of Amr Ali, with the management of the NRG mice by Simon Wang and Hannah She, generating data for Figure 13. Immunoblotting of Hep3B cells was performed by Simon Wang.

I declare that to the best of my knowledge, the contents of this document do not infringe on the works of others and that credit is appropriately given.

Chapter 1 – Introduction

#### 1.1 The liver and liver cancer

The liver is a major organ of the digestive system that primarily metabolizes toxins, clears pathogens, and aids in digestion with the production of bile. Additionally, the liver also plays an important role in hormone regulation and carbohydrate, lipid, and amino acid metabolism. Harmful toxins, viruses, bacteria, and macromolecules enter the liver from the hepatic portal vein, where liver enzymes catabolize and clear them [1].

However, circulating viruses, such as hepatitis B (HBV) and C (HCV) virus, toxins, and fatty acids can accumulate in the liver, resulting in liver injury, inflammation, and lipotoxicity, culminating in fibrosis and eventually cancer [2]. Hepatocyte injury contributes to immune cell dysfunction in the liver in cell types such as Kupffer cells, neutrophils, and monocytes [2]. This generates an autoreactive environment and further liver injury, inflammation, and activation of cell types such as hepatic stellate cells (primarily responsible for the development of fibrosis)[3]. Unfortunately, this also disrupts the critical function of cell types, such as CD8 T cells responsible for immune surveillance, and limits the efficacy of immunotherapeutic strategies [4].

Hepatocellular carcinoma (HCC) is a malignant tumor of the hepatocytes and is the most common type of primary liver cancer, making up 80-90% of all liver cancer cases [5]. Development of abnormal liver nodules, including preneoplastic lesions, such as hyperplastic and dysplastic nodules, which progressively harbor more morphological and molecular abnormalities, precede the development of HCC [6]. As genomic instability reaches a critical point, preneoplastic liver lesions evolve, and cancer (neoplastic nodules) appear [7].

## 1.2 Liver cancer epidemiology

As of 2022, the estimated global incidence of liver cancer ranked 6<sup>th</sup> [8]. Globally, Liver cancer incidence and deaths are predicted to increase by 63% and 67%, respectively, translating to an estimated 1.4 million new diagnoses and 1.3 million mortalities in the next 20 years [9]. Importantly, in Canada, liver cancer mortality rates rank second worst out of all cancer types, with a 5-year survival rate of 18%, in part due to difficulty in detecting liver cancer early and the limitations in treatments [10].

Liver cancer predominantly affects men, consisting of roughly 70% of new cases and deaths. Furthermore, cirrhosis as a result of HBV, HCV, alcohol-related liver disease (ALD), and metabolic-dysfunction associated steatotic liver disease (MASLD), among other factors, is considered the single greatest HCC risk factor and is an underlying factor in more than 90% of HCC cases [11]. Currently, the global burden of disease database revealed that the percentage incidence of HCC for each etiology is as follows; HBV at 41%, HCV at 28.5%, ALD at 18.4%, MASLD at 6.8%, and other factors at 5.3% [12]. HBV is an especially prevalent etiological factor for HCC, with an estimated 1.5 million new cases in 2019 and an estimated 296 million people living with the disease as of 2019 [13]. HCV also has an estimated 1.5 million new cases per year, with an estimated 58 million people living with the disease. HCV is the leading cause of viral HCC at 40% in countries with a high sociodemographic index [12, 14]. In total, HBV accounts for 75-80% of viral HCC in the world; however, it predominantly affects Africa and Asia and is reflected in the high incidence of virus-related HCC, accounting for up to 80% of cases, while Western regions were around 20% [14]. Instead, western regions are observing an increase in HCC from non-viral origins and instead from chronic liver damage due to metabolic syndromes and lifestyle choices, such as with MASLD. MASLD prevalence has increased globally to 24% in 2010, primarily affecting North American, South American, European, Middle Eastern, and Asian regions [15]. Correspondingly, MASLD-related HCC represents about 20% of HCC cases [16]. Correlatively, regions with high rates of excessive alcohol consumption, such as Australia, Central Europe, and Eastern Europe, also had higher rates of ALD-related HCC compared to the rest of the world [14].

HCC is continuously on the rise and presents a major burden in the lives of individuals and on worldwide healthcare infrastructure. Advances in the prevention and treatment of HCC are an immediate necessity to alleviate the already overburdened global healthcare system and improve health outcomes.

## 1.3 Liver cancer etiology and risk factors

#### 1.3.1 Viral HCC

HBV and HCV are chronic infections that result in liver cirrhosis, which progresses to HCC 80-90% of the time, making them major risk factors for the development of HCC [17].

#### 1.3.1.1 HBV

When infecting hepatocytes, HBV inserts its viral genetic material into the human genome and proliferates. Unsurprisingly, pathways such as the silencing of p53 and the constant activation of the phosphoinositide 3-kinase (PI3K)/Ak strain transforming (Akt)/mammalian target of rapamycin (mTOR) pathway are the same pathways upregulated in the uncontrolled growth of cancer cells. The continuous and chronic necrosis-regeneration cycle sustains inflammation, resulting in cirrhosis, genomic instability, and hepatocarcinogenesis [17].

#### 1.3.1.2 HCV

Unlike HBV, HCV infects hepatocytes without integrating its viral genetic code. Instead, HCV proteins are released by the virus to modify the regulation of transcription, cytokine production, growth kinetics, and lipid metabolism [17]. This allows for increased proliferation. Furthermore, liver cirrhosis occurs much more frequently in the presence of HCV compared to HBV [18].

Overall, chronic infection by HBV or HCV leads to genomic instability and hepatocarcinogenesis [17].

#### 1.3.2 MASLD

In recent years, the main factors contributing to HCC have shifted from virus-related liver disease caused by HBV and HCV to non-viral liver disease as a result of vaccines and anti-viral therapies [5]. Meanwhile, lifestyle factors have increased the prevalence of MASLD-associated HCC [5]. MASLD is defined as the sole cause of steatotic liver disease within any of the following cardiometabolic criteria [19]:

- BMI  $\geq$  25 kg/mm<sup>3</sup> or waist circumference > 94 cm in males and 80 cm in females
- Fasting serum glucose  $\geq$  5.6 mmol/L or a 2-hour post-load glucose level  $\geq$  7.8 mmol/L or HbA1c  $\geq$  5.7% or type 2 diabetes (T2D) or T2D treatment
- Blood pressure  $\geq 130/85$  mmHg or antihypertensive drug treatment
- Plasma triglycerides ≥ 1.70 mmol/L or lipid-lowering treatment
- Plasma HDL-cholesterol ≤ 1.0 mmol/L in males and 1.3 mmol/L in females or lipidlowering treatment

#### 1.3.2.1 MASLD risk factors

Consumption of a western diet and decreased rates of physical activity trigger the development of metabolic diseases, including obesity, diabetes mellitus, and dyslipidemia[17]. Diabetes mellitus alone increases the risk of HCC by 2-3 times and contributes to around 7% of global HCC incidences [20]. In a meta-analysis, obesity was found to independently increase the risk of HCC-related mortality by 2-fold [21].

The increase in circulating intermediates (glucose, fatty acids) and hormonal dysregulation (insulin resistance) with metabolic dysfunction drives ectopic fat accumulation in the liver[17]. MASLD can quickly progress to metabolic-dysfunction-associated steatohepatitis (MASH) (~30% of MASLD patients) and eventually cirrhosis (10-20% of MASH cases) [22], While 70-80% of MASLD-related HCC diagnoses already have cirrhosis, HCC can also arise independent of cirrhosis [23, 24]. Therefore, limiting this progression is essential.

#### 1.3.2.2 MASLD pathogenesis

MASLD is characterized by steatosis, the accumulation of lipids in the liver as a result of increased fatty acid uptake, increased de novo lipogenesis, decreased beta-oxidation of fatty acids, and lipid export [25]. The excessive buildup of lipids leads to oxidative stress and the production of reactive oxygen species as lipids are oxidized, as seen in figure 1. This interferes with mitochondrial function and induces endoplasmic reticulum stress. The dysfunction of these organelles triggers apoptotic pathways that release inflammatory cytokines, triggering an innate and adaptive immune response.

The key inflammatory cytokines involved in the progression of MASLD are leptin, tumor necrosis factor-alpha (TNF-α), and interleukin-6 (IL-6) [2]. Leptin is normally a hormone involved in the maintenance of energy homeostasis and is released when the body has a high reserve of triglycerides. Consequently, leptin concentrations are high in MASLD and are involved in carcinogenic pathways that promote fibrosis and angiogenesis by activating signaling pathways that increase the secretion of TNF- α and IL-6. Additionally, leptin also binds to leptin receptors on hepatocytes and later pre-HCC and HCC cells, activating the PI3K/Akt/mTOR pathway and Janus kinase/signal transducer and activator of transcription proteins (JAK/STAT) pathway [26]. In response to cell stress, TNF-α is primarily released by macrophages, but in the context of MASLD, adipose tissue releases TNF-α to promote metabolic disorder and carcinogenesis [27]. The release of TNF-α initiates inflammation and fibrosis pathways through inhibitor of nuclear factor kappa-B kinase subunit beta (IKKβ) production, with downstream targets that produce nuclear factor kappa-light-chain-enhancer of activated B cells (NF-κB) and its entry into the nucleus. IKKβ is also being activated by toll-like receptors (TLRs) in the presence of free fatty acids. NF-κB plays a large role in fibrosis and is a proto-oncogenic and oncogenic pathway [27, 28]. All these factors contribute to the dysregulation of liver metabolism, resulting in steatosis and steatohepatitis, which are characteristic of progression to MASH and the pathogenesis of MASLDrelated HCC, as seen in figure 1.

Meanwhile, IL-6 is another inflammatory cytokine that contributes to the progression of MASH and HCC by activating signal transducer and activator of transcription 3 (STAT3), which induces proliferation, apoptosis escape, and angiogenesis [17]. IL-6 is secreted by macrophages in response to pattern recognition receptor activation by pathogen-associated molecular patterns (PAMPs), which bind to TLRs. In MASLD, circulating PAMPs include more than

lipopolysaccharide and flagellin (bacteria), with abundant lipid species also binding to different members of the TLR family and triggering inflammatory signaling from macrophages, driving MASH and hepatocarcinogenesis [2].

At the same time, oncogenic pathways are elevated with MASLD. Impaired insulin signaling and elevated insulin-like growth factor (IGF-1) secretion stimulate hepatocyte proliferation and inhibit apoptosis [2]. This occurs via IGF-1 receptors (IGF1Rs), regulating downstream PI3K/Akt/mTOR signaling [2]. As the genomic stability of hepatocytes deteriorates, IGF-1 plays an important role in hepatocarcinogenesis and the propagation of cancer pathways [17].

#### 1.3.3 ALD

ALD is an injury to the liver as a result of excessive alcohol consumption, though the definition of excessive alcohol consumption varies by geography, ethnicity, sex, and many other factors. For many of the same reasons that MASLD-related HCC cases are on the rise, ALD resulting in HCC is also on the rise. Global alcohol consumption has seen an increase in consumption over the past decade. It is projected to continue increasing, with an estimated 2.3 billion people regularly consuming alcohol as of 2018. However, the trend is not uniform across all geographic regions, such as Africa, which has seen a decrease in the percentage of people who regularly consume alcohol [29, 30]. Alongside viral infection and metabolic diseases, ALD is one of the most prevalent, if not the most pervasive, chronic liver disease worldwide. Two million deaths per year are ALD-related, half of which are due to complications with cirrhosis, one of the most common precursors for hepatocarcinogenesis [31-33]. In 2015, ALD contributed to up to 30% of all HCC-related deaths [14].

Similar to the excessive consumption of food, alcohol abuse results in fat depositing in the liver, resulting in inflammation and damage (figure 1), with a high likelihood of progressing to HCC from chronic liver damage. Compared to 7% of cases progressing to cirrhosis in MASLD, 36% of ALD cases progress to cirrhosis [34]. Like the disease progression of MASLD, ALD damages the liver by generating reactive oxygen species (ROS) when metabolizing ethanol with alcohol dehydrogenase into acetaldehyde, an oxidative and carcinogenic product. Acetaldehyde is further metabolized into acetyl-CoA by acetaldehyde dehydrogenase, though redox reactions still occur before breaking down. If acetaldehyde is not processed, it can bind to the deoxyribonucleic acid (DNA) and form DNA adducts that interfere with the normal replication and transcription of the cell, resulting in potentially carcinogenic results. Ethanol also induces steatosis by preventing peroxisome proliferation-activated receptor alpha, a regulator of fatty acid metabolism, from binding to DNA to metabolize fatty acids in the presence of high fatty acid concentrations and instead maintaining de novo lipogenesis [35]. This is especially problematic because the consumption of alcohol increases the concentration of hepatic fatty acids. As exposure to ethanol and its products is prolonged, the similarities to the disease of progression in MASLD continue with damage to the liver accumulating, inflammation persisting in the liver, and the dysfunction of immune cells, culminating with the induction of cirrhosis with a high likelihood of HCC development seen in figure 1.

Alcohol consumption has a synergistic effect on propagating hepatocarcinogenesis with other risk factors, such as metabolic diseases (figure 1) and viral hepatitis [36, 37].

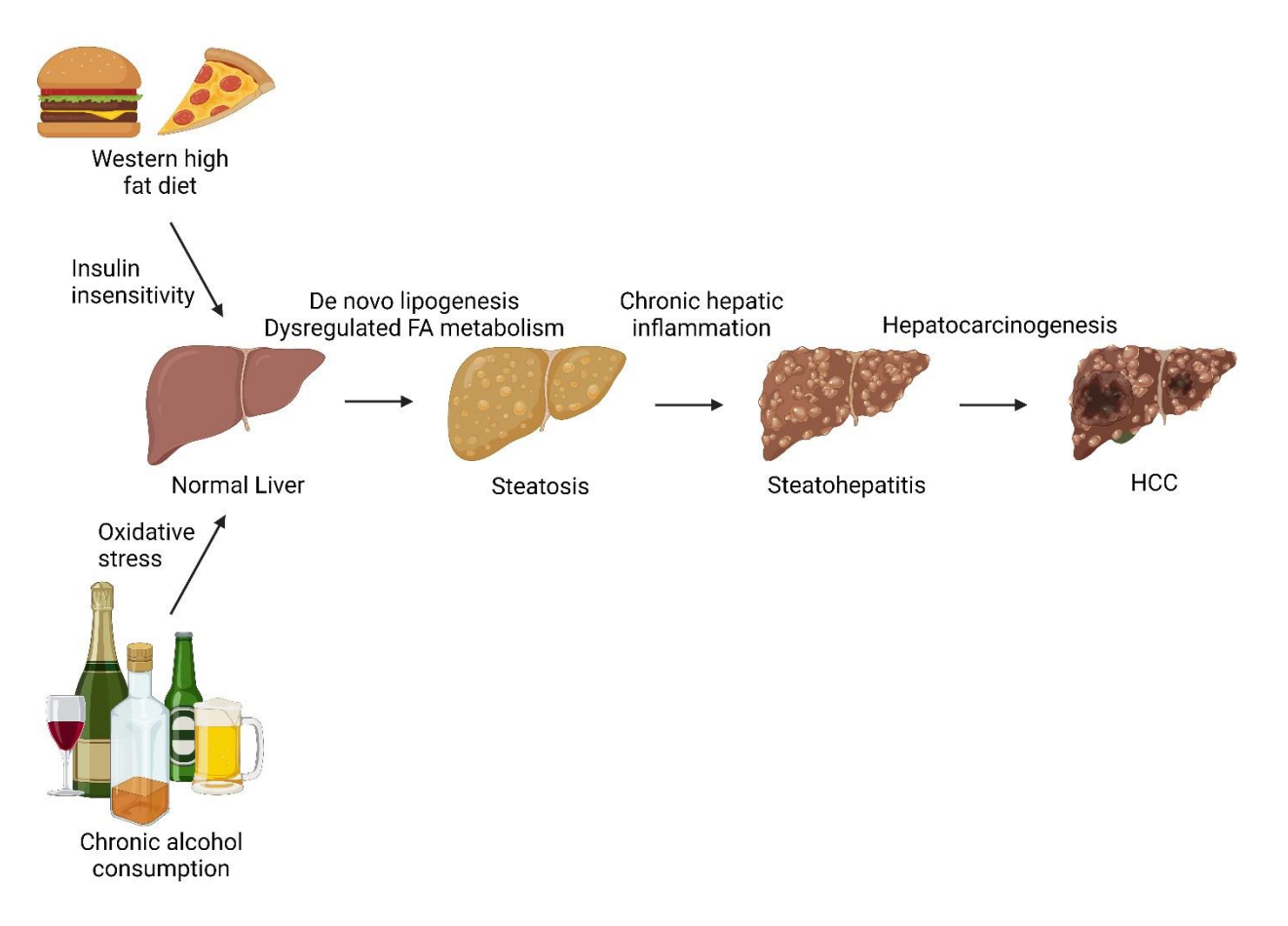


**Figure 1. Pathogenesis of HCC from MASLD and ALD.** High-fat diets and chronic alcohol consumption are diverging mechanisms by which the liver is damaged but converge into a common pathway for HCC pathogenesis. Hyperlipidemia and ethanol catabolism increase hepatic lipid deposition, leading to steatosis. Continued dysregulated fatty acid metabolism and chronic hepatic inflammation result in steatohepatitis and cirrhosis. Dysplastic cells form nodules where hepatocarcinogenesis occurs, resulting in progression to HCC.

#### 1.3.4 Other

The accumulation of carcinogens in the liver, such as aflatoxins, tobacco, vinyl chloride, arsenic, and others, are also HCC risk factors that cause hepatocyte injury, DNA damage, and cirrhosis. For example, aflatoxin is a well-known liver carcinogen from Aspergillus fungus that contaminates consumables. It suppresses p53 by mutation, while other toxins contribute to hepatocarcinogenesis by causing genomic instability, oxidative stress, and telomere shortening.

Finally, hereditary diseases that increase the risk of HCC by increasing inflammation in the liver and damaging hepatocytes include hereditary hemochromatosis, α1-antitrypsin deficiency, Wilson's disease, and hepatic porphyria, resulting in hepatocarcinogenesis [17].

## 1.4 HCC diagnosis

The first line of HCC diagnosis is screening at-risk individuals for HCC based on a list of criteria, including underlying conditions, age, sex, ethnicity, lifestyle, genetics, and other factors. The most common factors during screening are HBV, HCV, cirrhosis, metabolic diseases, and alcohol abuse. These high-risk patients should be regularly tested for HCC.

Alpha-fetoprotein (AFP) is a glycoprotein in the serum used as a biomarker for HCC, though it is not always elevated in all HCC cases nor isolated to HCC. Therefore, it is an early screening tool for the diagnosis of HCC.

To verify abnormal AFP levels, a physical exam is conducted to assess for abnormalities. This is usually done in conjunction with imaging tests, such as ultrasound exams, computed tomography (CT) scans, and magnetic resonance imaging (MRI). Additional blood tests are conducted to assess the performance of the liver by measuring certain liver-specific products for abnormal concentrations, such as alanine transaminase and aspartate transaminase concentrations. If an abnormal mass or lesion is detected, liver biopsies are taken with the assistance of an ultrasound or CT scan to procure fine-needle aspiration biopsies or core needle biopsies for histological assessment by pathologists. Liver biopsies are the most conclusive test, with a 96% sensitivity and a 95% specificity. A laparoscopy can be performed in extreme cases when biopsy needles cannot be properly guided by imaging techniques [38].

### 1.4.1 Staging of liver cancer

Treatment of HCC begins with staging, with the most common staging system being the Barcelona Clinic Liver Cancer (BCLC) system since this system helps select the appropriate treatment options for a patient [39]. The BCLC system considers the following characteristics for scoring:

- How many tumors are in the liver, and their sizes
- How well a patient can perform daily activities with the performance status (PS) scale, ranging from 0 to 4, increasing in inability to perform daily function
- The health of the liver with the Child-Pugh score, with A being normal liver function,
   B being mild to moderate liver damage, and C being severe liver damage
  - Observe bilirubin levels in the blood, albumin levels in the blood, blood clotting time, the presence of fluid in the abdomen, and brain function.

From these characteristics, the BCLC system is divided into 5 stages, summarized in table 1.

Table 1. BCLC system of categorizing HCC

Stage	Tumor number and	Performance status	Child-Pugh Score
	size		
0 (very early stage)	Any tumor <2 cm	0	A
A (early stage)	Single tumor ≤ 3 or all tumors < 3cm	0	A or B
B (intermediate stage)	Many tumors	0	A or B
C (advanced stage)	Local or spread	1 or 2	A or B
D (end stage)	Local or spread	3-4	С

## 1.5 HCC prevention

Preventative measures include vaccination against HBV and direct-acting antiviral therapy for HCV, reducing virological response, thereby reducing the risk of HCC by up to 80% [40]. With the rise of MASLD driving HCC, early preventative strategies include addressing lifestyle risk factors, for example, exercising, limiting food intake, and limiting tobacco and alcohol [41]. Additionally, widely used metabolic and anti-inflammatory agents are suggested to have chemoprevention activity that may be able to reduce the risk of HCC, including the antiinflammatory aspirin, the anti-cholesterol agents statins, and the diabetes agent metformin [42-44]. In a meta-analysis of 12 cohort studies, aspirin was shown to reduce the risk of HCC by 30% (adjusted HR 0.70, 95% CI 0.60-0.81), though subjects already with cirrhosis saw no benefits [45]. Another meta-analysis of aspirin's effect on HCC development involving 18 studies found an even higher risk reduction of HCC with aspirin (adjusted HR 0.54, 95% CI 0.44-0.66) [42]. The antiinflammatory and anti-platelet effects of aspirin can be attributed to the improvements in risk reduction of HCC, with inflammation being a hallmark of MASH. Lipophilic statins also appear to reduce the risk of HCC in Swedish patients with HBV or HCV virus, with a 4.8% lower 10-year risk of HCC (absolute RD -4.8%, 95% CI -6.2 to -3.3%; adjusted HR 0.56, 95% CI 0.41-0.79) and 7.9% lower mortality (absolute RD -7.9%, 95% CI -9.6 to -6.2%), though further studies are required [43]. Metformin has also demonstrated a 50% reduction of HCC in a meta-analysis of

activity inhibiting the mTOR pathway, proliferation, and angiogenesis [44, 46]. Furthermore, as the dominant cause of HCC shifts to MASLD, surveillance programs for at-risk patients, especially

anti-diabetic drugs due to its anti-cancer activity through AMP-activated protein kinase (AMPK)

in patients who have already developed cirrhosis, and the potential expansion of these surveillance

programs to patients with advanced liver fibrosis and MASLD are critical. Surveillance is a cost-effective method of detecting HCC, with semi-annual ultrasonography recommended in high-risk populations, though it has been argued that this is insufficient [47]. Current discussions revolve around who to categorize as high-risk to reduce unnecessary costs on the system and patient, both physically and mentally [5].

#### 1.6 HCC treatment

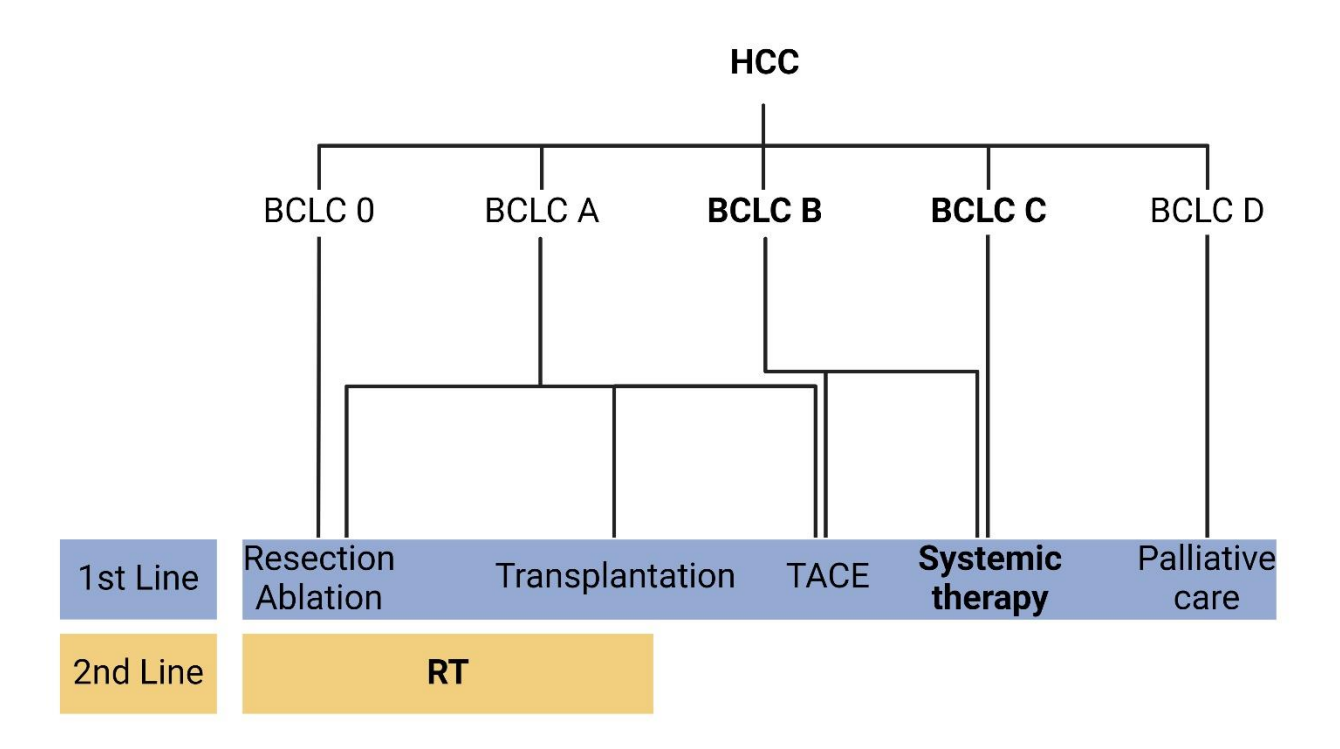


**Figure 2. Flow chart of HCC treatment options by BCLC staging system.** First-line therapies include resection, ablation, liver transplantation, trans-arterial chemoembolization (TACE), systemic therapy, and palliative care, depending on the severity of HCC and the eligibility of patients for specific treatments. Secondary treatments include RT.

#### 1.6.1 Local therapies

#### 1.6.1.1 Surgical Resection

Based on the BCLC score, different treatment options are available. At BCLC 0, surgical resection is the preferred treatment choice in patients with good liver function. Surgical resection is the second most effective method of removing HCC behind liver transplantation at the cost of liver function. Additionally, the conditions that gave rise to HCC in the liver would still likely persist, risking recurrence. Therefore, surgical resections are generally supplemented with adjuvant therapies. For example, patients with cirrhosis are not ideal candidates for surgical resection. While cirrhotic patients with good liver function can also undergo resection with minimal post-operative complications according to most metrics, a recent study showed that post-surgical liver decompensation can reach 50% of cirrhotic cases with good liver function [39]. Recurrence occurs in as high as 50% of surgical resection cases. Therefore, surgical resection is ideal for HCC patients without early disease or cirrhosis.

#### 1.6.1.2 *Ablation*

Ablation is another treatment for early-stage HCC, generally used when resection is impossible. Alcohol ablation, known as percutaneous ethanol injection (PEI), is the more traditional and widespread method of ablation, though, in recent years, radiofrequency ablation (RFA) and microwave ablation (MWA) have gained traction [40].

PEI is guided by ultrasound or CT scanning to inject the tumor with ethanol to deliver chemical burns at the target site and is most effective in eliminating tumors smaller than 2 cm in one session, though more sessions can be arranged to remove larger tumors with rarely any severe complications.

RFA and MWA have become the predominant ablation methods because they can ablate larger tumors in one session with few side effects. RFA and MWA consist of guiding a needle that generates heat to the site of the tumor either by electrical currents (RFA) or electromagnetic waves (MWA) under the guidance of ultrasound or CT scanning. RFA is predominantly used on smaller tumors less than 3 cm, while MWA is used with larger tumors [39]. Side effects include bleeding at the site of ablation, and at this point in time, no method of ablation is better than the other, with selection being highly dependent on local guidelines that can change on a case-by-case basis.

#### 1.6.1.3 Liver transplantation

Patients with BCLC A with a single tumor that can be reached surgically have resection as an option. Transplantation is a curative treatment option for HCC, but it is suitable only in selected patients. This includes having no extrahepatic spread of the tumor, having only a single tumor nodule size no larger than 5 cm, and a limited number of tumor nodules to less than 4 with none larger than 3 cm in diameter [39]. These constraints exist to limit the possibility of recurrence with transplantation since there is a very limited number of donor organs. A major drawback of liver transplantation is the long wait time, in which the tumor may spread or grow beyond the recommended constraints. Another consideration is that a liver transplantation has the potential to cure the entire liver.

#### 1.6.1.4 TACE

In the case that the aforementioned treatments are not available options, then ablation or trans-arterial chemoembolization (TACE) is possible.

TACE is a procedure guided by arteriograms to isolate the hepatic artery feeding the tumor for the injection of chemotherapeutics into the hepatic artery and its subsequent blockage with the injection of embolic material since HCCs primarily rely on blood from the hepatic artery. The result is the delivery of a concentrated dose of chemotherapeutics to the HCC tumor while minimizing the side effects of chemotherapeutics to the rest of the liver and reducing flow to the tumor. The reduced blood flow to the tumor also has the added benefit of keeping the chemotherapeutics in the vicinity of the tumor. Doxorubicin, cisplatin, and mitomycin C are common chemotherapeutics used in TACE. Gelfoam and Ivalon are standard embolization formulations to occlude blood flow to the tumor. The success of this procedure is defined by HCC receiving blood from the hepatic artery while the rest of the liver receives blood via the hepatic portal vein. Tumor necrosis is seen in 80% of cases, but the side effects of TACE could be just as damaging, such as liver failure and the formation of liver abscesses. The procedure can also be extremely painful regardless of the outcome. Studies have shown that the use of TACE compared to palliative therapy in unresectable HCC has no enhanced 4-year survival [48]. TACE is most applicable in concentrated tumors, such as HCC nodules, and is especially unapplicable in HCC tumors dispersed throughout the liver. Therefore, the application of TACE is usually limited to an adjuvant therapy.

#### 1.6.1.5 Chemotherapy

Chemotherapy is well documented as being a generally ineffective first-line treatment option and serves as second-line or adjuvant therapy. As mentioned before, regional administration of chemotherapy is done by TACE. Systemic administration of chemotherapy is usually isolated to antiangiogenic agents, such as thalidomide, since other types of chemotherapy generally elicit

a response in less than 25% of cases, with HCC patients with liver cirrhosis, which make up the majority of cases, being ineligible [39].

Attempts have been made to use a monotherapy regimen in combination with another first-line treatment, such as TACE and sorafenib, but this has not shown an increase in overall survival. However, in polytherapy regimens, 5-fluorouracil, leucovorin, and oxaliplatin (FOLFOX4) have demonstrated improvements in secondary endpoints while being just as effective in primary endpoints as monotherapy doxorubicin. Additionally, the Gemcitabine-Oxaliplatin (GEMOX) regimen showed some promise, with double the overall survival rate (19.9 vs 9.5 months) when there was a response, but the response rate was 22% [49]. Overall, more research is needed to identify which cases and with which adjuvant chemotherapy is beneficial.

#### 1.6.1.6 Radiotherapy

In the case that surgical resection or ablation is unsuitable for BCLC 0-A patients due to difficulty in achieving safe resection or the tumor is too close to critical structures to perform ablation, radiotherapy is an alternative. Radiotherapy is most commonly used as an adjuvant therapy in preparation for liver transplantation or with surgical resections. Compared to adjuvant TACE, adjuvant radiotherapy performed better in 3-year relapse-free survival at 45% compared to 27% and 3-year overall survival at 73% compared to 44% [50]. However, one major concern and limitation of radiotherapy is radiation-induced liver disease (RILD), a frequent side effect that occurs due to the radiosensitivity of normal liver tissues, limiting treatment effectiveness and severely decreasing the quality of life of the patient. If severe and chronic, radiation-induced liver fibrosis can occur, critically impairing liver function [51].

Conventional external beam radiation therapy (EBRT) targets cancer cells with a directed high-energy beam of ionizing radiation, generally in the form of photons (X-ray or gamma rays) generated from linear accelerators. In the past, conventional EBRT had limited use in treating HCC due to RILD. Past attempts to lower doses by lengthening the number of daily fractions have been shown to avoid RILD but negated the effectiveness of EBRT entirely in HCC. Advancements in EBRT, such as improved targeting and radiation delivery, have been proven to be effective while limiting RILD.

The advent of three-dimensional conformal radiotherapy (3DCRT) arose with advances in imaging techniques with CT and MRI scans. Detailed scans of the tumor site could now distinguish the tumor from the normal tissue surrounding the tumor, allowing for more targeted radiotherapy. The planning of radiotherapy regimens was revolutionized with the ability to specify the target of radiation beams so that the treatment is conformal to the tumor and avoids normal tissue damage.

Intensity-modulated radiation therapy (IMRT) is the next advancement in EBRT with better coverage of the tumor, more conformal delivery of radiation, and fewer off-target effects. IMRT achieves this by modulating the radiation intensity depending on where the beam targets. For example, beams closer to the main body of the tumor will deliver higher intensity of radiation while beams closer to normal tissue deliver lower intensity of radiation. However, IMRT may still significantly affect normal tissue in large HCC tumors. Studies comparing 3DCRT and IMRT showed that IMRT has improved 1-year survival at 43% and 70%, respectively, and 3-year survival rates at 28% and 47%, respectively, with the same 5% rates of RILD [52].

Stereotactic body radiotherapy (SBRT) is an EBRT technique that delivers very high doses of radiation to the tumor in shorter durations compared to other EBRT techniques. This technique requires extensive tumor imaging, image guidance, and patient immobilization to maintain on

target and prevent extreme radiation damage to normal tissue. SBRT usually achieves more than 90% local control in a dose-dependent manner but could also burden the patient with significant toxicities [53]. A meta-analysis pooling 30 SBRT cohorts showed that SBRT had an 87% local control rate of HCC and an 80% 1-year survival rate with only 6.4% late toxicity [54]. Compared to other local treatments, it had similar or better effectiveness, with less acute grade 3 or higher complications [52]. When compared to other EBRT techniques, SBRT has improved local control and 1-year survival rates.

Charged particle therapy (CPT) is another form of radiotherapy using charged protons instead of charged photons. The advantage of charged particle therapy is the finite range of the particle, which decreases the energy the particle is carrying rapidly to near zero and can be calculated to peak at the tumor site, reducing the off-target effects. CPT is an effective radiotherapy treatment, but a meta-analysis comparing CPT to SBRT showed comparable results [54].

Selective internal radiation therapy (SIRT) is a form of radiation therapy where 90-Yttrium, a β-emitting radioisotope, is injected into the tumor, most commonly large lesions. Though the treatment is effective, the side effects are severe and not limited to the liver. Additionally, studies have also shown that SIRT had a lower response rate and 1-year overall survival rate compared to other radiotherapy techniques [55]. The application of SIRT is limited to a case-by-case basis.

Due to the radiosensitivity of the liver and the nodular tendencies of HCC, SBRT is an increasingly popular method of treating HCC [56]. Although radiotherapeutic techniques have advanced and reduced radiation toxicity, radiation-induced liver disease is still an unpreventable complication that occurs in up to 66% of patients who undergo radiation [57]. The side effects of radiation drastically reduce the therapeutic ratio and make it a second-line therapy option.

### 1.6.2 Systemic therapy

If TACE is inapplicable for a patient with BCLC A or a patient with BCLC B, systemic therapies exist to treat HCC. About 50-60% of HCC patients are treated by systemic therapies, with half being diagnosed with advanced HCC and the other half with progression of HCC. Current systemic therapies include tyrosine kinase inhibitors, immunotherapies, and adoptive cell therapy.

#### 1.6.2.1 Tyrosine kinase inhibitors

Initially, sorafenib was the sole systemic therapy for advanced-unresectable HCC in 2007, working by inhibiting kinases such as VEGFR (vascular endothelial growth factor receptor), platelet-derived growth factor receptor (PDGFR), and RAF kinases [58]. Patients treated with sorafenib in the phase 3 trial had a median survival of 10.7 months, while patients on placebo had a median survival of 7.9 months. In 2018, Lenvatinib was approved for use against HCC. This agent works by inhibiting tyrosine kinases, such as VEGFRs, fibroblast growth factor receptors (FGFRs), and PDGFRs [59]. Compared to sorafenib, Lenvatinib showed equal potency in survival and improved secondary endpoints, such as overall response rate and progression-free survival. Other kinase inhibitors exist, such as regorafenib, cabozantinib, and ramucirumab, though they are used in niche scenarios when sorafenib and Lenvatinib alone are ineffective.

#### 1.6.2.2 Immunotherapy

Immune checkpoint inhibitors are newer therapeutics that have seen improvements in overall survival in HCC. The combination of atezolizumab (anti-programmed death-ligand 1 (PD-L1) antibody) and bevacizumab (anti-vascular endothelial growth factor (VEGF) A antibody) improved overall survival by 6 months compared to sorafenib [60]. Another combo treatment with

Durvalumab (anti-PD-L1 antibody) and tremelimumab (anti-cytotoxic T-lymphocyte associated protein 4 (CTLA4) antibody) also improved overall survival compared to sorafenib [61]. By themselves, immune checkpoint inhibitors have similar efficacy compared to sorafenib [61]. However, immune checkpoint inhibitors combined with anti-angiogenic drugs, including tyrosine kinase inhibitors, have synergistic activity against HCC via inhibition of the VEGF pathway [62]. The inhibition of VEGF normalizes vessels, improving drug delivery and immune cell infiltration. Unfortunately, the benefits of immune checkpoint inhibitors in combination with anti-angiogenics only offer advantages in viral HCC [63].

#### 1.6.2.3 Other therapies

Adoptive cell therapy, such as lymphokine-activated killer (LAK) cells, cytokine-inducted killer (CIK) cells, and chimeric antigen receptor (CAR) T cells, can target HCC-specific receptors for a more personalized and targeted therapy. LAK and CIK cell therapy trials observed some success with favorable overall survival, but the lack of in-house cell therapy infrastructure limits the feasibility and is affected by the time-sensitive nature of the disease. In CAR T cells targeting glypican-3 (GPC3), an HCC-associated antigen, preclinical models were promising, and a clinical trial is in progress (NCT05003895) [64].

# 1.7 Molecular and metabolic signaling in HCC

HCC tumors are very heterogeneous and will present with different mutations. In most cases, the disease will begin with impaired transforming growth factor beta (TGF- $\beta$ ) signaling, leading to overactive extracellular signal-regulated kinase (ERK) and mTOR pathways, with a high likelihood that p53 is impaired.

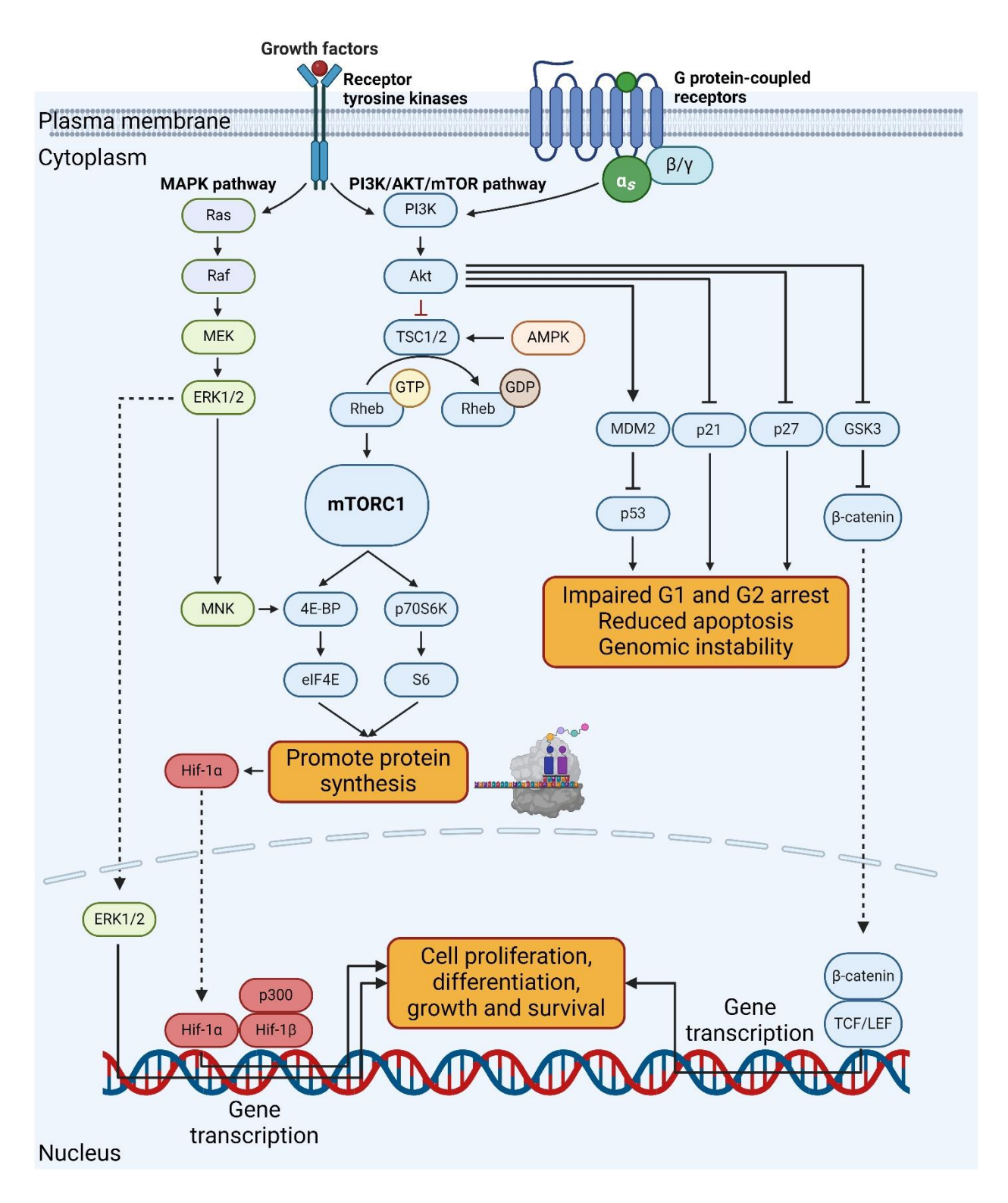


**Figure 3. mTOR and ERK signaling pathways.** The mTOR pathway is activated by receptor tyrosine kinases and G protein-coupled receptors. The PI3K/Akt/mTOR signaling cascade impairs cell cycle arrest and promotes protein synthesis, cell proliferation, and survival. The ERK pathway is activated by receptor tyrosine kinases and promotes cell

proliferation, differentiation, and growth while converging with the mTOR pathway with mitogen-activated protein kinase interacting protein kinases (MNK) phosphorylation of 4E-binding protein 1 (4E-BP) to promote protein synthesis. The increase in protein synthesis increases Hif-1α expression, promoting cell proliferation and survival.

### 1.7.1 MAPK pathway

The mitogen-activated protein kinase (MAPK) pathways are essential pathways that translate a range of extracellular stimuli into a corresponding cell response through a series of protein kinase cascades (see model in Figure 3). There are three distinct MAPK pathways in mammalian cells: the ERK pathway, the JNK/SAPK pathway, and the p38 pathway.

The most defined MAPK pathway is the ERK pathway described in figure 3 and is usually upregulated in many different types of cancers, including HCC. The upregulation of this particular MAPK pathway results in cell proliferation, differentiation, and cell cycle progression. The ERK pathway is initiated by growth factors (GFs) stimulating tyrosine kinase receptors (RTKs) to trigger an ERK signaling cascade. The most common RTKs include epidermal growth factor receptor (EGFR), platelet-derived growth factor receptor (PDGFR), insulin-like growth factor receptor (IGFR), MET RTK, and fibroblast growth factor receptor (FGFR). The ligands of these RTKs are GFs, with the most common GFs being epidermal growth factor (EGF), platelet-derived growth factor (PDGF), insulin-like growth factor (IGF), hepatocyte growth factor (HGF), and fibroblast growth factor (FGF). The binding of GFs to RTKs dimerizes the RTK, and intermediary proteins pass the signal from activated RTKs to the ERK pathway beginning at Raf. For example, an activated EGFR phosphorylates growth factor receptor binding protein 2 (GRB2), which recruits son of sevenless 1 (SOS) for a GTP-catalyzed activation of Ras to bind to Raf for its activation [65]. Raf phosphorylates dual specificity mitogen-activated protein kinase kinase 1

(MEK1) and MEK2, which in turn phosphorylates ERK1 and ERK2 (see Figure 3). Upon phosphorylation, ERK1/2 is translocated into the nucleus to alter gene expression, phosphorylating transcription factors to promote cell proliferation, differentiation, angiogenesis, apoptosis resistance, and cell cycle progression [66-68]. Phosphorylated ERK1/2 phosphorylates transcription factors, including ETS Like-1 protein (ELK1), c-Myc, c-Fos, and c-Jun, promote the formation of activator protein-1 (AP-1) complexes, which bind to promoter and enhancer regions of genes involved in cell proliferation, differentiation, and cell cycle progression [69].

For example, the cell cycle is regulated by target genes encoding cyclin D1, which binds with cyclin-dependent kinase (CDK) 4 and 6 to regulate G1/S transition for cell cycle progression. The binding of cyclin D1 to CDK4 phosphorylates and inhibits retinoblastoma protein (Rb) from preventing the transcription factor E2F from promoting the genes needed for transition into the S phase, including as cyclin E. Cyclin E binds with CDK2 to further inhibit Rb, thereby increasing cyclin E, and also phosphorylate p27 for proteolysis. Cyclin D1-CDK4 also inhibits p27 and p21 inhibition of cyclin E-CDK2 to promote G1/S transition [70].

### 1.7.2 PI3K/Akt/mTOR pathway

The PI3K/Akt/mTOR pathway is involved in cell survival, growth, and proliferation in response to extracellular stimuli. The PI3K/Akt/mTOR pathway is commonly dysregulated during carcinogenesis, contributing to treatment resistance due to its constant activation [71].

Figure 3 describes the mTOR signaling pathway beginning with G protein-coupled receptors and RTKs triggering the PI3K/Akt/mTOR pathway. PI3K is comprised of p85, the regulatory subunit, and p110, the catalytic subunit. p85 binds to activated RTKs, recruiting p110 to form PI3K. In many cancer types, the p110 subunit is mutated to either be hyperactivated or

insensitive to p85 regulation. PI3K propagates the signal to Akt with the p110 subunit phosphorylating PIP2 to PIP3, which can be dephosphorylated by phosphatase and tensin homolog (PTEN). For this reason, PTEN is commonly known as a tumor suppressor since it regulates PI3K/Akt signal transduction, and its loss is often the precursor to carcinogenesis. For Akt to be activated, PIP3 binds to inactive Akt in the plasma membrane, phosphorylating and activating Akt, which, in turn, activates downstream targets in the cytoplasm and the nucleus, where it translocates. In most cases, Akt mutation does not occur, but gain-of-function mutations can cause constitutive activation and localization in the cytoplasm and nucleus. Hyperactivation mutations can also produce cellular responses consistent with carcinogenesis [71]. The activation of Akt phosphorylates a variety of downstream substrates:

- Phosphorylation of B cell lymphoma-2 associated agonist of cell death (BAD) inactivates the protein, promoting apoptosis escape and cell survival [72]
- Phosphorylation of IKK activates a signal cascade that alters gene expression to favor cell survival and proliferation [28]
- Phosphorylation of forkhead box class O (FOXO) inhibits the protein, resulting in cell cycle progression, cell survival, and metabolic reprogramming [73, 74]
- Phosphorylation of mouse double minute 2 homolog (MDM2) inhibits p53, a key cell regulator known as a tumor suppressor, promoting cell cycle progression, apoptosis escape, and genomic instability [75]
- Phosphorylation of p21 and p27 inhibits their function of regulating G1/S progression, resulting in cell cycle progression [76]

- Phosphorylation of glycogen synthase kinase 3 (GSK3) inhibits their function of regulating the β-catenin pathway, which promotes cell cycle progression, cell proliferation, and growth [77]
- Phosphorylation of tuberous sclerosis complex 2 (TSC2) inhibits its regulation of mTORC1, which increases biosynthesis, cell growth, and cell survival [78]

### 1.7.3 mTOR pathway

The mTORC1 pathway is regulated by Akt through the inhibitory phosphorylation of TSC2, allowing for Ras homolog enriched in brain (RHEB), a guanosine triphosphate (GTP)-binding protein, to activate mTORC1 in a GTP-mediated step (figure 3). Once activated, mTORC1 phosphorylates its downstream targets, 4E-BP1 and ribosomal protein S6 kinase beta-1 (p70S6K). The phosphorylation of 4E-BP1 has an inhibitory effect and causes 4E-BP1 to dissociate from eukaryotic translation initiation factor 4E (eIF-4E), increasing cap-dependent mRNA translocation. The phosphorylation of p70S6K activates downstream targets S6rp and eIF4B, promoting ribosome biogenesis and increasing cap-dependent translocation, respectively. The dual activation of 4E-BP1 and p70S6K results in the increased protein synthesis required in carcinogenesis [79].

In addition to being regulated by Akt, mTORC1 is also regulated by AMPK through the phosphorylation of the upstream regulator TSC2, which enhances the inhibitory activity of TSC2 on mTOR, countering phosphorylation of TSC2 by Akt, which inhibits TSC2 activity. AMPK also regulated mTORC1 with the phosphorylation of the Raptor subunit of mTOR, a negative regulator of mTOR activity [80].

#### 1.7.4 Hif-1α

Usually, Hif-1 $\alpha$  responds to the oxygen level, with high levels marking Hif-1 $\alpha$  for degradation. During normoxia, Hif-1 $\alpha$  is localized to the cytoplasm by factor inhibiting HIF, preventing the recruitment of coactivators required for translocation into the nucleus [81]. In hypoxic conditions, Hif-1 $\alpha$  regulators are repressed, and Hif-1 $\alpha$  is translocated into the nucleus, where it makes up a larger unit with Hif-1 $\beta$ , called hypoxia-inducible factor (HIF), managing the transcription activity of hundreds of genes in response to oxygen levels [82]. The regulation of Hif-1 $\alpha$  is not limited to oxygen levels and can be activated by hormones and cytokines, such as insulin, IL-1 $\beta$ , CDKs, and ROS, as well as hyperlipidemia [83].

Hif-1α expression is promoted by both the ERK pathway and the mTOR pathway via 4E-BP1 inactivation by ERK1/2 and mTORC1, resulting in subsequent eIF4E promotion of cap-dependent translation of HIF-1α (figure 3). S6 ribosomal protein (S6rp) phosphorylation by p70S6K also increases Hif-1α synthesis with the increase in ribosomes. The ERK and mTOR pathways also stabilize Hif-1α by suppressing p53, Rb, and Bcl2 while activating Myc and Ras [83]. Regulation by oxygen in tumors is repressed due to the hypoxic tumor microenvironments, which stabilizes Hif-1α in tumors [84]. In many cases, Hif-1α activation can create a feedback loop where it overexpresses growth factors, such as VEGF and PDGF, that activate ERK and mTOR signaling cascades to further increase Hif-1α activity [83].

The effects of Hif-1 $\alpha$  activity in cancer include angiogenesis, metastasis, alterations in energy metabolism, cell survival, and cell proliferation. Tumors rely on the formation of vascular networks to continue growing and not collapse under their own mass. Hif-1 $\alpha$  promotes the transcription of proangiogenic factors, such as VEGF, to form new vasculature in the tumor. A common occurrence prior to cancer metastasis is an epithelial-mesenchymal transition (EMT), and

many components that trigger EMT are induced by Hif-1 $\alpha$ , such as Snail and TWIST, which suppress the E-cadherin scaffold that roots cells in place [83]. In addition to promoting EMT, Hif-1 $\alpha$  also contributes to intravasation, extravasation, and pre-metastatic niche formation [85]. Shifts in energy metabolism are required to sustain cancerous growth, most commonly in glucose and fatty acid metabolism. Hif-1 $\alpha$  modulates glycolytic shift by increasing glucose uptake through the expression of GLUT (glucose transporter) 1, GLUT3, and GLUT4 [83]. At the same time, Hif-1 $\alpha$  shifts energy production away from the mitochondria by producing proteins that inhibit glycolytic products from entering the mitochondria while increasing aerobic glycolysis by promoting lactate dehydrogenase A expression [83, 86]. In many types of cancer, abnormally increased lipid metabolism can be observed for energy or biosynthesis and cell growth. Hif-1 $\alpha$  promotes sterol regulatory-element binding protein-1 expression, which triggers the expression of several proteins in fatty acid synthesis [87]. Overall, limiting Hif-1 $\alpha$  activity in cancer, especially in HCC, may have important clinical implications.

# 1.7.5 TGF- $\beta$ pathway

Mouse and human studies have revealed the TGF-β1 to likely be one of the main instigators of pulmonary fibrosis while having 2 other isoforms. TGF-β can elicit a cellular response through the intracellular SMAD and non-SMAD signaling pathways. In the intracellular SMAD signaling pathway, TGF-β transmits a signal when it binds to a transmembrane serine/threonine kinase type II (TβRII), which then recruits and phosphorylates to activate a transmembrane serine/threonine kinase type I (TβRI) complex [88, 89]. Once active, TβRI phosphorylates receptor-regulated SMAD (R-SMAD) 2/3, forms a heteromeric complex with the common SMAD (co-SMAD) 4, and is translocated to the nucleus. The SMAD2/3/4 complex regulates the transcription of TGF-β

target genes, such as those involved in pro-inflammatory and profibrotic pathways, by acting as transcription factors, interacting with other transcription factors as activators or repressors, and interacting with chromatin remodeling factors. Inhibitory SMADs (I-SMADs) 6 and 7 regulate SMAD signaling by binding to T $\beta$ RI to prevent recruiting R-SMADs [88, 89]. This pathway is the primary pathway TGF- $\beta$  promotes fibrosis.

The non-SMAD signaling pathways begin with the joining of the TβRI:TβRII complex with the binding of TGF-β but activates pathways, such as the MAPK pathway, JNK pathway, PI3k/AKT/mTOR pathway, NF-κB production, and RhoA pathway. These pathways include transcriptional and translational regulation of cellular responses for survival and inflammatory pathways [88, 89]. These pathways are also implicated in cancer growth and survival. Non-SMAD signaling pathways crosstalk with each other, and the SMAD signaling pathway produces the response to injury.

TGF- $\beta$  is generally produced by most cells in response to stress or injury. In the liver, TGF- $\beta$  is upregulated in various liver diseases and is involved in every stage. Initially, TGF- $\beta$  signaling is beneficial during liver diseases, participating in the recruitment of immune cells and repairing liver injuries. At this stage, TGF- $\beta$  signaling is antiproliferative and is a tumor suppressor. However, as liver diseases persist chronically, the continued production and secretion of TGF- $\beta$  loses its tumor suppressive effects, with malignant and dysplastic cells overcoming the anti-cancer effects from chronic TGF- $\beta$  exposure, resulting in deactivated tumor suppressor signaling cascades, such as SMAD-dependent regulation of the cell cycle, or overactive hepatocarcinogenic pathways, such as EGFR and PDGF ligand and receptor production [3, 90-94]. Instead, these cells respond to TGF- $\beta$  signaling cascades that promote hepatocarcinogenesis, such as EMT, which is often involved in cancer metastasis [95]. In addition to cellular changes, TGF- $\beta$  contributes to

remodeling the surrounding liver environment into an HCC tumor microenvironment. TGF- $\beta$  signaling increases the production and secretion of connective fibers by the surrounding cells and activates hepatic stellate cells that are now myofibroblastic, creating scaffolding for angiogenesis, inflammation, metastasis, and immune cell evasion. The result is further liver injury and scarring [3]. Furthermore, TGF- $\beta$  also has an immunosuppressive role in which TGF- $\beta$  signaling deactivates natural killer (NK) cells by suppressing NKG2D, a key activating receptor of NK cells. T-cells are also affected by TGF- $\beta$  signaling, with the suppression of T-cell activation or the conversion of T-cells to regulatory T-cells, which further suppresses T-cell activation [3, 96-98].

# 1.8 Cell response to radiotherapy

Radiotherapy relies on normal tissue being less susceptible to ionizing radiation than cancer cells. Double-strand breaks (DSBs) are more likely to occur during the M phase when the chromosomes condense. This often results in apoptosis or mitotic cell death as chromosomal aberrations accumulate. Cancer cells are highly proliferative and divide more often, increasing the likelihood of being irradiated during the M phase. Furthermore, cancer cells often have reduced DNA damage repair capabilities due to mutations or alterations to cell cycle control, accumulating DNA damage from other stages and eventually resulting in cell death. Normal tissue that is not the target of radiotherapy receives a lower dose of radiotherapy and has a higher capacity for DNA damage repair compared to cancer cells. This, in combination with appropriate fractionation of radiation treatment, allows for repairs of normal cells [99].

The energy carried by ionizing radiation is capable of breaking the chemical bonds of essential cellular components, such as proteins and DNA. The breaking of chemical bonds in DNA

can cause single-strand breaks (SSBs) and DSBs, which may result in cell death if the damage is not repaired [99].

Reactive oxygen species (ROS) are generated by ionizing radiation, energizing electrons to the point that the electron is liberated from the atoms, at which point, any chemical bonds are also broken and create highly reactive ions [99]. One of the most common ROS is hydroxyl radicals generated from energizing water molecules. Hydroxyl radicals react with many essential cellular components, including proteins and DNA. These interactions destabilize the DNA and create mutations that could result in apoptosis. ROS indirectly damages DNA and is one of radiotherapy's foremost perpetrators of genetic damage [100].

Cells have many checkpoints in the cell cycle to prevent cell division in the event of genomic instability and react by activating DNA repair mechanisms. Typically, the cell cycle resumes once all the repairs are made. However, if the cell cannot repair the damage, it will become senescent or apoptotic. Senescence is when the cell arrests the cell cycle to prevent further lineages of the damaged cell. When cells become senescent, pro-inflammatory signals are released to recruit immune cells to clear damaged cells. However, the pro-inflammatory response can contribute to long-term normal tissue damage. Additionally, radiation-induced senescence can result in the body being unable to replace the damaged cells if the progenitor cells enter senescence, resulting in diminished tissue function [101]. The continuous inflammatory and fibrotic signals eventually lead to tissue remodeling, resulting in fibrosis in the affected tissue. The development of fibrosis is especially prevalent with defective autophagy, which was found in the fibrotic tissue of patients suffering from idiopathic pulmonary fibrosis [102].

### 1.9 Radiation-induced liver disease

When treating patients with hepatic radiation, about 6-66% of patients develop radiation-induced liver disease (RILD) within 4-8 weeks, although the range can be as broad as 2 weeks or 7 months (see Figure 4 for a model) [57, 103]. Unfortunately, RILD has no methods of prevention or cure due to the poorly understood mechanisms of RILD development. Despite the trade-offs, radiotherapy has been shown to perform more effectively than other therapies, such as TACE. RILD can be divided into acute and chronic phases. The pathogenesis of RILD is illustrated in figure 4.

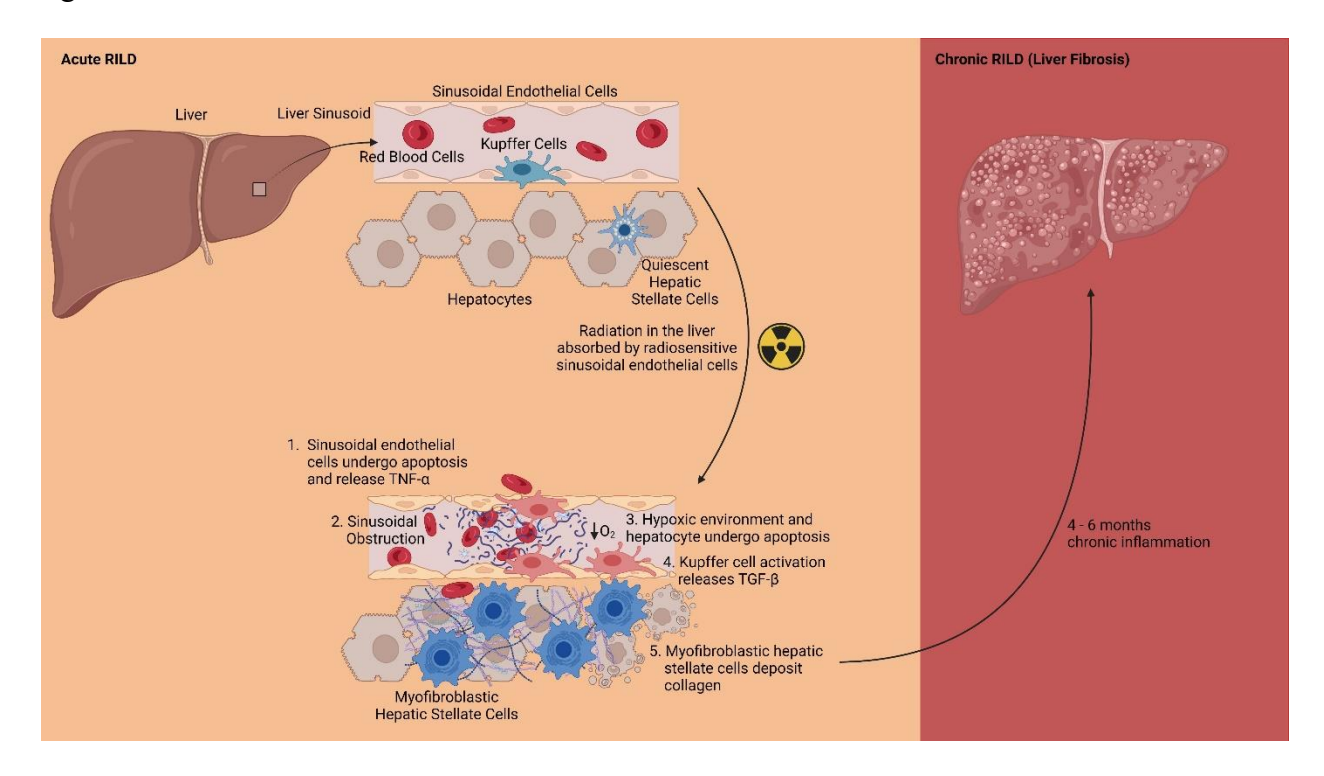


**Figure 4: Pathogenesis of RILD.** Acute RILD occurs when sinusoidal endothelial cells absorb radiation and undergo apoptosis, releasing TNF- $\alpha$ . The breakdown of sinusoidal endothelial cells releases red blood cells out of the vessels, triggering fibrinogen conversion to fibrin, which blocks blood flow, known as sinusoidal obstruction. The occlusion of blood vessels decreases oxygenation downstream, creating a hypoxic environment resulting in hepatocyte apoptosis and inflammation. TNF- $\alpha$  and inflammation activate Kupffer cells, which release TGF- $\beta$ , recruiting and activating quiescent hepatic stellate cells into

myofibroblastic hepatic stellate cells. Myofibroblastic hepatic stellate cells deposit collagen, leading to liver fibrosis in the chronic stages of RILD.

### 1.9.1 Acute phase

Early stages of RILD include tissue and molecular damage by radiation and ROS, prompting an inflammatory response to the region of injury [104]. The apoptosis of sinusoidal endothelial cells is one of the main events in RILD, resulting in the disruption of microcirculatory blood flow. The interruption to blood flow causes damage to hepatocytes, forms clots in the central vein and hepatic sinusoids, and deposits fibrin in the liver. The congested liver environment becomes hypoxic, which leads to more apoptotic events and liver dysregulation [105]. Additionally, this stage is accompanied by hepatocellular death due to the radiation-induced release of TNF- $\alpha$  by Kupffer cells, which sensitizes hepatocytes to radiation-induced apoptosis [106]. In response to liver injury, quiescent hepatic stellate cells differentiate into activated myofibroblasts. This is believed to take place through mTOR suppression by AMPK phosphorylation and proliferates to compensate for the large-scale deaths of hepatocytes [107].

## 1.9.2 Chronic phase

As the primary collagen-producing cells in the liver, activating myofibroblastic hepatic stellate cells is a crucial trigger for **radiation-induced liver fibrosis (RILF)** [51]. The increase and activation of TGF- $\beta$ 1 post-radiation activate profibrotic pathways that result in collagen deposition, the inhibition of fibrin catabolism, and extracellular matrix (ECM) remodeling, promoting radiation-induced liver fibrosis. Liver fibrosis marks the chronic phase of RILD.

### 1.9.3 Modelling chronic RILD in mice

A preliminary analysis of H&E stains of 10Gy irradiated mouse liver after 6 months was conducted by a pilot study in mice by a clinically trained pathologist, which found radiation damage in the liver, as shown in figure 5. This mouse model found key pathological hallmarks of RILD, such as patchy sinusoidal dilatation, fibrin deposition, and hemorrhage, which are all signs of veno-occlusive disease. Sinusoidal endothelial cells are very radiosensitive; thus, the liver microvasculature is easily disrupted. When red blood cells are exposed to the environment outside vessels, fibrins accumulate, resulting in sinusoidal obstruction [105]. Signs of an inflammatory reaction to the radiation are evidenced by inflammatory cell infiltration in the liver parenchyma and liver periportal. Sinusoidal endothelial cells release TNF- $\alpha$  as they undergo apoptosis, triggering a response from Kupffer cells. Damage to sinusoidal endothelial cells disrupts blood flow in the liver, depriving hepatocytes of oxygen and creating a hypoxic environment unsuitable for hepatocytes. Consequently, hepatocytes also undergo apoptosis, which was directly observed or inferred with hepatocytes with pyknotic nuclei, which is the permanent condensation of chromatin observed during apoptosis [106]. More inflammatory cytokines are released, recruiting inflammatory cells. The existing inflammatory cells in the liver, Kupffer cells, become activated and hyperplastic, indicating a reaction to radiation and inflammation. Kupffer cells release TGFβ, activating and recruiting myofibroblastic hepatic stellate cells, which will be the main contributor of collagen deposition via secretion of ECM proteins, eventually culminating into liver fibrosis in late stage RILD [103].

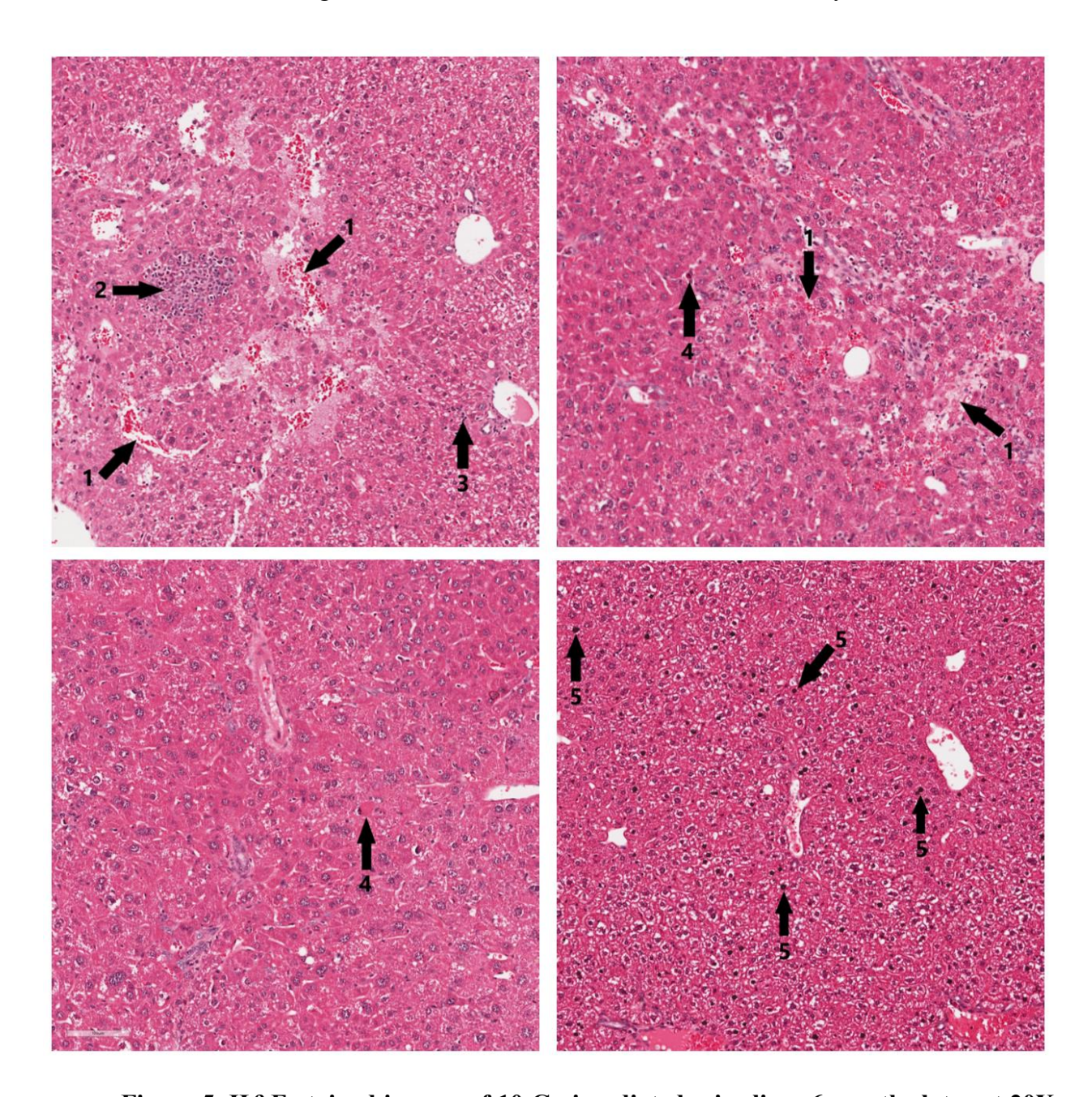


Figure 5. H&E-stained images of 10 Gy irradiated mice liver 6 months later at 20X magnification with preliminary morphological analysis by a trained pathologist. 1) Patchy sinusoidal dilation, fibrin deposition, and hemorrhage. 2) Inflammatory cell infiltration. 3) Kupffer cell hyperplasia. 4) Increased apoptotic cells. 5) Increased hepatocytes with pyknotic nuclei.

# 1.10 Molecular pathways involved in normal tissue damage by irradiation

## 1.10.1 Transforming growth factor $\beta$ (TGF- $\beta$ )

Studies have shown that an increase in TGF-\(\beta\)1 expression is followed by profibrotic events, including collagen synthesis and deposition [89]. Macrophages, Kupffer cells, hepatic stellate cells, and liver sinusoidal endothelial cells secrete TGF-\beta1 after radiation, which triggers profibrogenic pathways, recruits fibroblasts, and converts fibroblasts to myofibroblasts. TGF-\(\beta\)1 proliferates fibroblasts by promoting the transcription and release of fibroblast growth factor (FGF)-2. Furthermore, fibroblasts differentiate into myofibroblasts via the SMAD signaling pathway, activating the alpha-smooth muscle actin ( $\alpha$ -SMA) promoter. The activation of myofibroblasts triggers the synthesis of collagen-rich ECM containing  $\alpha$ -SMA, which is contractile and directly deforms the lung architecture [108]. Myofibroblasts are recruited by profibrotic signals downstream of TGF-β signaling from intrapulmonary fibroblasts, EMT, and circulating fibrocytes. In addition to driving fibrosis, TGF-β1 inhibits collagen catabolism and promotes the production and remodeling of the ECM to contain more connective proteins [89, 109]. TGF-β induces EMT through canonical SMAD signaling by repressing E-cadherin transcription with transcription repressors SNAIL, ZEB, and TWIST. E-cadherin is essential to joining epithelial cells to each other and the basement membrane [110]. Non-SMAD signaling pathways can also promote EMT through ERK activation, which promotes cytoskeletal remodeling. Downstream products of ERK, such as AP-1, also enhance SMAD transcription involved in TGF-β induced EMT [111]. These pathways, when dysregulated, also promote cancer growth and metastasis.

### 1.10.2 Epithelial-to-mesenchymal transition (EMT)

EMT is essential in embryogenesis, tissue regeneration, and cancer metastasis. Due to radiation damage, EMT occurs in many tissues and organs, including the heart, lungs, and liver. An EMT occurs when epithelial cells change to a mesenchymal cell phenotype via basement membrane degradation, to which epithelial cells are usually polarized. In the context of radiationinduced normal tissue damage, the cause of the depolarization is ionizing radiation. The phenotype shift is marked by mesenchymal cells' ability to migrate and produce more ECM components. When tissue damage occurs, EMT is a response to replace damaged cells and repair the wound. Usually, when the wound is healed, mesenchymal cells re-epithelialize. However, fibrosis is a possible complication of tissue regeneration due to malfunctioning tissue repair pathways. As a result of injury, profibrotic signals from inflammatory cells and fibroblasts trigger EMT. In the presence of ECM secreted by myofibroblasts rich in collagens and other fibers, a microenvironment forms suitable for fibrosis development. As a result of prolonged inflammatory signaling, mesenchymal cells completely leave the basement membrane and accumulate near connective tissues, where the mesenchymal cells will differentiate into a fibroblastic phenotype, thickening these connective tissues [110]. Profibrotic signals will recruit fibroblasts derived from the migrated mesenchymal cells to alveolar walls and propagate profibrotic signals, resulting in the progression of fibrosis [88]. The promotion of EMT by TGF-β has been implicated as a method of cancer metastasis. Canonical SMAD signaling pathways promote breast cancer, and SMAD signaling involving SNAIL transcription factors promotes skin carcinogenesis [112, 113]. Scientific debates also center on whether EMT is a precursor to cancer metastasis [114].

### 1.10.3 Tumor necrosis factor $\alpha$ (TNF- $\alpha$ )

TNF- $\alpha$  is an inflammatory cytokine primarily produced in the acute phase of radiation-induced injury by activated macrophages, T-cells, and natural killer cells. The production of TNF- $\alpha$  persists throughout the acute phase, driving pro-inflammatory signaling pathways and sensitizing organs to acute radiation injury, which is especially evident in the lung [115, 116]. Mice deficient in TNF- $\alpha$  are less sensitive to RILD, which points to TNF- $\alpha$  as a driver of RILD [117, 118]. The overproduction or dysregulation of TNF- $\alpha$  is also implicated in some cancers' proliferation and progression through MAPK, NF- $\kappa$ B, AP-1, and IL-8 signaling pathways [119, 120]. These pathways overlap with pathways TGF- $\beta$  activates implicated in carcinogenesis, such as MAPK and AP-1 [120].

#### 1.10.4 Interleukins

The microenvironment of the injury site dramatically affects the body's response to the injury. Interleukins greatly influence the inflammatory signals that recruit and activate inflammatory cells. IL-1, 6, and 7 are responsible for the pro-inflammatory state in RILD that recruits inflammatory cells to the injury site [121]. M2 macrophages can act as immunoregulators by secreting the anti-inflammatory IL-10, but in the presence of TGF-β, IL-4, and IL-13, M2 macrophages secrete ECM and are profibrotic [122]. IL-13 is a driver of RILD, with knockdown studies showing significantly less RILD, likely by not recruiting M2 macrophages post-radiation, reducing TGF-β levels, and not activating the expression of profibrotic genes [123].

## 1.11 Radioprotective drugs

Glucocorticoids alleviate acute radiation pneumonitis symptoms, and patients usually respond positively to corticosteroid treatments [124, 125]. This course of treatment is especially true for patients suffering from radiation pneumonitis who are showing apparent symptoms and are not at risk of or have a lung infection, in which administering corticosteroids would be detrimental to fighting the infection [126]. Prednisone and dexamethasone are examples of glucocorticoids that alleviate the symptoms of radiation pneumonitis, although their effects are not permanent, and recurrence is possible. Mouse studies suggest that administering dexamethasone prior to radiation increases survival by decreasing inflammatory cell infiltration and cytokine release [127]. Despite these benefits, glucocorticoids have significant drawbacks, such as increased blood pressure and swelling. However, NSAIDs have similar anti-inflammatory properties to steroids without these drawbacks. The consensus for treating RILD with glucocorticoids is mixed, with some studies showing that glucocorticoids have a positive effect, while others found no benefit [128-130].

# 1.11.1 Potential radioprotective properties of Salsalate

Willow bark had been used by humans medicinally centuries before the active ingredient was identified in 1826. The active ingredient is salicylate, and its role in plants is to activate the plant's defense mechanisms against plant infections. Acetylsalicylic acid, known as aspirin, is a synthetic salicylate derivative used to treat inflammatory diseases. Once ingested, aspirin is quickly broken down to salicylate by cellular esterases.

Salsalate is two salicylates joined at the ester group, where the hydroxyl groups on the second carbon and the carboxyl group of each salicylate join to form an ester bond (figure 6).

Salsalate is an NSAID used to treat rheumatoid arthritis. Like aspirin, Salsalate is quickly cleaved once ingested.

The benefits of salsalate compared to aspirin include a reduced risk of gastrointestinal bleeding [131, 132]. Aspirin has a risk for gastrointestinal bleeding mediated by the acetylation of serine-530 of cyclooxygenase-1 (COX-1), which leads to the blockade of thromboxane A synthesis and reduced platelet aggregation [133]. Additionally, gastrointestinal bleeding from the use of aspirin is also due to the disruption of the hydrophobicity of the bicarbonate mucus layer protecting the stomach lining, damage to gastrointestinal mucosal epithelial cells, and interfering with the permeability of the gastrointestinal tract [132, 134].

**Figure 6.** Chemical structure of salicylate and its dimer Salsalate. Salicylate is the active ingredient of aspirin. Salsalate is a pair of salicylate molecules joined by an ester group, which is quickly metabolized into salicylate after ingestion.

Salicylate was chosen as the active ingredient in aspirin due to its anti-inflammatory and anti-cancer properties. Aspirin is a non-steroidal anti-inflammatory drug (NSAID) and suppresses

inflammation primarily by inhibiting COX-1/2 properties [135]. Inflammation in radiation-injured tissue recruits immune cells to repair the damage but can result in chronic inflammation, leading to more tissue damage and the development of fibrosis.

Many studies have shown that aspirin and its derivatives can potentially mitigate radiation-induced injury and fibrosis. Peng et al. determined that aspirin combats fibrosis development by preventing fibroblast differentiation via the autophagy pathway, activated by inhibiting the PI3K/AKT/mTOR pathway [136]. Similarly, Salsalate slowed the progression of polycystic kidney disease by reducing mTOR activity via cAMP signaling, indicating that aspirin and aspirin derivatives target the PI3K/AKT/mTOR pathway implicated in the development of fibrosis [137]. In the liver, aspirin inhibits the activation of hepatic stellate cells, which, upon differentiating into myofibroblastic hepatic stellate cells, becomes the main contributor to collagen deposition and drives liver fibrosis by suppressing TLR4/NF-κB [138]. The suppression of NF-κB decreases collagen deposition because NF-κB transcriptionally promotes the production of P4HA2, a central enzyme in collagen synthesis [139]. This suppression is achieved by aspirin preventing the translocation of NF-κB into the nucleus, likely through the inhibition of p65 or IKK-β signaling [140]. The suppression of mTOR, P4HA2, and the activation of AMPK via cAMP signaling is also observed to have anti-cancer effects [139, 141, 142].

The possibility of mitigating radiation-induced liver damage with Salsalate appears promising, given the positive outcomes in treating liver fibrosis, which is also the late stage of RILD, and similar diseases with aspirin. Aspirin and its derivatives are most used for their anti-inflammatory properties. A rat study of aspirin's effect on acute radiation toxicity revealed that aspirin protects against radiation toxicity by reducing oxidative damage and inflammation [143].

## 1.11.2 Other potential radioprotective drugs

Histone deacetylases (HDACs) exert epigenetic control by remodeling the chromatin by removing acetyl groups from histones [144]. Deacetylation of histones closes the chromatin structure and suppresses gene expression by restricting transcription factors from accessing the DNA [145]. The dysregulation of HDACs is associated with many diseases, including fibrosis and cancer [146].

HDAC inhibitors have been approved for treating a few diseases, such as cutaneous and peripheral T-cell lymphoma, and are being investigated for applications in many other cancers [147]. HDAC inhibitors target carcinogenic pathways analogous to specific fibrotic pathways, such as pathways for cell migration [148]. The potential for therapies against radiation-induced diseases is plentiful. Vasudevan et al. found that the expression of HDAC5 promoted EMT in certain urothelial carcinoma cell lines [149]. The inhibition of HDACs suppressed EMT via non-SMAD TGF-β pathways [150]. Additionally, HDAC inhibitors prevent the differentiation of fibroblasts to myofibroblasts by blocking TGF-β signaling [151]. Travers et al. observed less cardiac fibrosis with the administration of HDAC inhibitors on mice due to the downregulation of ECM remodeling and cardiac fibroblast activation [152]. HDAC6 inhibitors prevented the production of the key inflammatory cytokines in radiation-induced injuries, IL-1 and IL-6, which construct the environment necessary for fibrosis development [153, 154]. Although a promising emerging therapeutic with the potential to treat radiation-induced injuries, HDAC inhibitors can be toxic, and the role of HDACs is not entirely understood, which can result in harmful or the opposite of the desired effect [155].

## 1.12 Anti-cancer effects of Salsalate/salicylate

Salsalate and salicylate have shown promise as anti-cancer agents for prostate and lung cancer by suppressing growth and sensitizing cancer to radiotherapy. It was demonstrated that salicylate targets cancer survival and metabolic pathways, such as the mTORC1-HIF1 $\alpha$  and AMP-activated protein kinase [142]. Furthermore, the pathways targeted to maximize cancer killing and minimize radiation-induced injury overlap and may be central to increasing the therapeutic ratio. Therefore, the anti-cancer properties of salicylate can work in conjunction with radiotherapy to eradicate cancer, while the anti-inflammatory properties of salicylate can help ensure patient survival post-treatment.

Aspirin has already been suggested as a primary therapy for reducing the risk of developing HCC. From a metabolic standpoint, MASLD animal models demonstrated that Salsalate improved homeostasis and decreased liver steatosis via mitochondrial uncoupling, using existing lipids while decreasing lipid synthesis [156]. Salsalate can also ameliorate MASLD by activating AMPK, which inhibits de novo lipogenesis, inflammation, and fibrosis while promoting fatty acid oxidation, autophagy, and mitochondrial homeostasis [157].

Inherently, these diseases share many pathways to liver disease that aspirin and its derivatives target, such as the mTOR pathway, the inflammatory cascade, the pro-fibrotic cascade, and NF-κB signaling [136-139, 158]. These pathways are also closely related to carcinogenesis, which is why aspirin, Salsalate, and salicylate have been studied for potential anti-cancer efficacy. Salicylate was shown to diminish clonogenic survival of prostate and lung cancer cell lines, with the mechanism attributed to AMPK activation by salicylate inhibiting the mTOR pathway and lipogenesis [142].

There is also evidence that salicylate enhanced the effect of radiation on prostate cancer in mouse models by blocking mTOR activity triggered by radiation, reducing biosynthesis, cell-cycle progression, and survival pathways [141]. The combined effects of salicylate and radiation are further evidenced when combined with metformin, where prostate cancer growth was reduced in mouse xenograft models and enhanced the effects of radiation while reducing the increased oxygen consumption rate associated with radiation. Additionally, this study found that Hif-1 $\alpha$  levels were reduced when prostate cancer cells were treated with a combination of metformin, salicylate, and radiation [159].

More recently, our group examined whether salicylate could improve the efficacy of the tyrosine kinase inhibitor, Lenvatinib, in HCC, especially from MASH. This study found synergistic suppression of HCC cells in vitro with the drug combination of salicylate and Lenvatinib. The drug combination suppressed the mTOR and MAPK pathways and angiogenesis. The orthotopic mouse xenografts also showed improved survival in mice treated with the drug combination. In addition to the anti-cancer efficacy of the combined drug treatment, the MASH mouse model also saw metabolic improvements, such as a reduction in steatosis and fibrosis [E. Tsakiridis et al. In Review].

### 1.13 Rationale

Based on the limitations of treating advanced HCC, there is an apparent demand for improving first-line treatments for advanced non-viral HCC. The radioprotective properties of Salsalate could improve the therapeutic ratio of radiotherapy [136-138]. Radiotherapy is currently a second-line therapy for treating HCC due, in part, to complications associated with this treatment modality. The extensive vascularization and sensitivity of sinusoidal endothelial cells to radiation

often results in RILD [104]. RILD occurs frequently, drastically reducing the efficacy of radiotherapy for combating HCC. This is especially difficult due to the frequently large size of HCC nodules, requiring larger fields of radiotherapy, thereby increasing the amount of radiation absorbed by the surrounding normal tissue. Salicylate may mitigate RILD and improve the therapeutic ratio of the treatment, possibly enabling the delivery of higher doses of radiation with reduced toxicity.

Furthermore, salicylate could sensitize HCC cells to radiotherapy, similar to what was observed in prostate and lung cancer cells [141, 142, 159]. Previous work from our group shows that salicylate also directly combats HCC by suppressing HCC proliferation via AMPK suppression of mTOR [141, 142, 159]. Therefore, the possibility of a salicylate-radiotherapy combination is based on an improved cell response to radiation as a result of salicylate-induced sensitization, while surrounding normal tissue is also protected by salicylate from radiation toxicity.

Additionally, the possibility of combining Salsalate and radiotherapy with the first-line systemic therapy, Lenvatinib, presents the possibility of a three-pronged attack against HCC. Lenvatinib inhibits tyrosine kinases, such as VEGFR, PDGFR, EGFR, and FGFR, reducing survival and angiogenesis via MAPK suppression [68]. Targeted radiotherapy combats HCC with ionizing radiation, breaking the chemical bonds between essential cellular components, inducing senescence, apoptosis, and potentially inducing a localized immune response, while Salsalate protects the liver and the surrounding tissue from radiation toxicity [138]. Both Salsalate and Lenvatinib are expected to positively affect the tumor microenvironment, increasing treatment efficacy.

Based on compelling evidence from previous works on HCC and other cancer types, both within and outside of our group, we were prompted to investigate whether Salsalate could mitigate

radiation-induced liver damage and whether the incorporation of Salsalate could enhance the responses to radiotherapy and Lenvatinib in HCC models.

# 1.14 Hypothesis

Salsalate can improve the efficacy of standard therapies in unresectable HCC by reducing radiation-induced fibrosis and enhancing the anti-tumor efficacy of radiotherapy and Lenvatinib.

# 1.15 Aims

#### The specific aims of this work were to:

- 1. Investigate the potential radioprotective effects of Salsalate on normal liver tissue.
- 2. Assess the anti-tumor efficacy of Salsalate alone and in combination with radiotherapy and Lenvatinib.
- 3. Begin an early analysis of the mechanism of action of salicylate.

McMaster University – Medical Sciences

MSc. Thesis – Simon Wang

Chapter 2 – Methodology

# 2.1 Materials

Materials were purchased from Fisher Scientific (Toronto, ON), Sigma Aldrich (Oakville, ON), and BioRad (Mississauga, ON).

## 2.1.1 Antibodies

Antibodies were purchased from Cell Signaling Technologies and Abcam.

Table 2. List of antibodies used for immunoblotting and immunohistochemistry

Primary	Primary	Primary	Application	Secondary	Secondary	Secondary
antibody	antibody	antibody		antibody	antibody	antibody
	manufacturer	dilution			manufacturer	dilution
	and catalog				and catalog	
	number				number	
p-p70	9205S	1:1000	WB	Anti-	7074S	1:10000
p70	9202S	1:1000		rabbit		
p-ERK	4370S	1:1000		IgG,		
ERK	4695S	1:1000		HRP-		
GH2AX	2577S	1:500		linked		
ETS1	14069S	1:500		antibody		
ATF3	33593S	1:500				
РНН3	9701S	1:1000				
PLK1	4513S	1:1000				
p-S6rp	9234S	1:1000				
S6rp	2217S	1:1000				
Hif-1α	14179S	1:500				
p27	3698S	1:500				
p21	2947S	1:500				
Cyclin D1	2978S	1:500				
CDK4	12790S	1:1000				
β-actin	5125S	1:1000				
β-tubulin	86298S	1:1000		Anti-	7076P2	
				mouse		
				IgG,		
				HRP-		

MSc. Thesis – Simon Wang

				linked	
				antibody	
GAPDH	2118	1:1000		Anti-	
TNF-α	11948T	1:1000		rabbit	
TGF-β	Ab215715	1:1000		IgG,	
IL-6	12912T	1:1000		HRP-	
CD3	ab16669	1:1000		linked	
NF-κB	8242T	1:1000		antibody	
α-SMA	ab5694	1:1000			
Col1A1	72026T	1:1000			
F4/80	70076S	1:1000 /	WB / IHC		
		1:200			

# 2.2 Animal radioprotection experiments

C57BL/6 mice were chosen due to their widespread use in studies investigating the effects of radiation on mice and their availability. Furthermore, this strain is considered "fibrosis prone" and develops fibrosis in response to radiation-induced injury. Female C57BL/6 mice were chosen for their closer timeline to radiation-induced diseases in humans than male C57BL/6s [160].

A total of 48 mice were used. 20 were reserved for the survival experiment and 28 for analysis of acute vs chronic effects of RILD. A total of 16 controls, 10 receiving control diet and 6 receiving salsalate diet, were used between the 2 experiments.

#### 2.2.1 Effect of SAL on survival after RILD induction

The female C57BL/6 mice used for the survival analysis are outlined in Table 3 in green, with those highlighted in blue as part of both the survival analysis and histological assessment. All treatments began when the mice were 12 weeks old. The mice in the radiation and radiation with Salsalate groups were treated with two fractions of 10 Gy for 20 Gy of radiation. Based on the

compilation of previous literature by Dabjan et al. (2016) and a pilot study we conducted, testing multiple doses of radiation, 20 Gy in 2 fractions yielded the most desirable outcomes [160]. The salsalate drug diet began 7 days prior to radiation. Dexamethasone (5 mg/kg), an anti-inflammatory drug, was administered once post-radiation to increase the likelihood of survival immediately following radiotherapy without affecting subsequent molecular responses [161].

#### 2.2.2 Acute vs chronic RILD / Benefits of SAL

Mice were divided randomly into four groups: 6 each in control and Salsalate, and 8 each in radiation alone and radiation with Salsalate, with irradiated mice further subdivided into an acute and chronic group of four mice for each treatment group. Furthermore, the mice in the radiation and radiation with Salsalate groups were treated with one fraction of 10 Gy. All treatments began when the mice were 16 weeks old in an effort to increase the likelihood of animals reaching the desired endpoint.

**Table 3. Animal treatment groups** 

Group	Treatment	Purpose	Mice Used	Duration
Control	No treatment	Baseline of normal mice	10	6 months
Salsalate	Treated with Salsalate	Baseline of Salsalate treated	6	6 months
	infused in rodent diet	mice		
Radiation	Treated with 10 Gy	Acute effects of irradiated	4	3 months
	radiation	mice		

		Chronic effects of irradiated	4	6 months
		mice		
	Treated with 2x10 Gy	Survival of irradiated mice	8	6 months +
	radiation			
Radiation	Treated with 10 Gy	Acute effects of irradiated	4	3 months
+	radiation and Salsalate	and Salsalate treated mice		
Salsalate	infused in rodent diet	Chronic effects of irradiated	4	6 months
		and Salsalate treated mice		
	Treated with 2x10 Gy	Survival of irradiated and	8	6 months +
	radiation and Salsalate	Salsalate treated mice		
	infused in rodent diet			

<sup>\*</sup>In yellow, mice were used for histological assessment; in green, mice were used for survival analysis; and in blue, mice were used for histological evaluation and survival analysis.

# 2.2.3 Liver radiation delivery

Radiation delivery was administered after dedicated radiation simulation was performed using wax mouse phantoms, followed by appropriate dosimetry calculations by the Juravinski Cancer Centre radiotherapy physics team.

Radiation was delivered with a clinical linear accelerator (Varian Truebeam). Mice were anesthetized with gas anesthesia using isoflurane for the duration of the radiation delivery. Mice were radiated 6 at a time, using a plexiglass box divided into 6 corrals. The field size is 2x22 cm, and the mice were aligned to ensure that the liver (upper abdomen and lower thorax) would receive radiation. The mice were radiated so that half the dose was delivered anteriorly and posteriorly at

51.3 mu/cGy and 52.3 mu/cGy, respectively, using 6 MV. The radiation dose was confirmed with a mouse-sized phantom containing thermoluminescent dosimeters that were irradiated alongside mice in the corral and were analyzed by Dr. Thomas Farrell (Department of Medical Physics) and the dosimetry team of the Juravinski Cancer Centre. After radiation treatment, animals were supported by placing liquid gels and heating pads in the cages. The mice were monitored for the duration of the experiment for weight changes and diet consumption. 15% weight loss prompts the administration of 1 mL of 10% saline solution. 20% weight loss, severe symptoms, or physical signs indicating suffering require close monitoring or euthanasia.

#### 2.2.4 Rodent diet

Salsalate was administered through the rodent chow diet at 2.5 mg/kg of Salsalate 1 week before treating the mice with radiation and for the duration of the experiment after radiation. The custom 2.5 mg/kg Salsalate Teklad diet was made by Envigo using Salsalate manufactured by Cayman Chemicals. The amount of rodent diet consumed by each cage was weighed and used to calculate the approximate average Salsalate concentration per mouse.

In the survival study, mice were sacrificed as they met the definitions of endpoint and lasted for approximately 6 months. In the acute vs. chronic study, 3 months post-radiation treatment, the acute mouse groups outlined were sacrificed, and the chronic group was at 6 mo.

These time points were determined because chronic hepatic fibrosis usually develops after 6 months [160].

#### 2.2.5 Euthanasia & tissue collection

After mice reach the endpoint, a single dose of ketamine/xylazine is injected peritoneally, and cervical dislocation is performed. The lung, heart, and liver were extracted and preserved by formalin-fixed paraffin-embedded (FFPE). Formalin fixation lasted 72 hours before being transferred into 70% ethanol for long-term preservation. Each FFPE organ was sectioned and stained with H&E and PSR stains to evaluate tissues for radiation-induced damage and fibrosis. Blood was also taken from the mice before radiation, 3 months, and 6 months after radiation treatment by tail nick to observe the responses to radiation injury.

## 2.3 Histology

FFPEs are sectioned into 5-micrometre sections. The slides can be left to air-dry for 24-48h or incubated in a section dryer at 60°C for 30 minutes.

After deparaffinization, dehydration, and antigen retrieval, the primary antibody is incubated overnight in a humidity chamber. Primary antibody dilutions can be found in Table 2. Slides are then washed with 1X Tris-buffered saline-Tween-20 (TBST) (Tris, NaCl, HCL, and Tween 20), and the secondary antibody is incubated for 30 minutes. Slides are then washed twice with 1X TBST and streptavidin (1:50 dilution) for 15 minutes. Slides are then washed one time, each with 1X TBST and dH<sub>2</sub>O. Stains were visualized with NovaRED for 3 minutes before being thoroughly washed with dH<sub>2</sub>O. Hematoxylin counterstaining was applied for ~10 seconds and subsequently washed with dH<sub>2</sub>O until the wash was clear. After counterstaining, the slides are dehydrated again and washed with xylene before being mounted with a large drop of Permount Mounting Medium (Fisher Scientific # SP15-100) and left to dry overnight. Stain analysis includes visual quantification and digital quantification.

PSR stains are also performed by the McMaster Immunology Research Centre (MIRC) Histology Lab to observe the pattern of collagen deposition in the collected tissues.

H&E staining was used to identify morphological features and anomalies for further analysis.

# 2.4 Digital histological quantification

To digitally quantify histological analyses, 10 high-power fields are taken at random and quantified. For F4/80 IHC stains, QuPath 0.5.1 was used for visual quantification by counting, and the results are expressed as the average number of macrophages. For PSR stains, ImageJ was used for area analysis by color deconvolution and thresholding, expressing the result as the percentage of positive PSR staining.

### 2.5 Cell lines

For the in vitro study of liver cancer, human HCC cell lines Hep3B, HepG2, and PLC/PRF/5, as well as Sk-Hep-1, a human liver adenocarcinoma cell line, were used.

Hep3B, HepG2, SK-Hep1, and PLC/PRF/5 were cultured in EMEM (Eagle's minimum essential medium) (Wisent Bio Products, Saint-Jean-Baptiste, CAN, Cat # 320-026-CL) with 10% fetal bovine serum (Wisent Bio Products, Cat # 098150) and 1% antibiotic-antimycotic. All cells were cultured at 37°C at 5% CO<sub>2</sub> and passaged according to cell confluence with the use of 0.25% trypsin-EDTA solution (Wisent Bio Products # 325-043-CL).

#### 2.5.1 Cell RT

Cells were irradiated by linear accelerators 100 cm overhead, with a 1 cm thick Vaseline bolus covering the plates.

## 2.6 Clonogenic assays

Clonogenic assays were performed with Hep3B, PLF/PRF/5, SK Hep1, and HepG2 cells by seeding 1000-2000 cells per well in a 12-well plate and treating them 6 hours later after cells had adhered to the plate, with sodium salicylate (Millipore Sigma # 567639) and Lenvatinib mesylate (Cayman Chemicals # 29832) infused in EMEM media, with 2-8 Gy radiation 24 hours after drug treatment. When the cells reach 80-90% confluence in the control conditions, the experiments end with 10 minutes of formalin fixation to the plates and are subsequently stained with crystal violet for 10 minutes. Excess crystal violet is washed with water until the background is clear and left to dry overnight. Plates are counted for the number of colonies that formed., with colonies defined as a cluster of cells consisting of more than 50 cells.

## 2.7 Proliferation assays

Proliferation assays were performed with Hep3B, PLF/PRF/5, and SK Hep1 cells by seeding 500 cells per well in a 96-well plate and treating them 6 hours later, after cells have adhered to the plate, with sodium salicylate (Millipore Sigma # 567639) and Lenvatinib mesylate (Cayman Chemicals # 29832) infused in EMEM media, with 2-8 Gy radiation 24 hours after drug treatment. When the cells reach 80-90% confluence in the control conditions, the experiments end with 10 minutes of formalin fixation to the plates and are subsequently stained with crystal violet for 10

minutes. Excess crystal violet is washed with water until the background is clear and left to dry overnight. To analyze the proliferation assay,  $100 \, \mu L$  of  $0.05 \, M \, NaH_2PO_4$  is pipetted into every well for  $10 \, minutes$ . The plate is then quantified by a spectrophotometer, measuring  $560 \, nm$  wavelength absorbance. Results are organized in Excel and analyzed using GraphPad PRISM.

#### 2.8 Immunoblotting

For immunoblot analysis of triple therapy, 500,000 Hep3B cells are seeded per well in 3 wells of a 6-well plate and treated 6 hours later, after cells have adhered to the plate, with sodium salicylate (Millipore Sigma # 567639) and Lenvatinib mesylate (Cayman Chemicals # 29832) infused in EMEM media, with 2-8 Gy radiation 24 hours after drug treatment. 24 hours after radiation, the experiment is stopped with lysis buffer, collected into microcentrifuge tubes, spun down in a centrifuge, and collected the supernatant. A BCA assay is performed to normalize the protein concentration for subsequent protein expression analysis using immunoblotting. Separation gels [40% acrylamide/Bis solution, 37.5:1 (BioRad # 1610148), dH<sub>2</sub>O, 1.5 M Tris-HCL pH 8.8, 10% sodium dodecyl sulfate (SDS), 10% ammonium persulfate (APS)] are cast in 1 mm thick gel casts with 15-well stacking gels. The concentration of the gel varies from 10-15% depending on the molecular weight of the target protein.10 µg of protein is loaded into gels submerged in 1X electrophoresis buffer (Tris base, glycine, SDS, and dH<sub>2</sub>O), with 2 µg of Precision Plus Protein Dual Color Standard (Bio-Rad) for gel electrophoresis, initially at 90 V and 3.0 A for protein separation into the separation gel, and then at 110 V and 3.0 A until ladder is separated to the bottom of the gel (~90 minutes). Proteins are then transferred from the gel to PVDF transfer membranes (BioRad # 1620177) using a wet transfer apparatus in 10% methanol transfer buffer (Tris, glycine, dH<sub>2</sub>O, and 95% methanol) at 90 V for 90 minutes, submerged in ice.

After transferring proteins to the PVDF transfer membranes, 5% bovine serum albumin in 1X TBST was used to block for an hour. Primary anti-rabbit and anti-mouse antibodies were diluted at 1:1000 if sensitive or 1:500 if insensitive and incubated overnight at 4°C. Secondary antibodies were diluted at 1:10,000 and applied for an hour after removing the primary antibody, and the membranes were washed 3x for 10 minutes with 1X TBST. Following secondary antibody incubation, membranes were washed 3x for 10 minutes with 1X TBST before detection. The enhanced chemiluminescence substrate was used for easily visualized proteins, and for weaker signals, the super signal substrate was used. Membranes were visualized with a chemiluminescence imager, and the blots were analyzed with ImageJ.

#### 2.9 Mouse xenograft experiments

Female NRG mice are xenografted with 2 million Hep3B cells injected subcutaneously in the right flank and grown to 150 mm<sup>3</sup> in a 200µl 1:1 EMEM:Matrigel solution when all treatments begin. Tumors were measured using a caliper throughout the experiment

Tumors were measured with a caliper, taking the length of the longest side and the weight of the perpendicular side. The volume is calculated with the formula  $V = \frac{1}{2} \times (\text{length} \times \text{width}^2)$ .

Salsalate treatment with radiation also starts at 150 mm<sup>3</sup> with radiation 4 days later. Salsalate is administered through diet at 300 mg/kg. The endpoint tumor size was set at 2500 mm<sup>3</sup>, with the related health endpoints including 20% weight loss, tumor ulceration, impaired breathing, failure to right itself, and failure to respond to touch. At the endpoint, the tumor was extracted and weighed. Half the tumor was fixed, and the other half was frozen.

Radiation was administered conformally to the xenografted tumor. Mice were anesthetized with isoflurane and placed in a conical restraining container, also receiving isoflurane, to position

the tumor for conformal radiation by a clinical LINAC at 90° and 270°. A wax bolus is also positioned over the radiation field as a bolus.

Endpoint tissue collections and preservation were performed as described above. Blood is also collected with cardiac puncture.

#### 2.10 Statistical analysis

Log-rank tests (Mantel-Cox) were performed to analyze Kaplan-Meier survival curves for significant differences between groups.

The tissue analysis consisted of 3-6 unpaired groups analyzing the difference in macrophage number per field or the percentage of collagen deposition per field, which is both a single factor. Therefore, a one-way ANOVA is the most applicable statistical test, with Tukey's highest significant difference test used for the multiple comparison procedure.

Similarly, the quantification of immunoblotting markers in section 3.1.3 was analyzed with a one-way ANOVA followed by Tukey's highest significant difference for multiple comparisons because each marker was a single unpaired factor for 3-6 groups.

For the analysis of proliferation and clonogenic assays, a two-way ANOVA was used with Tukey's highest significant difference test for multiple comparisons. This test was chosen because more than two unpaired groups were analyzed for two factors: the type of drug treatment (no drug treatment, salicylate, Lenvatinib, and salicylate-Lenvatinib combination) and radiotherapy.

The immunoblotting results in 3.2.7 and 3.2.8 were subjected to statistical analysis because of the low number of repeats and the fact that these are preliminary results meant for a first look into the mechanisms behind salicylate, radiotherapy, and Lenvatinib treatment.

MSc. Thesis – Simon Wang

Outlier analysis is also performed using GraphPad PRISM. Drug synergy was determined using SynergyFinder 3.0 with the highest single agent (HSA) as the reference model [162]. HSA quantifies the excess inhibitory response over the highest single drug response from proliferation results. SynergyFinder 3.0 also generates a dose-response matrix and a synergy heat map for each treatment combination, with scores based on predicted drug interaction. Synergy scores of < -10 are antagonistic, scores between -10 and 10 are additive, and scores > 10 are synergistic.

McMaster University – Medical Sciences

MSc. Thesis – Simon Wang

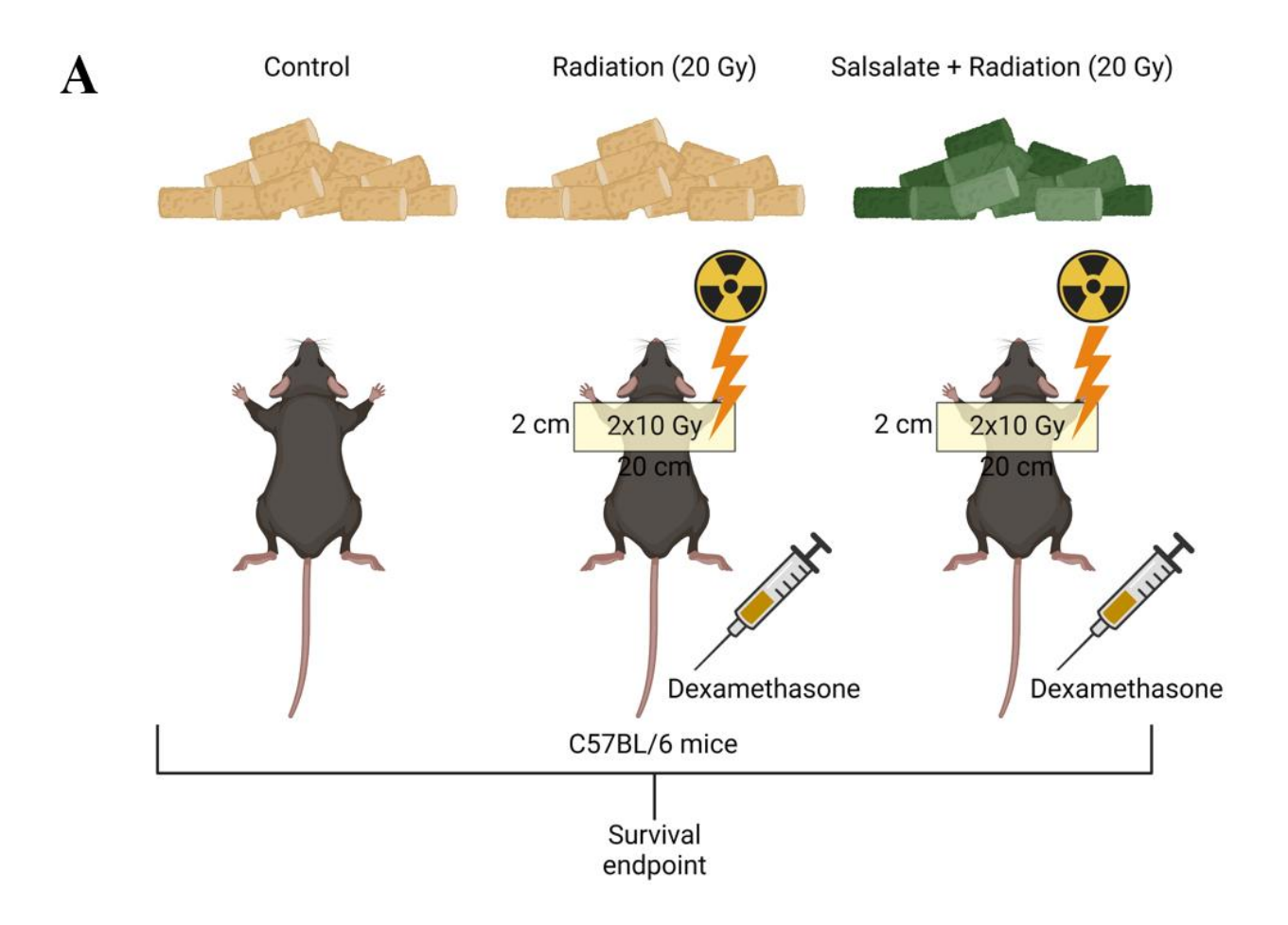
Chapter 3 – Results

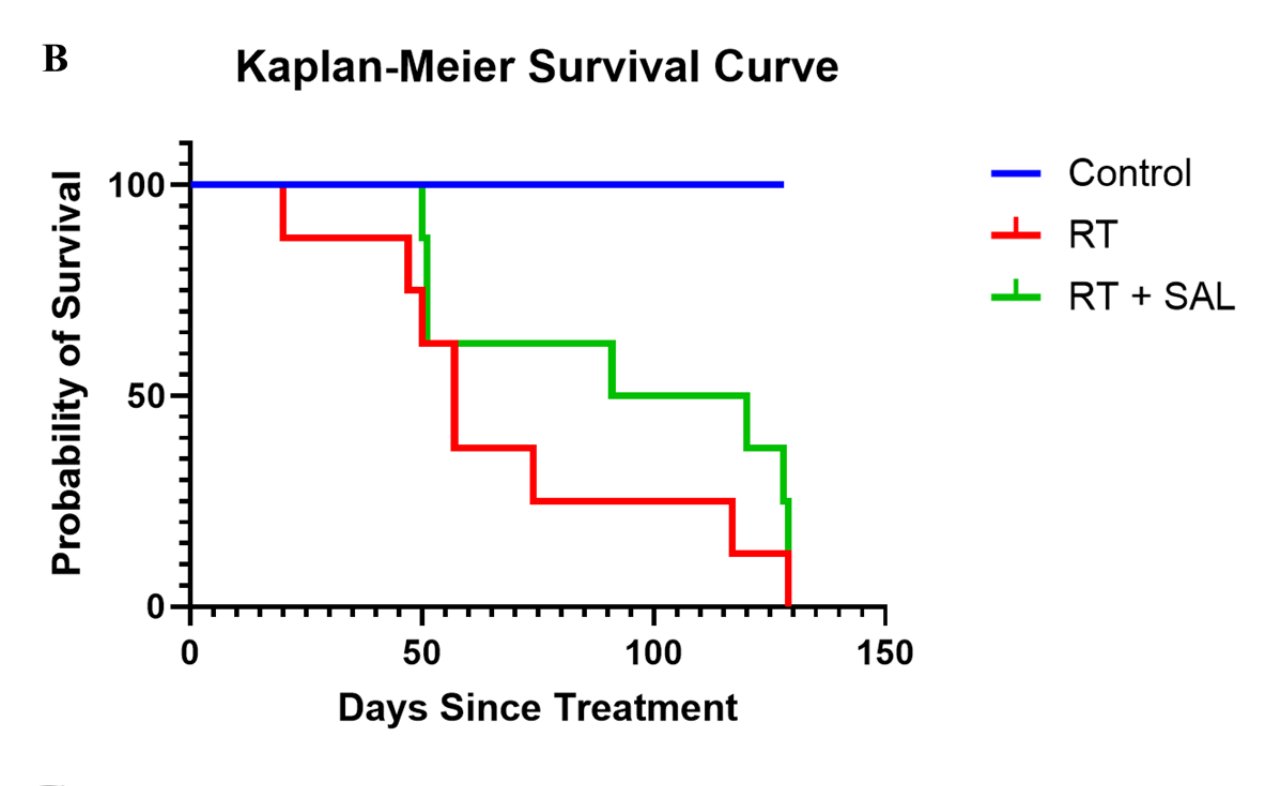
#### 3.1 Normal tissue protection by Salsalate

Given the anti-inflammatory activity of Salsalate and earlier data on the potential of aspirin to provide normal tissue cytoprotection from radiation, Salsalate was examined in this study to see if it could ameliorate the toxicity of liver radiotherapy, influence animal survival after abdominal radiotherapy, inhibit liver fibrosis, and limit inflammatory cell infiltration.

#### 3.1.1 Animal survival

To assess the potential radioprotective effects of Salsalate, a cohort of normal female C57BL/6 mice at 12 weeks old were pre-treated with Salsalate via diet at 300 mg/kg before receiving 20Gy of high-dose lower thorax and upper abdomen radiotherapy (which included the entire liver) 7 days after initiation of drug treatment, as seen in figure 7A. Figure 7B illustrates the K-M survival curves of animals in each group, and Figure 7C shows the animal median survival in two irradiated groups. Irradiated mice had a worse median survival at 57 days post-radiation compared to irradiated mice treated with Salsalate, with a median survival of 105.5 days. A Mantel-Cox log-rank test revealed that the control, irradiated, and irradiated mice treated with Salsalate had significantly different survival curves (p = 0.0202).





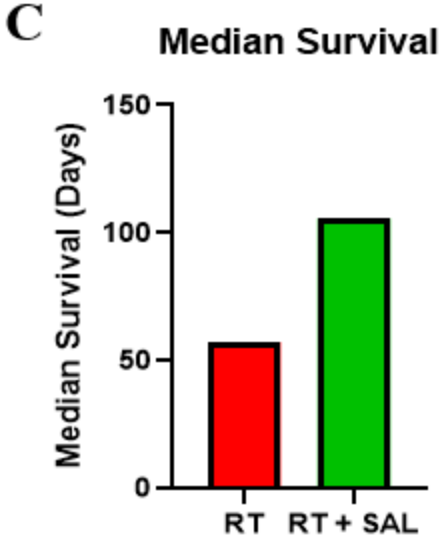


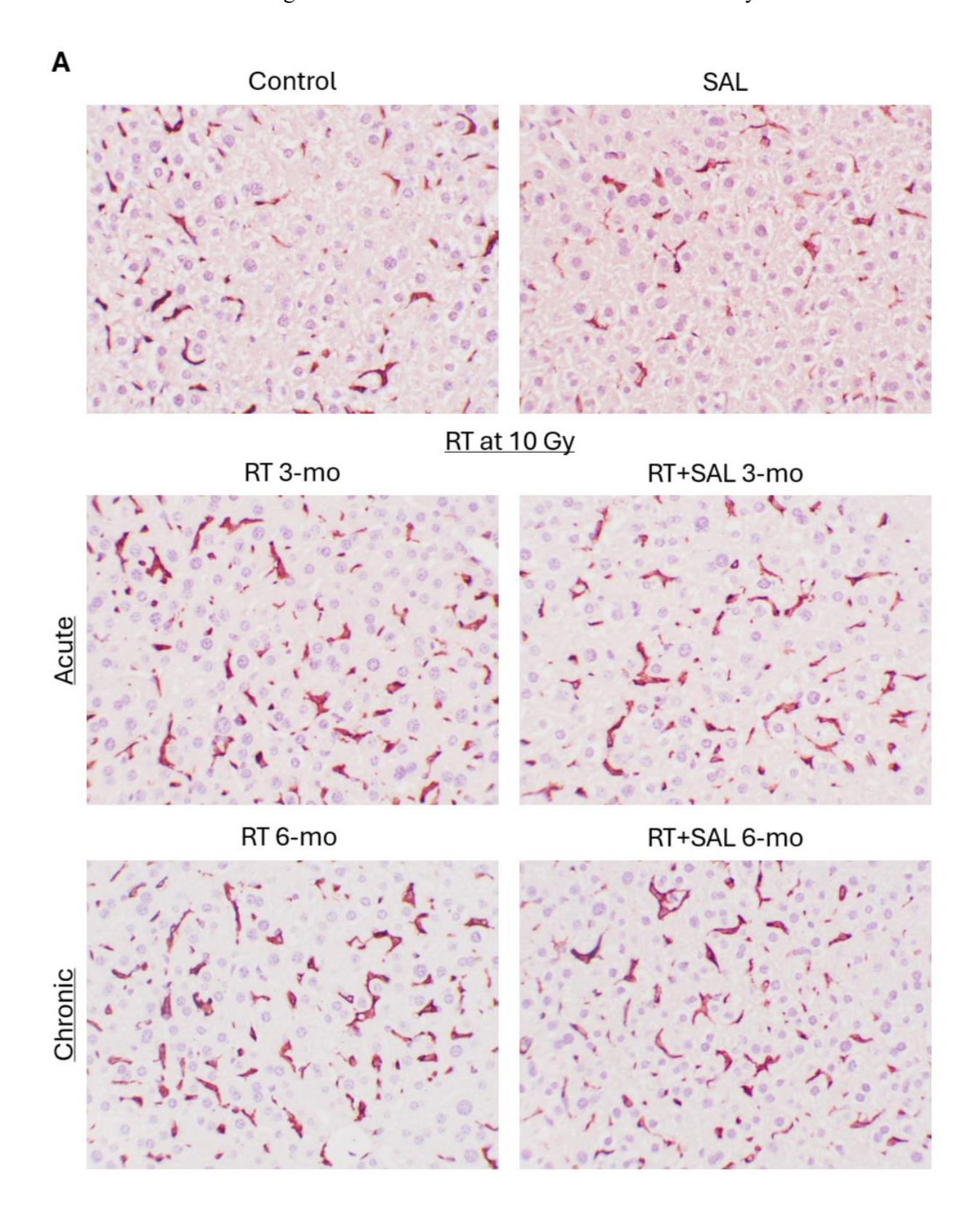
**Figure 7.** Effects of Salsalate therapy on survival of animals receiving whole liver radiotherapy. A) Infographic of C57BL/6 mice RT + SAL survival experimental design. B) Kaplan-Meier survival curves of control (n = 4), RT (n = 8), and RT + SAL (n = 8) animals. Log-rank (Mantel-Cox) test: p= 0.0202. C) Median survival time of RT and RT + SAL mice. The RT and RT + SAL groups received whole liver (lower thorax and upper abdomen) radiotherapy (20 Gy). Salsalate-treated animals received Salsalate (incorporated into their chow diet), starting 1 week before radiation and continuing throughout the experiment. The irradiation alone (RT) group received 20 Gy radiotherapy delivered in 2 fractions of 10 Gy each in consecutive days and a normal chow diet similar to control

animals, with no other intervention. All mice that received radiation were treated with a single dose of dexamethasone immediately after RT through an intraperitoneal injection. RT = radiation, SAL = Salsalate.

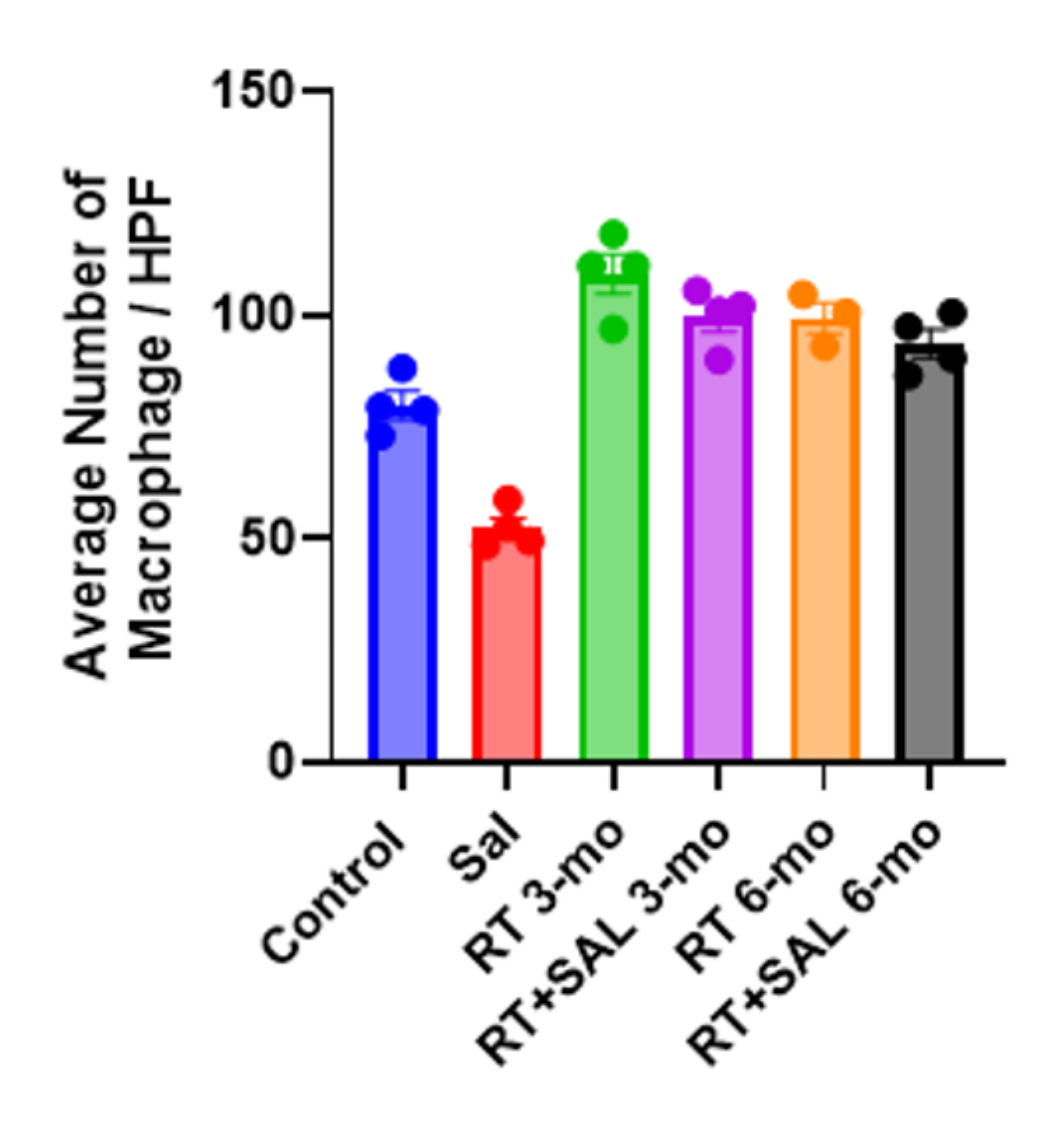
#### 3.1.2. Liver morphology and immune cell infiltration

Next, we aimed to analyze the effects of irradiation and Salsalate therapy on liver tissue morphology and immune cell infiltration. We examined the livers of animals collected in the survival experiments described above and tissue from animals from another cohort where RT and RT+SAL animals received only 10Gy of liver irradiation. In those experiments, RT and RT+SAL animals were sacrificed at two different time points of 3 and 6 months after treatment initiation in order to evaluate the progressive effects of irradiation on liver morphology and the potential protective effects of Salsalate during that period.

IHC analysis of macrophages revealed an increase in macrophages 3 and 6 months after irradiation in mice that received 10 Gy of liver irradiation. However, macrophages did not decrease with the treatment of Salsalate at either endpoint. In contrast, mice radiated with 20 Gy had a more significant increase in average macrophage number in the liver, and macrophages were significantly decreased with the treatment of Salsalate. Further, macrophages in mice radiated with 20 Gy were observed to be morphologically different from those in the control group and those treated with Salsalate before radiation.



### B Average Number of Macrophage in Mouse Liver



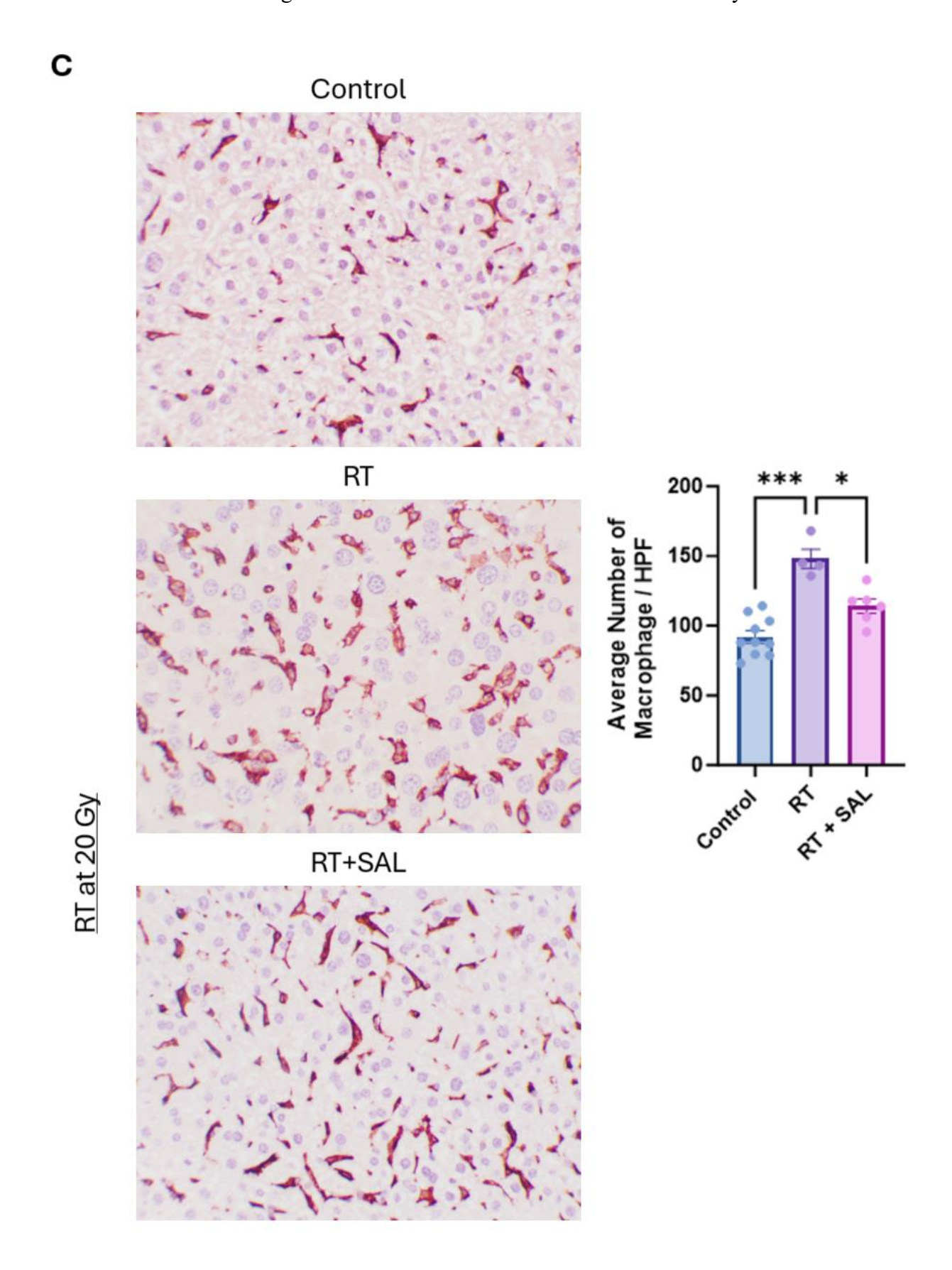
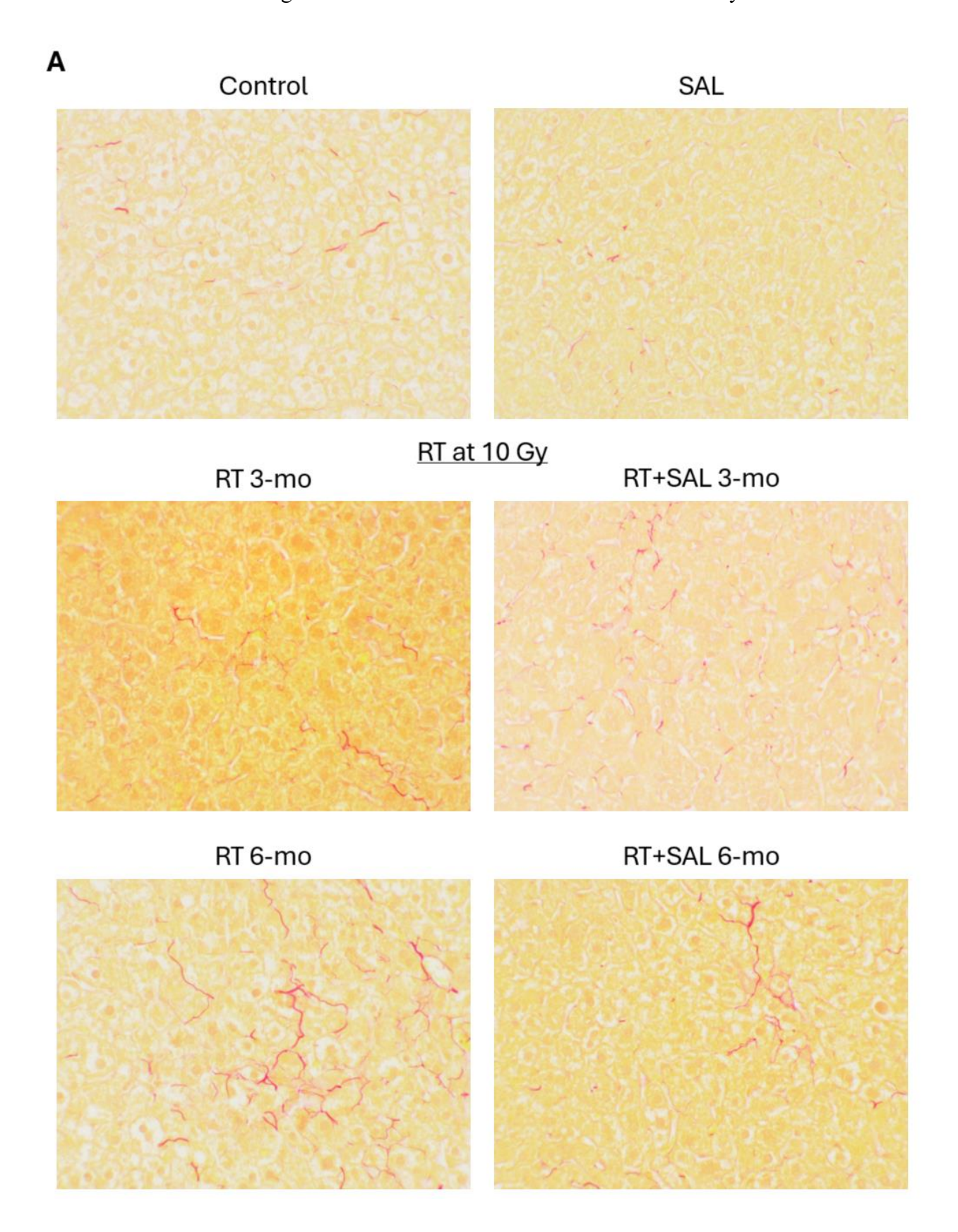


Figure 8. Representative images of macrophage (Kupffer) cells in mice liver in response to Salsalate and radiation. A) HPF representative images of IHC stain for F4/80 in mouse livers irradiated with 10 Gy and treated with Salsalate in the acute 3-month period and the chronic 6-month period. B) Quantification of macrophage number in 10 Gy irradiated mice livers from 10 random HPF of F4/80 IHC stains per sample. C) IHC stains for F4/80 in mouse livers irradiated with 20 Gy and treated with Salsalate for 6 months. D) Quantifying macrophage number in 20 Gy irradiated mice livers from 10 random HPF of F4/80 IHC stains per sample. IHC stains for F4/80 stains macrophages red and visualized here the number of macrophages in the liver of mice. The quantification of macrophages was assisted by the use of QuPath. 10 HPF images were taken at random portions of the liver for quantification. \*p < 0.05, \*\*p < 0.01, \*\*\*p < 0.001, and \*\*\*\*p = < 0.0001.

## 3.1.3. Salsalate regulates fibrosis, immune infiltration, and inflammatory processes in irradiated livers

#### 3.1.3.1 Morphological analysis

PSR stain, which stains collagen red, was used on the liver to assess for liver fibrosis by quantifying the amount of collagen deposition in the liver parenchyma. In the assessment of the liver parenchyma, an increase in collagen was observed in mice at 10 Gy radiation but only significantly at the 6-month time point, with an insignificant decrease with the addition of Salsalate in the animal diet.



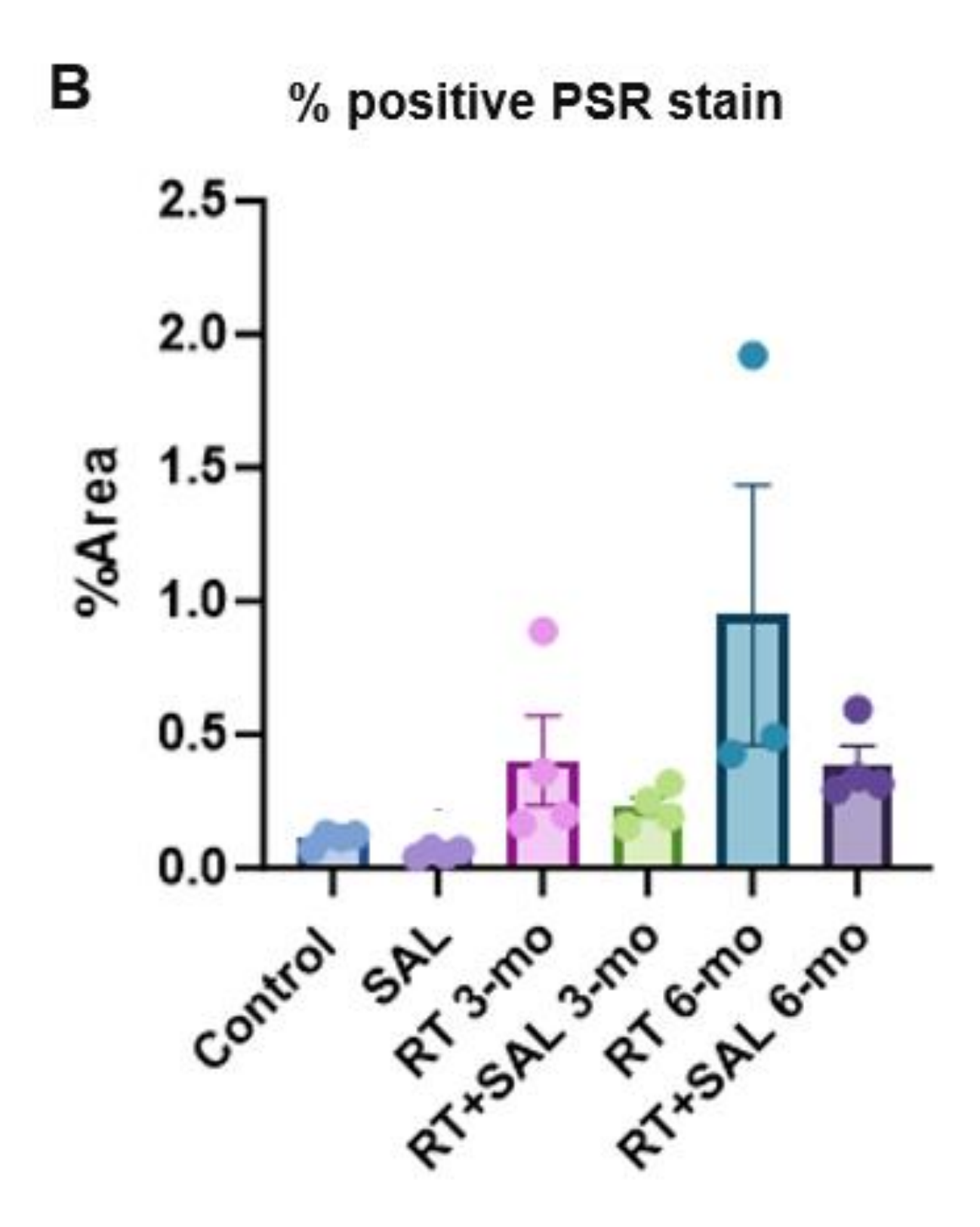


Figure 9. Effects of irradiation and Salsalate treatment on liver collagen deposition detected by PSR stain. A) Representative HPF images of mouse liver parenchyma

irradiated with 10 Gy of radiation and treated with Salsalate at the acute 3-month period and the chronic 6-month period, stained with PSR to visualize the pattern of collagen (stained red) deposition. B) Quantification of the percentage area that collagen occupied in the liver parenchyma. Quantified with ImageJ. 10 HPF images were taken at random portions of the liver for quantification. \*p < 0.05, \*\*p < 0.01.

#### 3.1.3.2 Immunoblotting analysis of liver tissue lysates.

To better understand the results obtained by the PSR stain, we performed an early analysis of fibrosis and immune cell infiltration markers with immunoblotting analysis of livers from treated animals. For that, liver lysates were generated from the second cohort of mice treated with 10 Gy radiation and Salsalate for 3 and 6 months.

IL-6 immunoblotting showed a significant increase (p < 0.01) in IL-6 in irradiated mouse liver, but Salsalate treatment in the irradiated liver did not have significantly decreased IL-6 expression. Immunoblotting analysis of liver tissue showed a trend for an increase in Col1A1 with radiation and a decrease in Col1A1 expression in irradiated mice treated with Salsalate. Further, we found that  $\alpha$ -SMA expression also significantly increased (p < 0.05) with radiation and was significantly suppressed (p < 0.01) by Salsalate in irradiated livers. NF- $\kappa$ B and CD3 expression both showed the same pattern of expression in response to radiation, with a significant increase (p < 0.05) in expression, but the addition of Salsalate treatment in irradiated liver decreased these markers insignificantly.

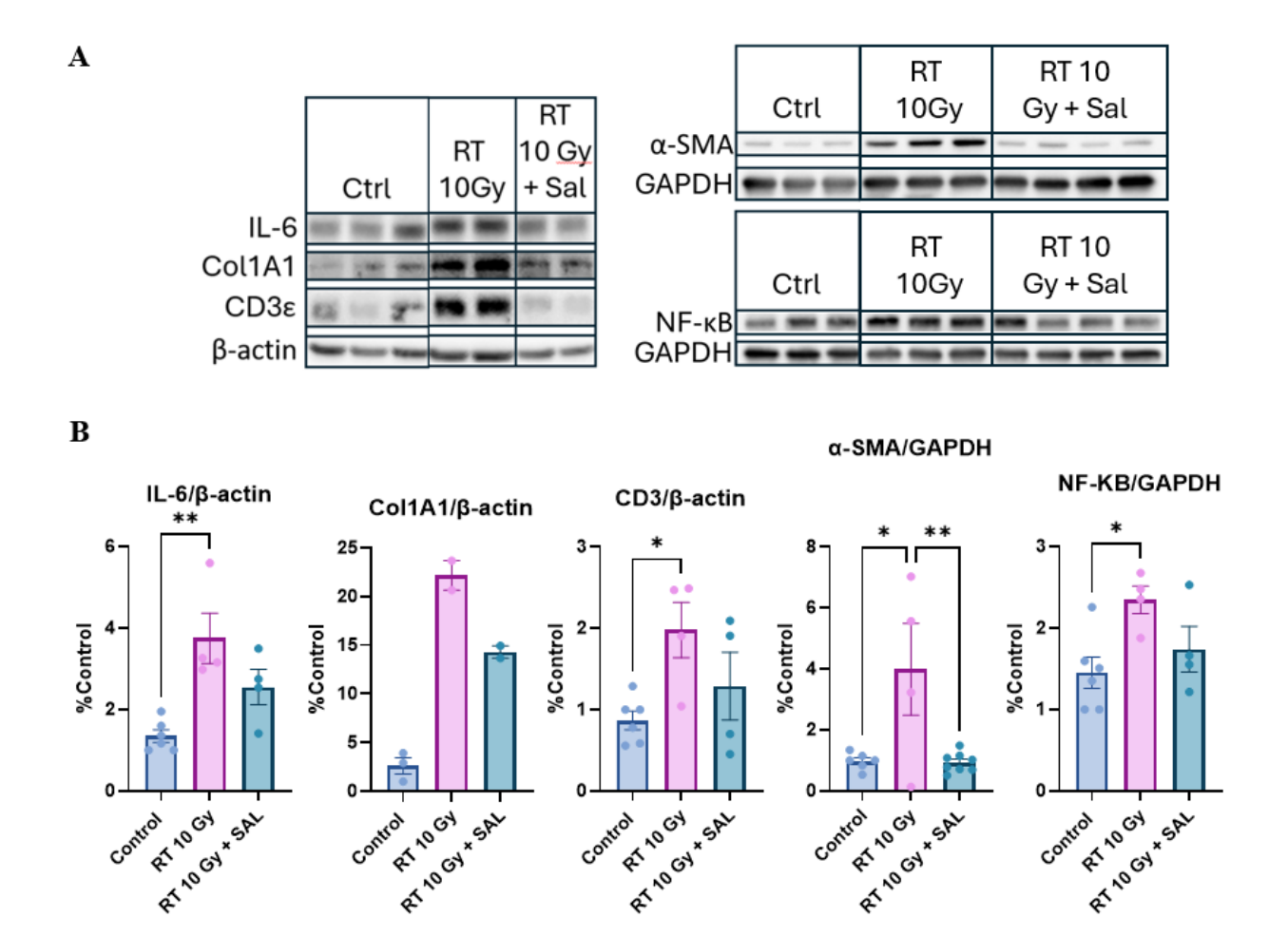


Figure 10. Key instigating proteins of RILD, IL-6, Col1A1, CD3, α-SMA, and NF-κB protein expression in mouse liver treated with radiation and Salsalate. A) Immunoblotting of IL-6, Col1A1, and CD3ε protein expression with housekeeping protein β-actin, and α-SMA and NF-κB with housekeeping protein GAPDH. B) Immunoblotting quantification of markers normalized to respective housekeeping proteins. Mouse liver extracted from mice treated with control (n = 6 in IL-6, CD3, α-SMA, and NF-κB, n = 3 in Col1A1), 10 Gy radiation (n = 4 in IL-6, CD3, α-SMA, and NF-κB, n = 2 in Col1A1), or both (n = 6 in IL-4, CD3, α-SMA, and NF-κB, n = 32 in Col1A1) for 6 months. Only markers with more than 3 datapoints were quantified. Quantified with ImageJ. \*p < 0.05, \*\*p < 0.01, and \*\*\*p < 0.001.

#### 3.2 Anti-tumor and radio-sensitizing effects of salicylate

#### 3.2.1 Salicylate drug dose-response.

When Salsalate is ingested, it is quickly hydrolyzed into 2 molecules of salicylate in the intestine. Therefore, salicylate was investigated in in-vitro experiments.

To assess the responsiveness of HCC cells to salicylate, proliferation experiments were conducted first on cells from the human HCC cell line, Hep3B. Hep3B cells were treated with salicylate doses ranging from 100  $\mu$ M to 2000  $\mu$ M for 8 days when control wells reached 80-90% confluence. Figure 11 illustrates the responsiveness of Hep3B cells to salicylate, which has an IC50 of 1071.14  $\mu$ M.

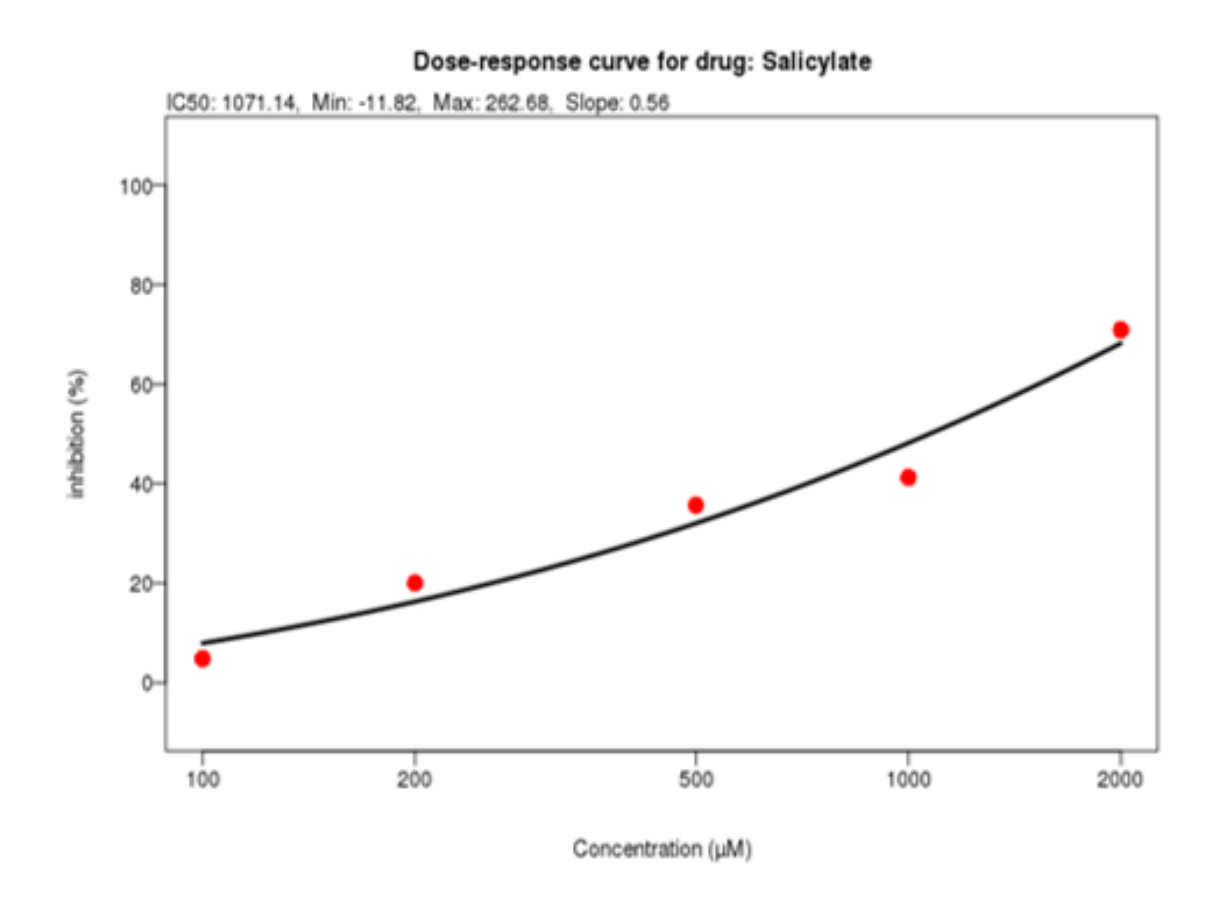


Figure 11. The dose-response curve of Hep3B cells to salicylate. Dose-response results were generated in a proliferation experiment with Hep3B cells treated with 100-2000  $\mu$ M salicylate for 8 days when cells reached 80-90% confluence.

Please note that for the purpose of experimental efficiency, the experiments described below were performed with salicylate alone and in combination with Lenvatinib and radiotherapy. For clarity, the effects of each treatment and combination are discussed separately. However, the results are shown in the figures in a combined form.

#### 3.2.2 Salicylate inhibits HCC cell clonogenic survival.

To assess the effects of salicylate on HCC, Hep3B cells were treated with 1 mM of salicylate, a clinically achievable and safe dose, for 8 days. Hep3B proliferation was inhibited by 16.6% (p < 0.01), indicating that salicylate can exhibit anti-tumor activity in HCC (figure 12A).

Clonogenic survival assays are the gold-standard assay for assessing the anti-tumor activity of drug and radiation treatments in vitro. Therefore, clonogenic assays were performed with a variety of HCC cell lines Hep3B, PLC/PRF/5, HepG2, and Sk-Hep-1 cells to evaluate the extent of clinically achievable concentrations of salicylate that can inhibit the oncogenic potential of these four liver cancer cell lines.

In Hep3B cells, 1 mM of salicylate inhibited clonogenic survival significantly (p < 0.01) by 16.5%, consistent with the proliferation results (figure 12B). PLC/PRF/5 cells were more sensitive to salicylate, with an average of 40.5% inhibition in clonogenic survival (p < 0.05). Similarly, HepG2 cells showed a 31.9% decline in clonogenic survival (p < 0.0001). Lastly, Sk-Hep-1, a liver adenocarcinoma cell line, was the most sensitive to salicylate, with 59.6% inhibition of clonogenic survival (p > 0.0001). The results of the clonogenic experiments clearly demonstrate

that salicylate is indeed an anti-cancer drug with a significant ability to inhibit the HCC cell oncogenic potential.

#### 3.2.3 HCC cell response to radiotherapy

The response of HCC cells to radiotherapy was first investigated with Hep3B cells in proliferation experiments using 2-8 Gy irradiation. In Figure 12A, Hep3B cells irradiated with 2 Gy of radiation proliferated 17.4% less (p < 0.001). Radiation decreased the proliferation of Hep3B cells dose-dependently, with 4 Gy of radiation inhibiting Hep3B proliferation by 43.9% (p < 0.0001), 6 Gy of radiation inhibiting Hep3B proliferation by 64.4% (p < 0.0001), and 8 Gy of radiation inhibiting Hep3B proliferation plateauing at 64.9% (p < 0.0001).

The above results were replicated in clonogenic survival assays performed with the Hep3B, PLC/PRF/5, HepG2, and Sk-Hep-1 cell lines. Radiotherapy significantly suppressed clonogenic survival in all cell lines in a dose-dependent fashion (p < 0.0001) with the exception of Sk-Hep-1 cells, which only showed increased sensitivity to high-dose (6-8 Gy) radiation also (Figure 12B).

#### 3.2.4 Salicylate in combination with radiation

Interestingly, when radiation and salicylate are used together, the two treatments have a synergistic interaction. Using the HSA model to probe for the efficacy of combining salicylate and radiotherapy in Hep3B cells from the results of proliferation experiments, an average HSA synergy score of 11.56±4.48 was found (figure 12C). This treatment combination had the greatest synergy at 1 mM salicylate and 2 Gy radiation, generating an HSA score of 19.17. In the proliferation experiments, salicylate and radiation in combination enhanced the inhibition of proliferation at 2

and 4 Gy more than the radiation alone (p < 0.0001), but the benefit of the addition of salicylate diminishes with high-dose radiotherapy.

Salicylate and its combination with radiation were also investigated for their combined effect on the oncogenicity (clonogenic survival) of liver cancer by treating cells with 1 mM salicylate and 2-8 Gy of radiation (figure 12B). In Hep3B cells, salicylate with 2 Gy radiation observed a 51.2% decrease in colony formation (p < 0.0001), compared to a 16.5% inhibition (p < 0.0001) in salicylate alone and a 45.2% inhibition in 2 Gy radiation alone. Appropriately, salicylate with 4 Gy radiation observed an 80.3% decrease in Hep3B colony formation (p < 0.0001), compared to salicylate alone (p < 0.0001) and a 75.1% inhibition in 4 Gy radiation alone. The absolute benefit of the addition of salicylate to radiotherapy diminished further with higher radiation doses. All in all, salicylate, in combination with radiation at all doses, does not appear to significantly inhibit the colony formation ability of Hep3B cells compared to radiation alone.

Clonogenic experiments with PLC/PRF/5 cells treated with radiation and Salsalate did not decrease tumorgenicity in the combined Salsalate-radiotherapy group compared to Salsalate individually, demonstrated by the lack of significant change in colony formation across all radiation doses between salicylate-treated PLC/PRF/5 cells and salicylate-radiotherapy-treated PLC/PRF/5 cells.

In contrast, HepG2 and Sk-Hep-1 cells had a response to salicylate-radiotherapy cotreatment similar to that of Hep3B cells. Salicylate-radiotherapy combinations in HepG2 and Sk-Hep-1 cells significantly inhibited the colony formation of these cell lines to a greater extent than the individual treatments in solely low dose 2-4 Gy radiation, though this effect was not observed in high dose 6-8 Gy radiation, where colony formation plateaued to the point that no discernible differences were observed between any of the treatments.

#### 3.2.5 Salicylate in combination with radiotherapy and Lenvatinib (triple therapy)

With the promising results of combining salicylate and radiotherapy to enhance the effectiveness of both therapies, the idea of incorporating another standard of care therapy to further improve tumor killing concluded with Lenvatinib. It is important to note that this portion of the investigation focuses on comparing the salicylate-radiotherapy-Lenvatinib combination (triple therapy) to the salicylate-radiotherapy combination. The individual effect of Lenvatinib or Lenvatinib-radiotherapy combination only serves as cursory comparisons.

Analysis of combining salicylate, radiotherapy, and Lenvatinib with SynergyFinder 3.0 and results from proliferation experiments involving Hep3B cells treated with 1 mM salicylate, 2-8 Gy radiotherapy, and 100 nM Lenvatinib for 8 days yielded an average HSA synergy score of 12.04±3.25, which is even greater than the salicylate-radiotherapy combination with an average HSA synergy score of 11.56±4.48. The treatment combination with the greatest synergy for triple therapy was at 1 mM salicylate, 2 Gy radiation, and 100 μM Lenvatinib, yielding an HSA score of 22.36. In the proliferation experiments, triple therapy with 2 and 4 Gy radiation inhibited the proliferation of Hep3B cells more than only 2 and 4 Gy radiation (p < 0.0001), but the increased inhibition of triple therapy diminished with high doses of 6 and 8 Gy radiotherapy.

To assess the potency of triple therapy on the colony formation ability of liver cancer, clonogenic assays were performed on Hep3B, PLC/PRF/5, HepG2, and Sk-Hep-1 cell lines treated with 1 mM salicylate, 2-8 Gy radiation, and 100  $\mu$ M Lenvatinib.

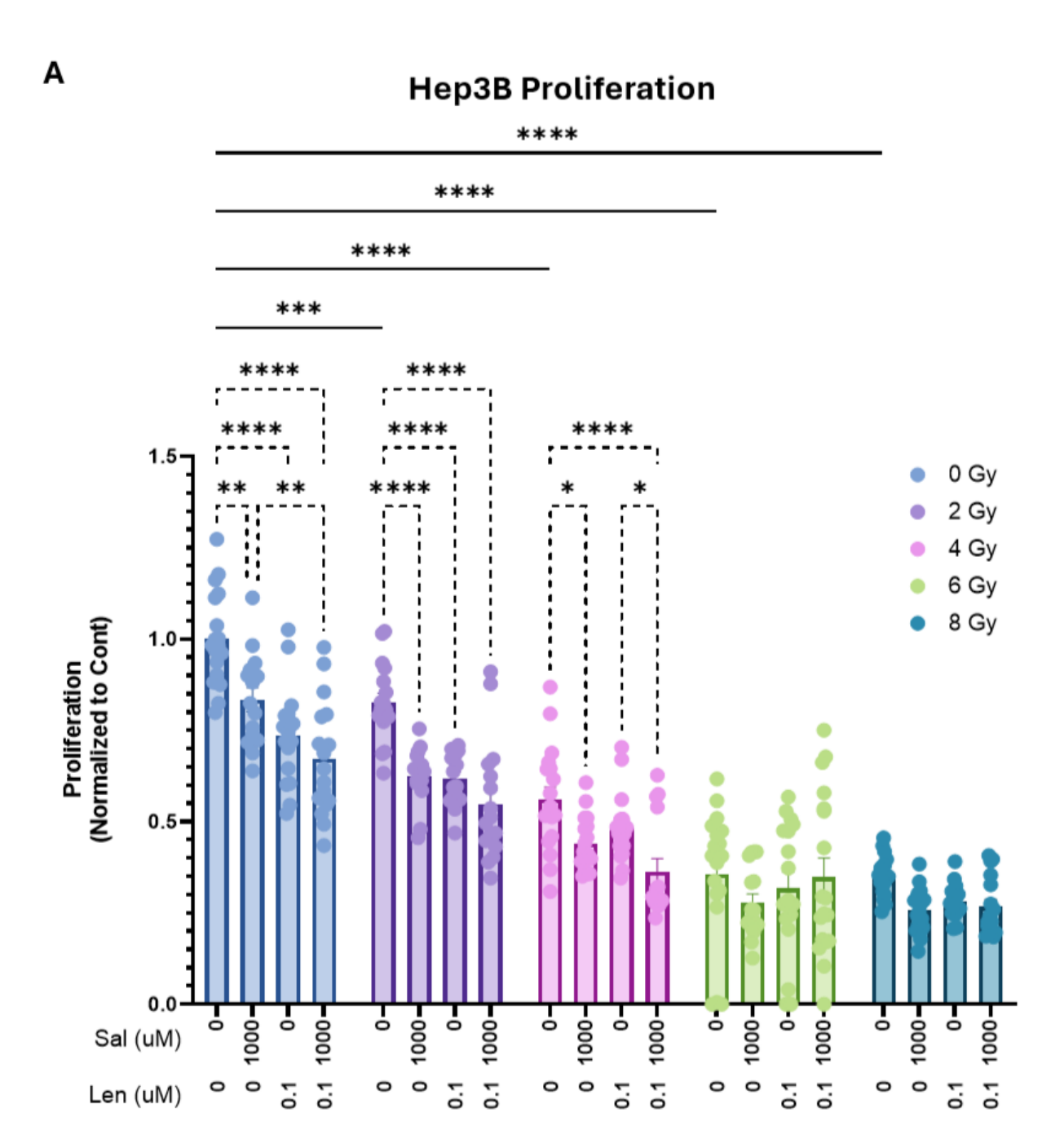
In Hep3B cells, triple therapy was most effective with 2 Gy radiation, with significantly improved inhibition to the colony formation of Hep3B cells compared to individual 2 Gy radiation (p < 0.0001), Lenvatinib-radiation (p < 0.01), and importantly salicylate-radiation combined (p < 0.0001)

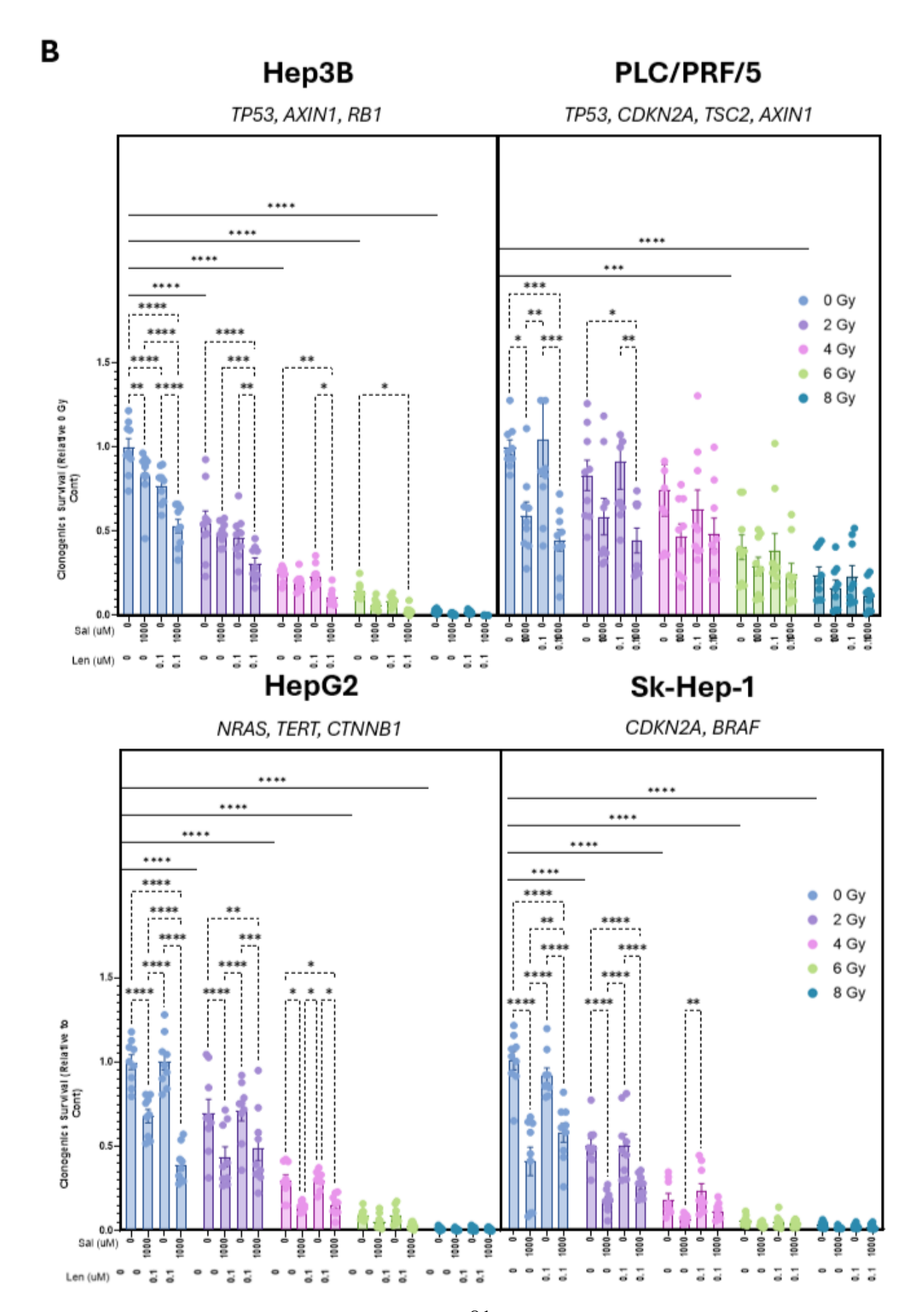
0.001). Although triple therapy improved the inhibition of Hep3B colony formation compared to its component monotherapies, there were no significant differences compared to the salicylate-radiotherapy combination in the 4 and 6 Gy settings. Colony formation was virtually entirely inhibited by 8 Gy radiation, so no comparisons were made between treatment groups.

Clonogenic experiment results in PLC/PRF/5 cells showed no significant improvement in colony formation inhibition compared to all treatments except for only 2 Gy radiation, Lenvatinib, and Lenvatinib-radiation. Interestingly, in addition to having low sensitivity to radiation, PLC/PRF/5 cells also appear to not respond to Lenvatinib. The suppression of colony formation between triple therapy and the salicylate-radiotherapy combination seemed to be primarily attributed to salicylate since Hep3B colony survival in radiotherapy and Lenvatinib-radiotherapy coincided, while Hep3B colony survival in salicylate-radiotherapy and triple therapy coincided.

HepG2 and Sk-Hep-1 cells responded similarly to PLC/PRF/5 cells, though HepG2 and Sk-Hep-1 cells were sensitive to radiotherapy, unlike PLC/PRF/5 cells. Triple therapy was more effective in suppressing colony formation than the individual therapies at 2 Gy in both cell lines and 4 Gy in Sk-Hep-1 cells. However, Lenvatinib had minimal additional benefit, with the colony survival of cells treated in triple therapy coinciding with cells treated with salicylate-radiotherapy in 2-4 Gy radiation. Like PLC/PRF/5 cells, HepG2 and Sk-Hep-1 cells appeared to not respond to Lenvatinib, with most inhibitory effects coming from salicylate-radiotherapy.

In summary, in Hep3B cells, triple therapy significantly inhibited colony formation across 2-6 Gy radiation doses, with enhanced effects compared to the salicylate-radiotherapy combination. In PLC/PRF/5 cells, the triple therapy showed more potent inhibition at lower radiation doses but had similar effects as the salicylate-radiotherapy combination at higher doses. HepG2 and Sk-Hep-1 cells showed minimal additional benefit from Lenvatinib, with triple therapy offering similar outcomes as the salicylate-radiotherapy combination. Overall, the effectiveness of triple therapy varied by cell line and radiation dose.





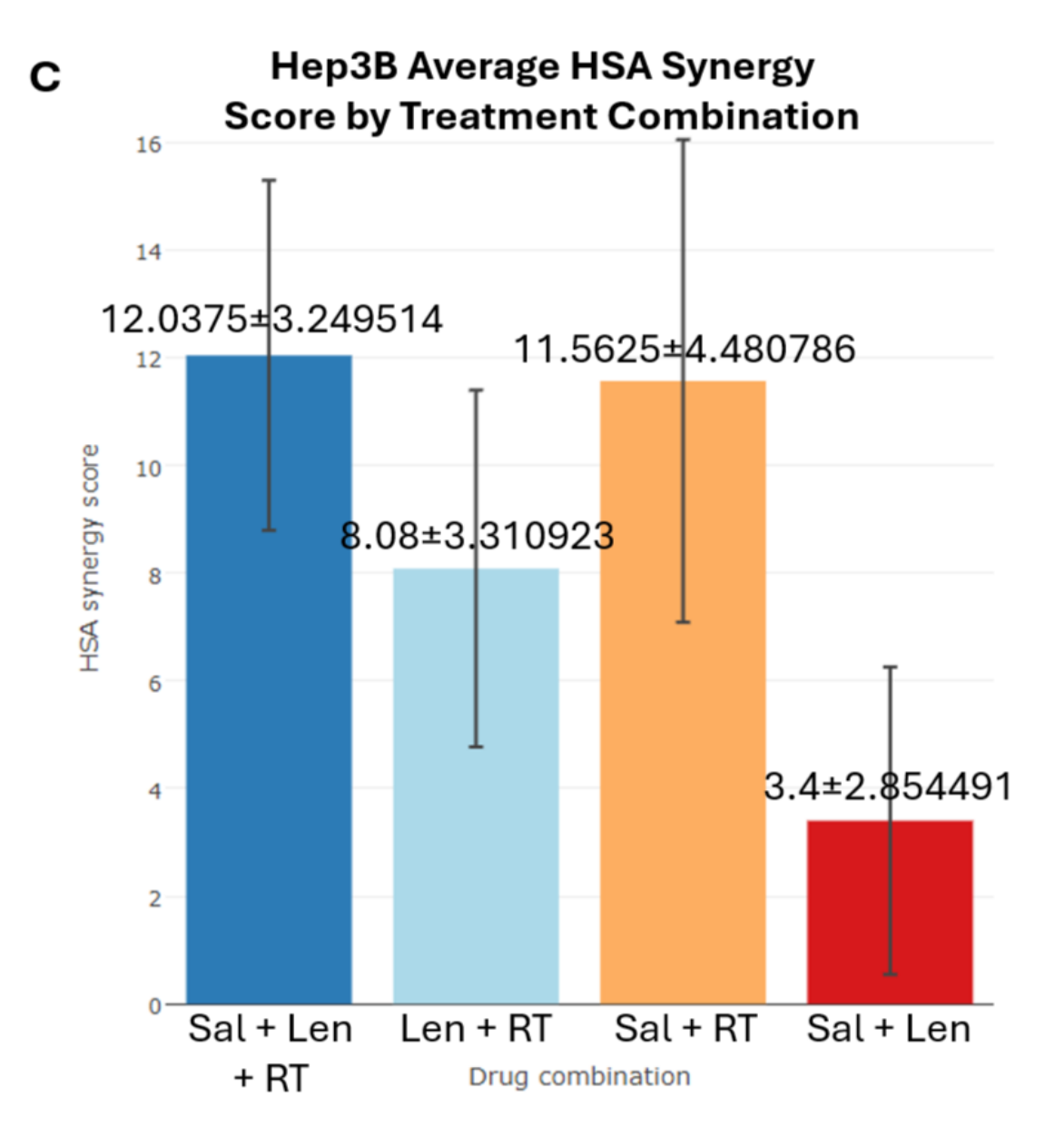
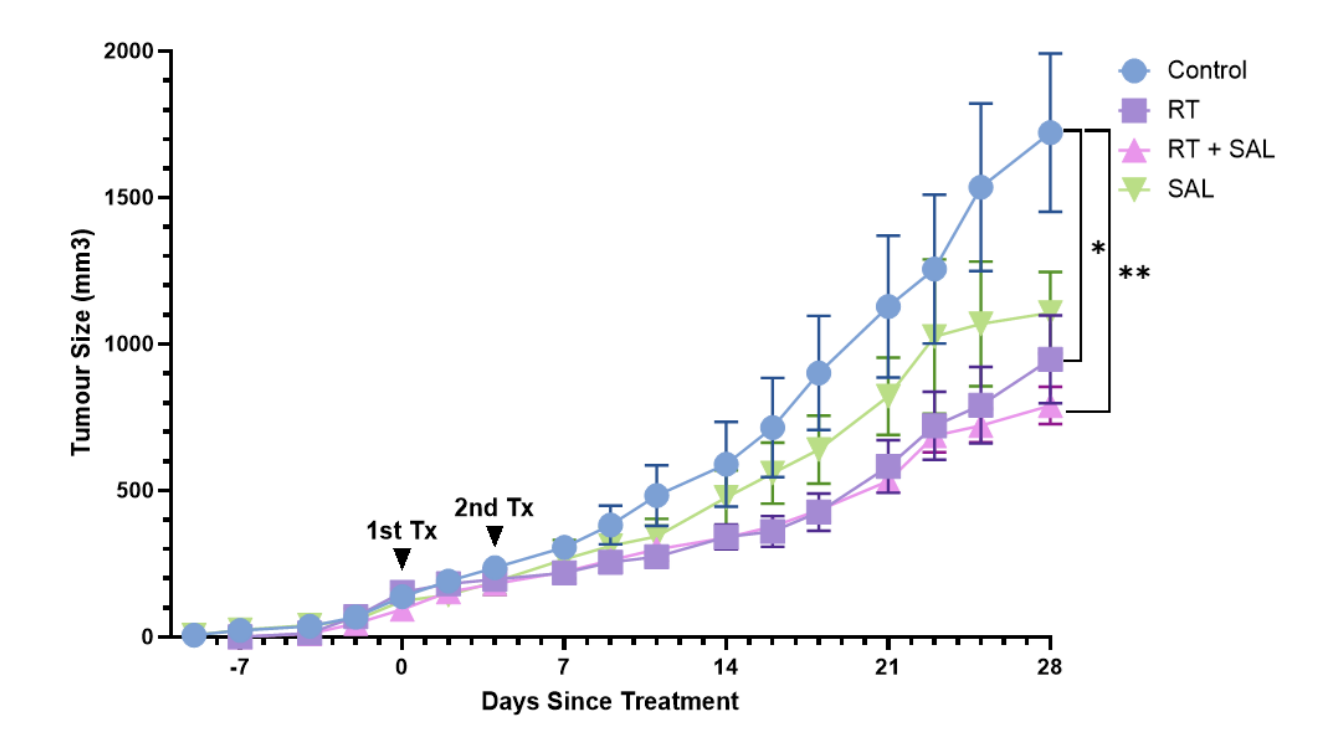


Figure 12. Proliferation of Hep3B cells, clonogenic survival of Hep3B, PLC/PRF/5, HepG2, and Sk-Hep-1 cells, and average HAS synergy scores of treatment groups. A) The effect of salicylate, radiation, and Lenvatinib on Hep3B cell proliferation. Two-way ANOVA comparison within each column, the rows, and within each row, the columns. B) Clonogenic survival of Hep3B, PLC/PRF/5, HepG2, and Sk-Hep-1 cells relative to the respective control groups. Two-way ANOVA comparison within each column, the rows, and within each row, the columns. C) The average HSA synergy score of each treatment combination involving salicylate, radiation, and Lenvatinib in Hep3B cells. \*p < 0.05, \*\*p < 0.01, \*\*\*p < 0.001, and \*\*\*\*p< 0.0001.

#### 3.2.6 Anti-tumor activity in-vivo.

Based on the in vitro results of salicylate and radiation inhibiting HCC cell growth, preparations were made to study whether these in vitro results translated in vivo. In an effort to observe whether salicylate and radiation could reduce HCC tumor growth in vivo, Hep3B cells were ectopically xenografted to NRG mice. After Hep3B xenografts reached ~100 mm<sup>3</sup>, the animals were first treated with Salsalate (300 mg/kg) for 4 days via the inclusion of the drug in the chow diet, followed by conformal tumor radiation (5 Gy) with parallel opposed radiotherapy fields at 90 and 270°. An endpoint of 2500 mm<sup>3</sup> was set for the xenograft size and the appropriate indicators of mice health throughout the experiment. The treatment with Salsalate, radiation, and Salsalate with radiation all decreased the growth rate of the tumors compared to the control tumor growth rates. Day 28 was chosen for the cut-off date because, after this date, treatment groups became incomplete due to mouse sacrifice as mice reached the criteria for endpoint sacrifice. 28 Days after treatment began, the control group had an average tumor size of 1721.61 mm<sup>3</sup>, the radiation group 947.78 mm<sup>3</sup>, the radiation-Salsalate group 790.17 mm<sup>3</sup>, the Salsalate group 1107.31 mm<sup>3</sup>, with the radiation (p < 0.05) and radiation-Salsalate (p < 0.01) groups significantly decreased compared to the control group. The in vivo work is still ongoing. Additional cohorts will increase the power of the existing groups, and mice treated with Lenvatinib in combination with salicylate and radiotherapy will be added.



**Figure 13. Growth of Hep3B cells xenografted in NRG mice.** Growth kinetics (volume in mm<sup>3</sup>) of **2** million Hep3B cells xenografted in NRG mice, treated with 300 mg/kg Salsalate chow diet and 5 Gy radiation. The drug diet is administered when tumors reach  $100 \text{ mm}^3$ , with the drug diet beginning 4 days before radiation. Tumor sizes are determined with calipers. RT = radiation, SAL = Salsalate. n(control) = 6, n(RT) = 8, n(RT+SAL) = 8, and n(SAL) = 8. A one-way ANOVA was performed at the cut-off date to determine whether each group differed significantly, where \* = p < 0.05, \*\* = p < 0.01.

#### 3.2.7 Modulation of cancer growth pathways by salicylate and combination therapies.

To pursue the molecular mechanism of action salicylate acts on, early immunoblotting analysis was performed on key targets involved in hepatocarcinogenesis, including the mTOR-Hif-1α and ERK signaling pathways. Hep3B cells were treated with salicylate for 48 hours and compared with untreated cells cultured in the same timeframe. The following results are preliminary work to probe for some of the most likely mechanisms behind salicylate, radiotherapy,

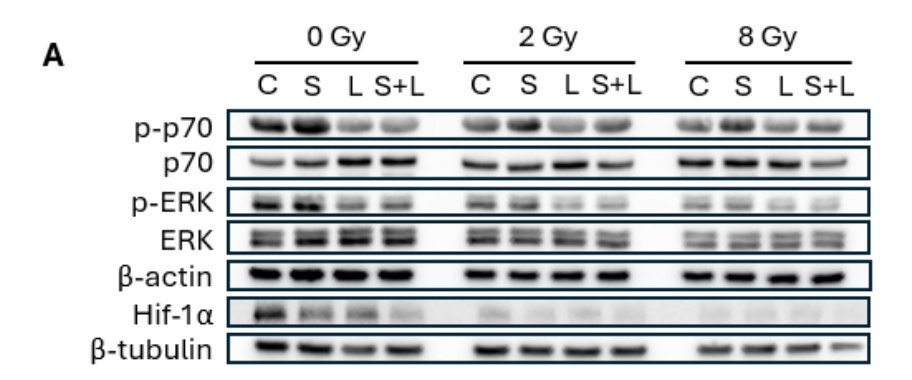
and Lenvatinib treatment. As a result, the power of these results was weak, so no statistical analysis was performed.

In Figure 14A, the control group had a lower expression of p70 compared to the salicylate group. Salicylate appeared to decrease the phosphorylation of p70 and Hif-1α expression compared to control. The phosphorylation of ERK did not appear to be affected by salicylate.

To assess the combinatory effects of radiation on these pathways, Hep3B cells were radiated and lysed 24 hours later. The phosphorylation of p70 was decreased to a similar extent by late 2 Gy and 8 Gy radiation. ERK phosphorylation appeared to be similarly decreased by 2 Gy and 8 Gy radiation. Following this trend, Hif-1α also appeared to be decreased by radiation.

To probe for markers in response to salicylate and radiation, Hep3B cells were treated with salicylate for 48 hours, and radiation was given 24 hours before stopping the experiment. The combination of salicylate and radiation did not appear to affect the phosphorylation or gene expression of p70, ERK, and Hif-1α more than the individual therapies.

To investigate the effect of triple therapy on these key cancer pathways, Hep3B cells were treated with 100  $\mu$ M Lenvatinib and found that no markers were significantly affected by triple therapy. However, Lenvatinib by itself appeared to decrease p70 phosphorylation, ERK phosphorylation, and Hif-1 $\alpha$  protein expression. Triple therapy appeared to decrease in a similar fashion to Lenvatinib but did not appear different.



В

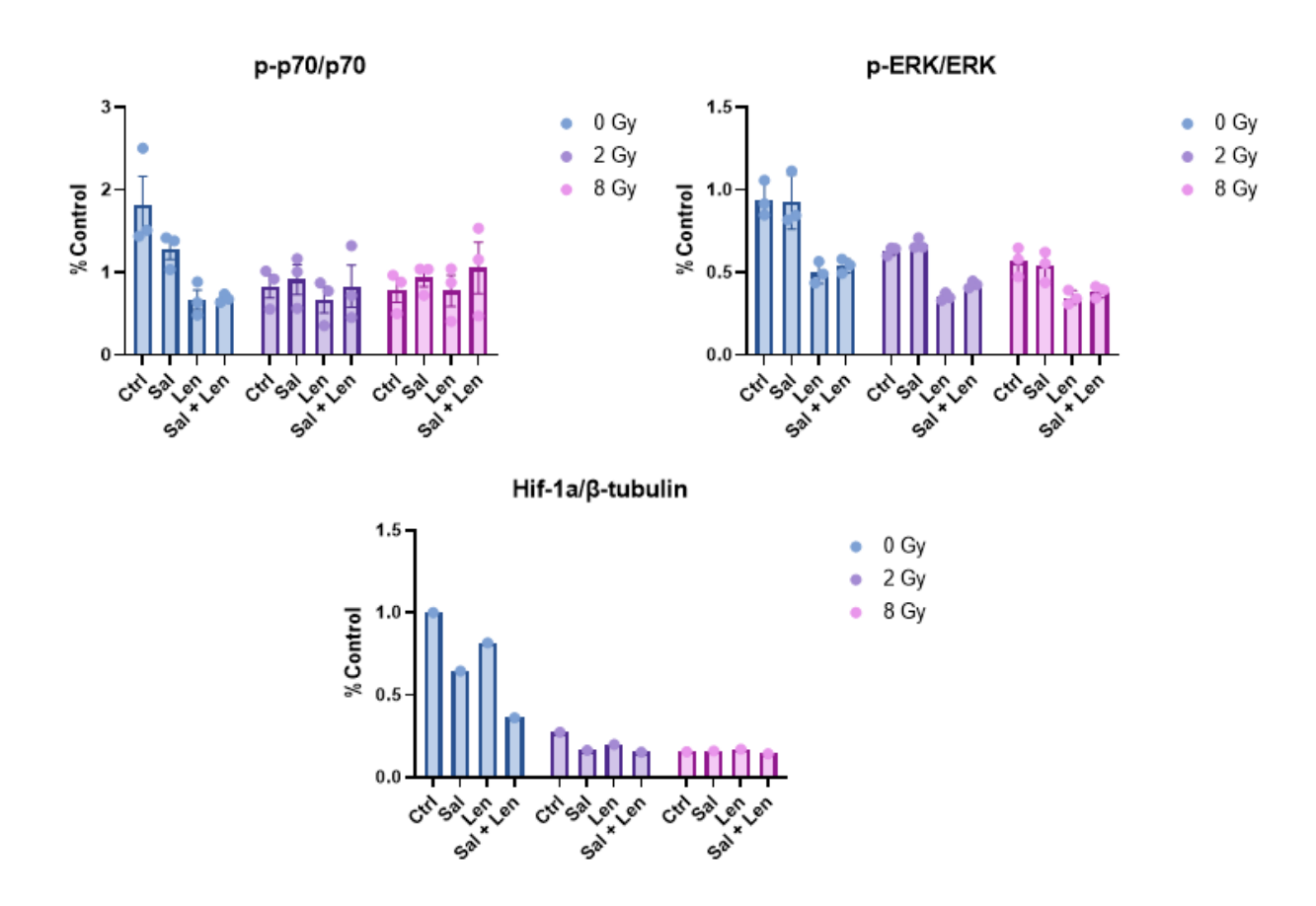


**Figure 14. Modulation of signaling pathways.** Levels of activating p70 and ERK phosphorylation expression, and Hif-1 $\alpha$  expression in Hep3B cells treated with salicylate, Lenvatinib, drug combination, and radiation. A) Markers of mTOR (phosphorylated and total p70 n = 3, Hif-1 $\alpha$  n = 1) and ERK (phosphorylated and total ERK n = 3) pathways by immunoblotting in Hep3B cell treated with 1 mM salicylate, 2 and 8 Gy radiation, and 100

nM Lenvatinib. B) Quantification of immunoblotting of phosphorylated proteins normalized to  $\beta$ -actin or  $\beta$ -tubulin over total proteins normalized to  $\beta$ -actin or  $\beta$ -tubulin in ImageJ. C = control DMSO, S = salicylate, L = Lenvatinib, S+L = salicylate and Lenvatinib drug combination. No statistical analysis was performed for this experiment, given the limited number of repeats performed by the time of this report.

These results suggest modulation of the mTOR-p70S6k/HIF1a and MAPK pathways by individual drug and radiation treatments. What appears to be inhibitory effects of dual treatments can be observed. However, these are very early results that require the generation of a larger number of experimental repeats for any conclusions to be drawn.

#### 3.2.8 Regulation of cell cycle and DNA replication markers.

Processes involved in the regulation of DNA replication and the cell cycle were also probed to explore whether salicylate modulates these cellular processes in Hep3B cells. Salicylate appeared to decrease the phosphorylation of histone H3, slightly increase cyclin D1 expression, and increase p27 expression. Histone H3 phosphorylation levels and cyclin D1 expression appeared to decrease with radiation dose-dependently. Radiation seems to reduce p27 expression. Salicylate-radiotherapy and triple therapy did not appear to have enhanced suppression of histone H3 phosphorylation, with most of the expression appearing to respond to radiation. Cyclin D1 appeared to be decreased by salicylate-Lenvatinib but radiation appeared to decrease cyclin D1 expression more. Within 2 Gy irradiated Hep3B cells, salicylate, and Lenvatinib appeared to further reduce cyclin D1 expression, with triple therapy appearing to enhance this effect further. Lastly, p27 appeared to increase in response to salicylate and Lenvatinib treatments in non-irradiated cells but showed limited response in irradiated ones. Cell cycle markers seem to be

modulated by salicylate, Lenvatinib, and radiotherapy, but the effects are limited by the power and sensitivity of the immunoblotting assay done so far, thereby reserving any further observations beyond superficial remarks.

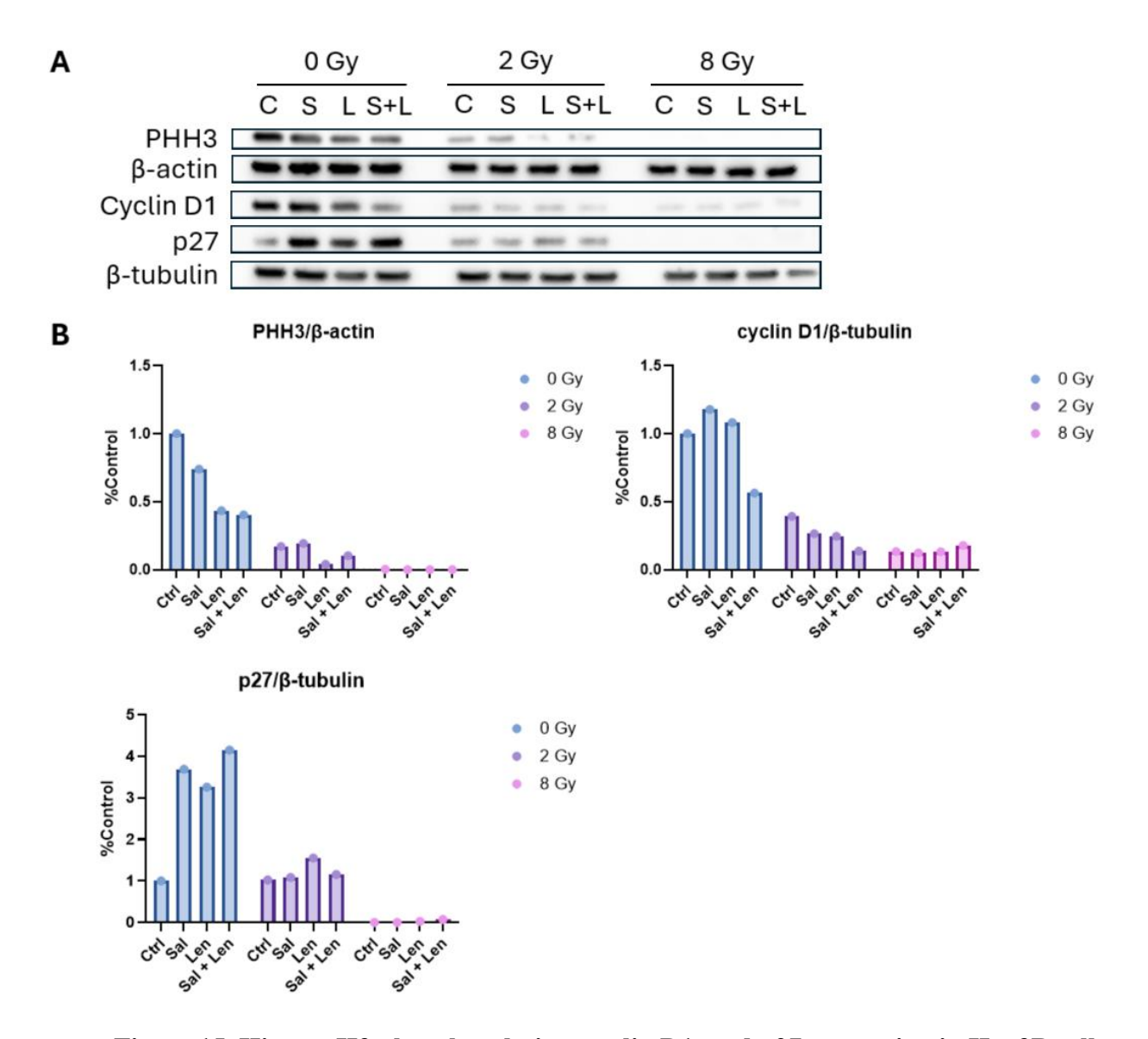


Figure 15. Histone H3 phosphorylation, cyclin D1, and p27 expression in Hep3B cells treated with salicylate, Lenvatinib, drug combination, and radiation. A) Cell cycle markers (all n=1), phosphorylated histone H3 (PHH3) normalized to  $\beta$ -actin, and cyclin D1 and p27 normalized to  $\beta$ -tubulin by immunoblotting in Hep3B cells treated with 1 mM salicylate, 2 and 8 Gy radiation, and 100 nM Lenvatinib. B) Quantification of immunoblotting of cell cycle markers. Immunoblots quantified with ImageJ. C = control DMSO, S = salicylate, L = Lenvatinib, S+L = Salicylate and Lenvatinib drug combination.

McMaster University – Medical Sciences

Chapter 4 – Discussion

MSc. Thesis – Simon Wang

The off-target effects of radiation remain a serious obstacle for treating HCC, as well as many other cancer types. This study aimed to improve the therapeutic ratio of radiotherapy investigating Salsalate for its radioprotective effects in liver tissue, as well as radio-sensitizing effects in HCC observed in previous work in prostate and lung cancer cell lines. Working with clinically achievable and relevant doses of Salsalate/salicylate, radiotherapy, and Lenvatinib, the following observations were found:

- Salsalate mitigated the response of inflammatory cells in irradiated livers, reduced expression of markers of fibrosis observed in RILD, and showed obvious trends to improve animal survival after high-dose whole liver irradiation
- Salicylate inhibited the proliferation and clonogenic survival of liver cancer cell lines individually and enhanced efficacy in most cell lines when combined with radiotherapy, both in vitro and in vivo
- The addition of Lenvatinib improved the inhibition of Hep3B cells by salicylate and radiotherapy, and early results point to modulation of critical cancer-promoting and cell cycle regulation markers

# 4.1 Potential protective effects of Salsalate against normal tissue radiation toxicity

The animal radiation survival study aimed to mimic conditions of EBRT treatments and found that irradiated mice treated with Salsalate had nearly double the median survival compared to irradiated mice, with 105.5 days compared to 57 days, respectively, suggesting potential radioprotective effects.

Additionally, histological analysis suggests that this may be due to Salsalate-mediated suppression of inflammation, resulting in reduced macrophage and T-cell recruitment in Salsalate-treated mice. Macrophages were observed in greater numbers in response to radiation. Kupffer cell size appeared enlarged (figure 8) in response to high-dose radiation, suggesting a potential state of activation, and was decreased in irradiated liver treated with Salsalate. Concurrently, CD3 expression (figure 10) also increased with radiation and with trends of reduction in the Salsalate-treated irradiated liver. A similar decrease in immune cell recruitment was also observed in an acute radiation study in a rat model, where neutrophil recruitment was decreased with aspirin [143].

This reduction in immune cell infiltration may be due to reduced inflammatory signaling. The anti-inflammatory property of Salsalate is likely suppressing key inflammatory cytokines released as a result of radiation damage, disrupting macrophage activation and, therefore, TGF-β release. IL-6 was also upregulated by radiation. Trends of a decrease in the Salsalate-treated irradiated liver would suggest a reduction of inflammation by Salsalate, though additional repeats and the probing of other inflammatory markers are required to confirm. IL-6, together with other inflammatory interleukins, IL-1 and 7, are responsible for recruiting inflammatory cells to the site of injury [121]. In the study by Liu et al. investigating the effects of aspirin on hepatic fibrosis, IL-6 was one of the inflammatory cytokines suppressed by aspirin [138].

Aspirin and aspirin derivatives have been demonstrated to prevent NF-κB nuclear translocation, leading to a decrease in collagen synthesis and the prevention of hepatic stellate cell differentiation into myofibroblastic hepatic stellate cells, which are the number-one contributor to collagen deposition and liver fibrosis [138-140]. Though a significant decrease in NF-κB expression was not observed, downward trends suggest Salsalate affecting its expression. NF-κB production is activated by SMAD-independent of downstream TGF-β signaling. In addition,

SMAD-independent pathways also activate the MAPK/JNK, mTOR, and RhoA signaling cascades for cell survival and inflammation, where the mTOR pathway is also involved in fibroblast differentiation via the autophagy pathway [88, 89, 136].

Previous work and studies by Peng et al. 2023 and Leonhard et al. 2019 observed aspirin and Salsalate, respectively, suppressed mTOR activity. Increased collagen deposition in the parenchyma of the irradiated liver and the decreasing trends of deposition in Salsalate-treated irradiated livers in Figure 9 suggest that pro-inflammatory and pro-fibrotic signaling cascades could have been suppressed. Furthermore, an apparent increase in Col1A1 and an increase in α-SMA expression with irradiated liver and their decreased expression in Salsalate-treated irradiated liver in Figure 10 point to the same conclusion, though more power is required. This trend in the in vivo liver expression of collagen building blocks in response to Salsalate after radiation correlates with findings by Peng et al. 2023, which demonstrated lung fibroblast cells treated with TGF-β upregulated Col1A1 and α-SMA but were suppressed when treated with aspirin [136]. Similarly, the results of the investigation by Liu et al. 2020 of a CCL4 rat model treated with aspirin found that Col1A1 and α-SMA were suppressed by aspirin [138]. Col1A1 and α-SMA are secreted by myofibroblastic hepatic stellate cells as extracellular matrix and are upregulated in response to radiation. This combination of factors could result in more than double the median survival time of Salsalate-treated irradiated mice.

#### 4.2 Anti-cancer benefits of salicylate and combination with radiotherapy

Radiotherapy is recognized as a potent method of killing cancer but has the drawback of causing equal harm to functional normal tissue vital for the well-being of the patient. As discussed in 4.1, Salsalate could address the issue of radiation toxicity in HCC patients, mainly due to the

high doses used to treat HCC. In contrast, other cancer types, such as lung and prostate cancer, have lower doses of radiation, usually around 2 Gy per fraction, increasing up to 8 Gy with hypofractionated radiotherapy [163, 164]. 8 Gy is usually the radiation dose per fraction for treating HCC with modern high-precision SBRT, with the biologically effective dose for many radiotherapy regimens reaching above 100 Gy, potentially requiring 15 Gy per fraction [165]. The proliferation and clonogenic experiments conducted in our study demonstrate that radiotherapy at an effective dose is effective in inhibiting the proliferation and tumorigenic potential of liver cancer.

The proliferation and clonogenic formation of several liver cancer cell lines were also assessed with salicylate treatment. Every cell line was inhibited by salicylate, though salicylate was least effective in the human HCC Hep3B cells and most potent in the human liver adenocarcinoma Sk-Hep-1 cells. Previous studies involving prostate and lung cancer cell lines have shown that adenocarcinomas are sensitive to salicylate [141, 142, 159]. The response of Hep3B cells to salicylate was significantly decreased but may be biologically irrelevant due to the small ~16.5% decrease in proliferation and clonogenic formation. Based on the aim of increasing the therapeutic ratio of radiotherapy with Salsalate in disease conditions and the anti-tumor and radio-sensitizing effects of salicylate observed in previous works, efforts were made to investigate how salicylate and radiation interacted in vitro.

Analysis of salicylate-radiotherapy synergy by SynergyFinder 3.0 suggests that there is a synergistic effect on Hep3B cells, yielding an HSA score of 11.56. The inhibition of Hep3B cells by both salicylate and radiation is very promising, especially with the positive results of Salsalate mitigating radiation damage in normal tissue. Indeed, proliferation and clonogenic assay results both showed a dose-dependent biologically relevant decrease in Hep3B proliferation and colony formation with the treatment of salicylate and radiotherapy. Hep3B cells treated with both

salicylate and radiotherapy had a greater proliferation and colony formation inhibition than individual treatments, and the inhibitory effect scaled in a dose-dependent manner, as seen in Figures 12A and B. These observations are likely attributed to the radio-sensitization of Hep3B cells by salicylate to radiation observed in other cell lines [141]. Combining the radio-sensitization of cancer cells with the promising results of the radioprotective effects of Salsalate on normal tissue, potentially enabling higher radiation doses with fewer complications, combined salicylate-radiotherapy treatment is a promising prospect for HCC patients.

Positive in vitro experimental results prompted in vivo experiments. In ectopic xenograft models, radiotherapy-salsalate and radiotherapy significantly decreased the tumor growth rate and the tumor size at the endpoint, visualized in Figure 13. More cohorts are required for a clearer understanding of the role each treatment plays in reducing Hep3B growth and statistical power. In vivo, salicylate, radiation, and salicylate-radiation combination decreased the growth rate of tumors relative to the control group. HCC tumors are usually hypoxic by nature due to the formation of large nodules and rely on Hif-1α to sustain growth. Given the in vitro evidence of salicylate decreasing Hif-1α protein expression, the decrease in salsalate-treated groups may be partly due to salicylate indirectly targeting Hif-1a through AMPK activation and inhibiting the mTOR pathway. AMPK activation and mTOR suppression were suggested as a mechanism for Salsalate to sensitize prostate cancer cells to radiotherapy in mouse models by Broadfield et al. 2019 [141]. Hif-1α promotes angiogenesis to counter hypoxia, which contributes to supplying the tumors with all the essential nutrients for growth. If Hif-1\alpha suppression by Salsalate occurs in these tumors, then this is a possible mechanism by which tumors have diminished growth capabilities compared to the control tumors. It is well documented that radiation reduces growth by initially killing many of the cancer cells and senesce damaged cancer cells, reducing the number of cells

able to replicate, thereby reducing the growth rate. In theory, the combination of salicylate and radiation would amplify these effects, potentially further reducing the initial population of cancer cells and then continuously slowing down tumor growth.

Previous studies have shown that salicylate also inhibits cancer cell growth and the suppression of cancer pathways, namely the mTOR pathway, by the induction of AMPK [142]. Immunoblotting, which still requires more repeats for the markers discussed and is only offering a preliminary look at some prominent markers of cancer pathways, revealed that salicylate suppressed mTOR activity, shown by the decreasing trends in p70 phosphorylation and Hif-1α expression. Radiation also appeared to decrease the expression of p70 phosphorylation and expression of Hif-1α, as well as ERK phosphorylation. This observation, if accurate and significant with more experimental repeats, contradicts current findings, which state that the ERK pathway is usually active after radiation in a compensatory function. In fact, studies have shown that the inhibition of the ERK pathway sensitizes cells to radiation since the pathway responds to radiation and plays a role in radio-resistance [166]. It is well known that the other mammalian MAPK pathways, JNK/SAPK and p38, respond to radiation damage and cell stress, and crosstalk between all three mammalian MAPK pathways exists [67]. Regardless, the decreasing trends of ERK1/2 in Hep3B cells is a positive outcome, as the ERK pathway is one of the primary cancer pathways driving growth and survival. The mTOR pathway is also not commonly observed to be decreased by radiation; instead, it confers radio-resistance and promotes cell survival in response to radiotherapy [167]. Similarly, Hif-1\alpha is described to be stabilized by the activation of the mTOR pathway, but we instead observe an apparent decrease of Hif-1α with radiation [168]. It is essential to consider that the treatment response is time-dependent, with radiation acutely affecting the aforementioned pathways and triggering early activation of ATM and DNA repair pathways,

typically inactive at 24-48 hours. The activation of these pathways generally is bimodal, with later induction leading to survival and radio-resistance [169].

Radiation kills HCC cells by breaking the bonds of essential molecules within the cell, such as the DNA, or by inducing senescence. This effect can be observed with the apparent decrease in histone H3 phosphorylation levels, a marker of proliferation due to histone H3 phosphorylation uncoiling for DNA replication, with increasing radiation dosage. Cyclin D1 and p27 are two crucial regulators of the G1/S phase transition, with the accumulation of the former driving the transition while the accumulation of the latter inhibiting the transition. The more cyclin accumulates, the more p27 is degraded. It is, therefore, interesting that salicylate appeared to increase p27 while cyclin D1 appeared to remain unaffected by salicylate, but radiation appears to downregulate cyclin without triggering a p27 upregulation. A possible explanation may be that the snapshot at the end of the experiment is at a time when cyclin is in high concentration while p27 is at low levels, as it may not be required at this time point to mediate cell cycle arrest. Furthermore, only a single repeat has been performed and may not accurately reflect the reality of what is occurring within these cells at this timepoint. Additional time-course experiments are required to verify this observation.

#### 4.3 Combination with Lenvatinib

When adding Lenvatinib to salicylate and radiotherapy treatment of Hep3B cells, SynergyFinder 3.0 suggests this treatment combination is synergistic with an average HSA score of 12.04. This average HSA score is greater than the HSA score of the salicylate and radiotherapy combination, which is 11.56, suggesting greater effectiveness against Hep3B cell growth.

The triple therapy of salicylate, Lenvatinib, and radiation inhibited the growth and colony formation of the human HCC cell line Hep3B, demonstrated in Figures 12A and B, respectively. This is likely driven by salicylate, Lenvatinib, and radiation inhibiting Hep3B growth by three pathways. The following markers observed with immunoblotting are still a work in progress and require repeats to consolidate findings. Salicylate is suggested to inhibit tumor growth by inhibiting mTOR activity through AMPK activation, shown by the apparent decrease in p70 phosphorylation. Radiation, through DNA damage and generation of ROS in the intracellular space, inhibits molecular pathways vital to cell survival. Lenvatinib, as a tyrosine kinase inhibitor, blocks tyrosine kinase receptors, such as VEGFR, PDGFR, EGFR, and FGFR. This suppresses both the ERK signaling cascade and the mTOR pathway downstream of the receptors. This is observed with the apparent decrease in ERK and p70 phosphorylation expression in Figure 14, respectively, which was also observed in our earlier study investigating the Lenvatinib and Salicylate combination [E. Tsakiridis et al. In review].

In the drug combination, the individual effect of each treatment is seen as an additive effect in reducing HCC growth. The combined effect of salicylate and Lenvatinib can be hinted at in the protein expression of Hif- $1\alpha$ , as seen in Figure 14, which appeared to have a high baseline expression of Hif- $1\alpha$  and apparently decreased when individually treated with each drug but appeared more decreased in response to combined salicylate and Lenvatinib. The decrease in Hif- $1\alpha$  expression was also noted in previous findings with Lenvatinib and salicylate and also in salicylate and metformin combination studies [159]. Both the mTOR and MAPK pathway induce Hif- $1\alpha$  activity, which plays a role in cell survival and stress resistance, by preventing eIF4e and rpS6 activation, respectively, and both inhibiting eIF4e inhibitor, 4E-BP1. Furthermore, the effects of suppressing the mTOR and MAPK pathways would not be isolated to the inhibition of Hif- $1\alpha$ 

but to all their downstream targets, which are involved in biosynthesis, proliferation, and survival. Without these responses, HCC cells would be vulnerable to radiation and possibly unable to adapt to external stress, thereby potentially further inhibiting tumor expansion [170]. Additionally, protein analysis of Hep3B cells treated with triple therapy also appeared to decrease the phosphorylation of histone H3 and cyclin D1 expression, as seen in Figure 15, suggesting a decrease in proliferation and cell cycle progression. These results are preliminary observations into how triple therapy may modulate the cell cycle and could be subject to change with additional experimental repeats. Furthermore, the timepoints of these experiments may not be reflective of the actual effects of triple therapy on the cell cycle of Hep3B cells and are only a snapshot of what was occurring 24 hours after treatment.

# Highlights

A few highlights in the experimental design revolve around the use of RT. The experimental mouse model, designed for the investigation of the radioprotective effects of Salsalate, aimed to replicate clinical radiotherapy. The 20 Gy high dose RT is fractionated to 10 Gy over 2 days, with an injection of dexamethasone to alleviate patients of the acute effects of RT. The RT is delivered using linear accelerators used in clinical practice and operated by trained RT technicians, with settings close to that of actual RT treatments. Similarly, RT in the Hep3B xenograft model is also delivered by clinical linear accelerators and is conformal to the tumor, replicating modern RT techniques for treating cancer. In many studies, radiation is delivered in non-clinical settings or obsolete methods, such as delivering RT with exposure to radioisotopes or orthovoltage machines [143, 171-176]. Though helpful in observing raw radiation damage and potential treatments, clinical presentation of radiation-induced injuries may not progress similarly.

## Limitations

The analysis of protein expression in both the liver lysates and Hep3B cells was very limited and required more experimental replicates to confirm the results. The optimization of several key markers for the liver lysates, such as TNF-α, could have provided more context to the effects of Salsalate and radiation on the liver. Additionally, serum analysis of C57BL/6 mice by ELISA for systemic reactions to Salsalate and radiotherapy is ongoing.

A major difference between the first and second cohorts of C57BL/6 mice was that the radiation dose was different, with the first cohort receiving 20 Gy and the second cohort receiving 10 Gy. This was done because of the high mortality of 20 Gy radiation, preventing analysis of tissue that was exposed to treatment for the same duration. Although the mice irradiated with 10 Gy were undoubtedly adversely affected by radiation, the magnitude of these responses was not as strong as observed in the pilot study despite having a longer experimental timeline. Upon further review, other solutions to animal mortality could have been proposed other than reducing the radiation dose, such as the development of more conformal radiotherapy techniques.

Key markers affecting the tumorigenicity of Hep3B cells were ongoing and could have provided more invaluable insight into the mechanism by which salicylate, radiation, and Lenvatinib were affected. On this note, the analysis of cell cycle regulation markers in Hep3B cells was inadequate and only provided preliminary insight into the cell cycle regulation of Salsalate, radiation, and Lenvatinib. A proper cell cycle experiment involving synchronizing cells and probing for the proportion of cells in each cell cycle stage using flow cytometry would have provided stronger evidence than the protein expression of several key cell cycle regulation markers. Furthermore, Hep3B tumors were collected from in vivo experiments and have yet to be analyzed.

Immunohistology analysis would provide information on the tumor environment of Hep3B cells, such as with vascularization and hypoxia.

### **Future Directions**

After the conclusion of a pilot Lenvatinib cohort using a clinically relevant low dose of Lenvatinib dose, a wider cohort studying the combination of Salsalate and Lenvatinib is ongoing. This study aimed to assess a new dose of Lenvatinib incorporated into a normal chow diet in NRG mice. Like with the in vivo study with Salsalate and radiotherapy, Hep3B cells were xenografted into the right flank of NRG mice and grown to 150 mm<sup>3</sup> before beginning the Lenvatinib diet, with mice being followed carefully to the experimental endpoint.

We aim to answer the following questions:

How is tumor growth kinetics affected? What are the molecular pathways responsible for the changes observed? Specifically, we are also interested in understanding how triple therapy affects Hep3B tumor vascularization and the assessment of hypoxia to analyze the mechanism behind the inhibition of tumor growth. This would also extend to future in vivo studies investigating the combination of Lenvatinib with Salsalate and radiotherapy.

### Conclusion

The cytoprotective effects of Salsalate may be able to mitigate radiotherapy toxicity to the point of influencing animal survival after high-dose radiotherapy, likely by limiting fibrosis and

inflammatory processes in the normal liver, which, in combination with tumor suppressors, may indeed be able to improve the therapeutic ratio of radiation in HCC.

In addition, the combination of salicylate, Lenvatinib, and radiotherapy can potentially decrease the proliferation of HCC more than the individual therapies alone. Based on the experimental results and early analysis of the mechanism of action of triple therapy suggest that HCC cell growth may be inhibited through the suppression of the mTOR and MAPK pathways in non-irradiated and irradiated cells at clinically relevant doses.

The early in-vivo analysis demonstrates promise for the ability of Salsalate to enhance the anti-tumor efficacy of radiotherapy in HCC. Ongoing work aims to replicate these findings and explore the benefit of triple therapy.

This work provides early results indicating that the triple therapy of Salsalate, Lenvatinib, and radiotherapy may be a promising therapeutic approach in unresectable HCC. Given that all components of this therapy are approved therapeutics, this work may generate a basis for clinical investigation of the triple therapy concept in HCC patients.

## References

- 1. Ozougwu, J., *Physiology of the liver.* 2017. **4**: p. 13-24.
- 2. Kutlu, O., H.N. Kaleli, and E. Ozer, *Molecular Pathogenesis of Nonalcoholic Steatohepatitis-* (*NASH-*) *Related Hepatocellular Carcinoma*. Can J Gastroenterol Hepatol, 2018. **2018**: p. 8543763.
- 3. Gonzalez-Sanchez, E., et al., *The TGF-β Pathway: A Pharmacological Target in Hepatocellular Carcinoma?* Cancers (Basel), 2021. **13**(13).
- 4. Llovet, J.M., et al., *Immunotherapies for hepatocellular carcinoma*. Nat Rev Clin Oncol, 2022. **19**(3): p. 151-172.
- 5. Singal, A.G., F. Kanwal, and J.M. Llovet, *Global trends in hepatocellular carcinoma* epidemiology: implications for screening, prevention and therapy. Nat Rev Clin Oncol, 2023. **20**(12): p. 864-884.
- 6. Renne, S.L., et al., *Hepatocellular carcinoma: a clinical and pathological overview.* Pathologica, 2021. **113**(3): p. 203-217.
- 7. Farazi, P.A. and R.A. DePinho, *Hepatocellular carcinoma pathogenesis: from genes to environment.*
- 8. World Health Organization. *Absolute numbers, Mortality, Both sexes, in 2022*. 2024 [cited 2024 September 7]; Available from:

  https://gco.iarc.fr/today/en/dataviz/bars?mode=cancer&group\_populations=1&populations=900&types=1&key=total&sort\_by=value0.
- 9. World Health Organization. *Estimated number of deaths from 2022 to 2045, Both sexes, age [0-85+].* 2024 [cited 2024 September 7]; Available from: https://gco.iarc.fr/tomorrow/en/dataviz/bars?cancers=11&populations=900\_903\_904\_905\_908\_909\_935&types=1.
- 10. Brenner, D.R., et al., *Projected estimates of cancer in Canada in 2024*. CMAJ, 2024. **196**(18): p. E615-E623.
- 11. Ioannou, G.N., et al., *Incidence and predictors of hepatocellular carcinoma in patients with cirrhosis*. Clin Gastroenterol Hepatol, 2007. **5**(8): p. 938-45, 945.e1-4.
- 12. Liu, Y., et al., Global burden of primary liver cancer by five etiologies and global prediction by 2035 based on global burden of disease study 2019. Cancer Med, 2022. **11**(5): p. 1310-1323.
- 13. Devarbhavi, H., et al., *Global burden of liver disease: 2023 update.* J Hepatol, 2023. **79**(2): p. 516-537.
- 14. Akinyemiju, T., et al., *The Burden of Primary Liver Cancer and Underlying Etiologies From* 1990 to 2015 at the Global, Regional, and National Level: Results From the Global Burden of Disease Study 2015. JAMA Oncol, 2017. **3**(12): p. 1683-1691.
- 15. Younossi, Z., et al., *Global burden of NAFLD and NASH: trends, predictions, risk factors and prevention.* Nat Rev Gastroenterol Hepatol, 2018. **15**(1): p. 11-20.
- 16. Estes, C., et al., Modeling the epidemic of nonalcoholic fatty liver disease demonstrates an exponential increase in burden of disease. Hepatology, 2018. **67**(1): p. 123-133.
- 17. Suresh, D., A.N. Srinivas, and D.P. Kumar, *Etiology of Hepatocellular Carcinoma: Special Focus on Fatty Liver Disease*. Front Oncol, 2020. **10**: p. 601710.
- 18. Alberts, C.J., et al., Worldwide prevalence of hepatitis B virus and hepatitis C virus among patients with cirrhosis at country, region, and global levels: a systematic review. Lancet Gastroenterol Hepatol, 2022. **7**(8): p. 724-735.

- 19. Rinella, M.E., et al., *A multisociety Delphi consensus statement on new fatty liver disease nomenclature.* Hepatology, 2023. **78**(6): p. 1966-1986.
- 20. El-Serag, H.B., H. Hampel, and F. Javadi, *The association between diabetes and hepatocellular carcinoma: a systematic review of epidemiologic evidence.* Clin Gastroenterol Hepatol, 2006. **4**(3): p. 369-80.
- 21. Gupta, A., et al., Obesity is Independently Associated With Increased Risk of Hepatocellular Cancer-related Mortality: A Systematic Review and Meta-Analysis. Am J Clin Oncol, 2018. **41**(9): p. 874-881.
- 22. Ahmed, A., R.J. Wong, and S.A. Harrison, *Nonalcoholic Fatty Liver Disease Review:*Diagnosis, Treatment, and Outcomes. Clin Gastroenterol Hepatol, 2015. **13**(12): p. 2062-70.
- 23. Chavez-Tapia, N.C., et al., *Understanding the Role of Metabolic Syndrome as a Risk Factor for Hepatocellular Carcinoma*. J Hepatocell Carcinoma, 2022. **9**: p. 583-593.
- 24. McGlynn, K.A., J.L. Petrick, and H.B. El-Serag, *Epidemiology of Hepatocellular Carcinoma*. Hepatology, 2021. **73 Suppl 1**(Suppl 1): p. 4-13.
- 25. Geisler, C.E. and B.J. Renquist, *Hepatic lipid accumulation: cause and consequence of dysregulated glucoregulatory hormones.* J Endocrinol, 2017. **234**(1): p. R1-r21.
- 26. Mittenbühler, M.J., et al., *Hepatic leptin receptor expression can partially compensate for IL-6Ra deficiency in DEN-induced hepatocellular carcinoma*. Mol Metab, 2018. **17**: p. 122-133.
- 27. Sun, B. and M. Karin, *Obesity, inflammation, and liver cancer.* J Hepatol, 2012. **56**(3): p. 704-13.
- 28. Bai, D., L. Ueno, and P.K. Vogt, *Akt-mediated regulation of NFkappaB and the essentialness of NFkappaB for the oncogenicity of PI3K and Akt.* Int J Cancer, 2009. **125**(12): p. 2863-70.
- 29. Manthey, J., et al., *Global alcohol exposure between 1990 and 2017 and forecasts until 2030: a modelling study.* Lancet, 2019. **393**(10190): p. 2493-2502.
- 30. Rehm, J., A.V. Samokhvalov, and K.D. Shield, *Global burden of alcoholic liver diseases*. J Hepatol, 2013. **59**(1): p. 160-8.
- 31. Ganne-Carrié, N. and P. Nahon, *Hepatocellular carcinoma in the setting of alcohol-related liver disease*. J Hepatol, 2019. **70**(2): p. 284-293.
- 32. Asrani, S.K., et al., Burden of liver diseases in the world. J Hepatol, 2019. **70**(1): p. 151-171.
- 33. Seitz, H.K., et al., Alcoholic liver disease. Nat Rev Dis Primers, 2018. 4(1): p. 16.
- 34. Haflidadottir, S., et al., *Long-term follow-up and liver-related death rate in patients with non-alcoholic and alcoholic related fatty liver disease.* BMC Gastroenterol, 2014. **14**: p. 166.
- 35. Crabb, D.W., et al., *Molecular mechanisms of alcoholic fatty liver: role of peroxisome proliferator-activated receptor alpha.* Alcohol, 2004. **34**(1): p. 35-8.
- 36. Younossi, Z. and L. Henry, *Contribution of Alcoholic and Nonalcoholic Fatty Liver Disease* to the Burden of Liver-Related Morbidity and Mortality. Gastroenterology, 2016. **150**(8): p. 1778-85.
- 37. Hassan, M.M., et al., *Risk factors for hepatocellular carcinoma: synergism of alcohol with viral hepatitis and diabetes mellitus.* Hepatology, 2002. **36**(5): p. 1206-13.
- 38. Bialecki, E.S. and A.M. Di Bisceglie, *Diagnosis of hepatocellular carcinoma*. HPB (Oxford), 2005. **7**(1): p. 26-34.
- 39. Befeler, A.S. and A.M. Di Bisceglie, *Hepatocellular carcinoma: diagnosis and treatment*. Gastroenterology, 2002. **122**(6): p. 1609-19.
- 40. Marrero, J.A., et al., *Diagnosis, Staging, and Management of Hepatocellular Carcinoma:* 2018 Practice Guidance by the American Association for the Study of Liver Diseases. Hepatology, 2018. **68**(2): p. 723-750.
- 41. Kanwal, F., et al., *Risk factors for HCC in contemporary cohorts of patients with cirrhosis*. Hepatology, 2023. **77**(3): p. 997-1005.

- 42. Wang, Y., et al., *Aspirin Use and the Risk of Hepatocellular Carcinoma: A Meta-analysis.* J Clin Gastroenterol, 2022. **56**(7): p. e293-e302.
- 43. Simon, T.G., et al., *Lipophilic Statins and Risk for Hepatocellular Carcinoma and Death in Patients With Chronic Viral Hepatitis: Results From a Nationwide Swedish Population*. Ann Intern Med, 2019. **171**(5): p. 318-327.
- 44. Singh, S., et al., *Anti-diabetic medications and the risk of hepatocellular cancer: a* systematic review and meta-analysis. Am J Gastroenterol, 2013. **108**(6): p. 881-91; quiz 892.
- 45. Abdelmalak, J., et al., *The Effect of Aspirin Use on Incident Hepatocellular Carcinoma-An Updated Systematic Review and Meta-Analysis*. Cancers (Basel), 2023. **15**(13).
- 46. Saraei, P., et al., *The beneficial effects of metformin on cancer prevention and therapy: a comprehensive review of recent advances.* Cancer Manag Res, 2019. **11**: p. 3295-3313.
- 47. Singal, A.G., et al., *AASLD Practice Guidance on prevention, diagnosis, and treatment of hepatocellular carcinoma*. Hepatology, 2023. **78**(6): p. 1922-1965.
- 48. A comparison of lipiodol chemoembolization and conservative treatment for unresectable hepatocellular carcinoma. N Engl J Med, 1995. **332**(19): p. 1256-61.
- 49. Le Grazie, M., et al., *Chemotherapy for hepatocellular carcinoma: The present and the future.* World J Hepatol, 2017. **9**(21).
- 50. Wang, L., et al., *Postoperative adjuvant radiotherapy is associated with improved survival in hepatocellular carcinoma with microvascular invasion*. Oncotarget, 2017. **8**(45): p. 79971-79981.
- 51. Lee, U.E. and S.L. Friedman, *Mechanisms of hepatic fibrogenesis*. Best Pract Res Clin Gastroenterol, 2011. **25**(2): p. 195-206.
- 52. Chen, C.P., Role of Radiotherapy in the Treatment of Hepatocellular Carcinoma. J Clin Transl Hepatol, 2019. **7**(2): p. 183-190.
- 53. Matsuo, Y., Stereotactic Body Radiotherapy for Hepatocellular Carcinoma: A Brief Overview. Curr Oncol, 2023. **30**(2): p. 2493-2500.
- 54. Qi, W.X., et al., Charged particle therapy versus photon therapy for patients with hepatocellular carcinoma: a systematic review and meta-analysis. Radiother Oncol, 2015. **114**(3): p. 289-95.
- 55. Rim, C.H., et al., Comparison of radiation therapy modalities for hepatocellular carcinoma with portal vein thrombosis: A meta-analysis and systematic review. Radiother Oncol, 2018. **129**(1): p. 112-122.
- 56. Dawson, L.A., S. Hashem, and A. Bujold, *Stereotactic Body Radiation Therapy for Hepatocellular Carcinoma*. American Society of Clinical Oncology Educational Book, 2012(32): p. 261-264.
- 57. Guha, C. and B.D. Kavanagh, *Hepatic radiation toxicity: avoidance and amelioration*. Semin Radiat Oncol, 2011. **21**(4): p. 256-63.
- 58. Llovet, J.M., et al., *Sorafenib in advanced hepatocellular carcinoma*. N Engl J Med, 2008. **359**(4): p. 378-90.
- 59. Kudo, M., et al., *Lenvatinib versus sorafenib in first-line treatment of patients with unresectable hepatocellular carcinoma: a randomised phase 3 non-inferiority trial.* Lancet, 2018. **391**(10126): p. 1163-1173.
- 60. Finn, R.S., et al., *Atezolizumab plus Bevacizumab in Unresectable Hepatocellular Carcinoma*. N Engl J Med, 2020. **382**(20): p. 1894-1905.
- 61. Abou-Alfa, G.K., et al., *Tremelimumab plus Durvalumab in Unresectable Hepatocellular Carcinoma*. NEJM Evid, 2022. **1**(8): p. EVIDoa2100070.
- 62. Fukumura, D., et al., Enhancing cancer immunotherapy using antiangiogenics: opportunities and challenges. Nat Rev Clin Oncol, 2018. **15**(5): p. 325-340.

- 63. Pfister, D., et al., *NASH limits anti-tumour surveillance in immunotherapy-treated HCC.* Nature, 2021. **592**(7854): p. 450-456.
- 64. Sangro, B., et al., *Advances in immunotherapy for hepatocellular carcinoma*. Nat Rev Gastroenterol Hepatol, 2021. **18**(8): p. 525-543.
- 65. Thatcher, J.D., The Ras-MAPK signal transduction pathway. Sci Signal, 2010. **3**(119): p. tr1.
- 66. Cargnello, M. and P.P. Roux, *Activation and function of the MAPKs and their substrates, the MAPK-activated protein kinases.* Microbiol Mol Biol Rev, 2011. **75**(1): p. 50-83.
- 67. Zhang, W. and H.T. Liu, *MAPK signal pathways in the regulation of cell proliferation in mammalian cells*. Cell Res, 2002. **12**(1): p. 9-18.
- 68. Leowattana, W., T. Leowattana, and P. Leowattana, *Systemic treatment for unresectable hepatocellular carcinoma*. World J Gastroenterol, 2023. **29**(10): p. 1551-1568.
- 69. Shaulian, E. and M. Karin, *AP-1 in cell proliferation and survival*. Oncogene, 2001. **20**(19): p. 2390-400.
- 70. Diehl, J.A., Cycling to cancer with cyclin D1. Cancer Biol Ther, 2002. 1(3): p. 226-31.
- 71. Glaviano, A., et al., *PI3K/AKT/mTOR signaling transduction pathway and targeted therapies in cancer.* Molecular Cancer, 2023. **22**(1): p. 138.
- 72. Kizilboga, T., et al., *Bag-1 stimulates Bad phosphorylation through activation of Akt and Raf kinases to mediate cell survival in breast cancer.* (1471-2407 (Electronic)).
- 73. Manning, B.D. and L.C. Cantley, *AKT/PKB Signaling: Navigating Downstream*, in *Cell*. 2007. p. 1261-1274.
- 74. Zhang, X., et al., *Akt, FoxO and regulation of apoptosis*. Biochim Biophys Acta, 2011. **1813**(11): p. 1978-86.
- 75. Chibaya, L., et al., *Mdm2 phosphorylation by Akt regulates the p53 response to oxidative stress to promote cell proliferation and tumorigenesis*. Proc Natl Acad Sci U S A, 2021. **118**(4).
- 76. Guo, Q., et al., ARHGAP17 suppresses tumor progression and up-regulates P21 and P27 expression via inhibiting PI3K/AKT signaling pathway in cervical cancer. Gene, 2019. **692**: p. 9-16.
- 77. Duda, P., et al., *Targeting GSK3 and Associated Signaling Pathways Involved in Cancer.* Cells, 2020. **9**(5).
- 78. Chiang, Y.J., et al., *CBAP modulates Akt-dependent TSC2 phosphorylation to promote Rheb-mTORC1 signaling and growth of T-cell acute lymphoblastic leukemia*. Oncogene, 2019. **38**(9): p. 1432-1447.
- 79. Tian, T., X. Li, and J. Zhang, *mTOR Signaling in Cancer and mTOR Inhibitors in Solid Tumor Targeting Therapy.* Int J Mol Sci, 2019. **20**(3).
- 80. Steinberg, G.R. and D. Carling, *AMP-activated protein kinase: the current landscape for drug development.* Nat Rev Drug Discov, 2019. **18**(7): p. 527-551.
- 81. Mahon, P.C., K. Hirota, and G.L. Semenza, *FIH-1: a novel protein that interacts with HIF-1alpha and VHL to mediate repression of HIF-1 transcriptional activity.* Genes Dev, 2001. **15**(20): p. 2675-86.
- 82. Jiang, B.H., et al., *Dimerization, DNA binding, and transactivation properties of hypoxia-inducible factor 1.* J Biol Chem, 1996. **271**(30): p. 17771-8.
- 83. Jun, J.C., et al., *Hypoxia-Inducible Factors and Cancer.* Curr Sleep Med Rep, 2017. **3**(1): p. 1-10.
- 84. Evan, G.I. and K.H. Vousden, *Proliferation, cell cycle and apoptosis in cancer.* Nature, 2001. **411**(6835): p. 342-8.
- 85. Chang, J. and J. Erler, *Hypoxia-mediated metastasis*. Adv Exp Med Biol, 2014. **772**: p. 55-81.

- 86. Firth, J.D., B.L. Ebert, and P.J. Ratcliffe, *Hypoxic regulation of lactate dehydrogenase A. Interaction between hypoxia-inducible factor 1 and cAMP response elements.* J Biol Chem, 1995. **270**(36): p. 21021-7.
- 87. Furuta, E., et al., Fatty acid synthase gene is up-regulated by hypoxia via activation of Akt and sterol regulatory element binding protein-1. Cancer Res, 2008. **68**(4): p. 1003-11.
- 88. Hao, Y., D. Baker, and P. Ten Dijke, *TGF-beta-Mediated Epithelial-Mesenchymal Transition and Cancer Metastasis*. Int J Mol Sci, 2019. **20**(11).
- 89. Yue, X., B. Shan, and J.A. Lasky, *TGF-beta: Titan of Lung Fibrogenesis*. Curr Enzym Inhib, 2010. **6**(2).
- 90. Caja, L., et al., Dissecting the effect of targeting the epidermal growth factor receptor on TGF-β-induced-apoptosis in human hepatocellular carcinoma cells. J Hepatol, 2011. **55**(2): p. 351-8.
- 91. Gotzmann, J., et al., A crucial function of PDGF in TGF-beta-mediated cancer progression of hepatocytes. Oncogene, 2006. **25**(22): p. 3170-85.
- 92. Warner, B.J., et al., Myc downregulation by transforming growth factor beta required for activation of the p15(Ink4b) G(1) arrest pathway. Mol Cell Biol, 1999. **19**(9): p. 5913-22.
- 93. Polyak, K., et al., *p27Kip1*, a cyclin-Cdk inhibitor, links transforming growth factor-beta and contact inhibition to cell cycle arrest. Genes Dev, 1994. **8**(1): p. 9-22.
- 94. Laiho, M., et al., *Growth inhibition by TGF-beta linked to suppression of retinoblastoma protein phosphorylation*. Cell, 1990. **62**(1): p. 175-85.
- 95. Malfettone, A., et al., *Transforming growth factor-β-induced plasticity causes a migratory stemness phenotype in hepatocellular carcinoma*. Cancer Lett, 2017. **392**: p. 39-50.
- 96. Chen, J., J.A. Gingold, and X. Su, *Immunomodulatory TGF-β Signaling in Hepatocellular Carcinoma*. Trends Mol Med, 2019. **25**(11): p. 1010-1023.
- 97. Thomas, D.A. and J. Massague, *TGF-beta directly targets cytotoxic T cell functions during tumor evasion of immune surveillance*. Cancer Cell, 2005. **8**(5): p. 369-80.
- 98. Dhodapkar, M.V. and R.M. Steinman, *Antigen-bearing immature dendritic cells induce peptide-specific CD8(+) regulatory T cells in vivo in humans*. Blood, 2002. **100**(1): p. 174-7.
- 99. Hubenak, J.R., et al., *Mechanisms of injury to normal tissue after radiotherapy: a review.* Plast Reconstr Surg, 2014. **133**(1): p. 49e-56e.
- 100. Zhao, W., D.I. Diz, and M.E. Robbins, *Oxidative damage pathways in relation to normal tissue injury.* Br J Radiol, 2007. **80 Spec No 1**: p. S23-31.
- 101. Citrin, D.E. and J.B. Mitchell, *Mechanisms of Normal Tissue Injury From Irradiation*. Semin Radiat Oncol, 2017. **27**(4): p. 316-324.
- 102. Araya, J., et al., *Insufficient autophagy in idiopathic pulmonary fibrosis*. Am J Physiol Lung Cell Mol Physiol, 2013. **304**(1): p. L56-69.
- 103. Khozouz, R.F., S.Z. Huq, and M.C. Perry, *Radiation-induced liver disease*. J Clin Oncol, 2008. **26**(29): p. 4844-5.
- 104. Kim, J. and Y. Jung, *Radiation-induced liver disease: current understanding and future perspectives.* Exp Mol Med, 2017. **49**(7): p. e359.
- 105. DeLeve, L.D., H.M. Shulman, and G.B. McDonald, *Toxic injury to hepatic sinusoids:* sinusoidal obstruction syndrome (veno-occlusive disease). Semin Liver Dis, 2002. **22**(1): p. 27-42.
- 106. Christiansen, H., et al., *Irradiation leads to susceptibility of hepatocytes to TNF-alpha mediated apoptosis*. Radiother Oncol, 2004. **72**(3): p. 291-6.
- 107. Hu, Y.B., et al., Sestrin 2 Attenuates Rat Hepatic Stellate Cell (HSC) Activation and Liver Fibrosis via an mTOR/AMPK-Dependent Mechanism. Cell Physiol Biochem, 2018. **51**(5): p. 2111-2122.

- 108. Zhang, H.Y., et al., Lung fibroblast alpha-smooth muscle actin expression and contractile phenotype in bleomycin-induced pulmonary fibrosis. Am J Pathol, 1996. **148**(2): p. 527-37.
- 109. Arroyo-Hernandez, M., et al., *Radiation-induced lung injury: current evidence*. BMC Pulm Med, 2021. **21**(1): p. 9.
- 110. Kalluri, R. and R.A. Weinberg, *The basics of epithelial-mesenchymal transition*. J Clin Invest, 2009. **119**(6): p. 1420-8.
- 111. Davies, M., et al., Induction of an epithelial to mesenchymal transition in human immortal and malignant keratinocytes by TGF-beta1 involves MAPK, Smad and AP-1 signalling pathways. J Cell Biochem, 2005. **95**(5): p. 918-31.
- 112. Hoot, K.E., et al., *Keratinocyte-specific Smad2 ablation results in increased epithelial-mesenchymal transition during skin cancer formation and progression.* J Clin Invest, 2008. **118**(8): p. 2722-32.
- 113. Deckers, M., et al., *The tumor suppressor Smad4 is required for transforming growth factor beta-induced epithelial to mesenchymal transition and bone metastasis of breast cancer cells.* Cancer Res, 2006. **66**(4): p. 2202-9.
- 114. Huang, Y., W. Hong, and X. Wei, *The molecular mechanisms and therapeutic strategies of EMT in tumor progression and metastasis.* J Hematol Oncol, 2022. **15**(1): p. 129.
- 115. Damm, R., et al., *TNF-alpha Indicates Radiation-induced Liver Injury After Interstitial High Dose-rate Brachytherapy.* In Vivo, 2022. **36**(5): p. 2265-2274.
- 116. Roy, S., K.E. Salerno, and D.E. Citrin, *Biology of Radiation-Induced Lung Injury*. Semin Radiat Oncol, 2021. **31**(2): p. 155-161.
- 117. Zhang, M., et al., *Inhibition of the tumor necrosis factor-alpha pathway is radioprotective for the lung.* Clin Cancer Res, 2008. **14**(6): p. 1868-76.
- 118. Hill, R.P., et al., *Investigations into the role of inflammation in normal tissue response to irradiation*. Radiother Oncol, 2011. **101**(1): p. 73-9.
- 119. Suzukawa, K., T.J. Weber, and N.H. Colburn, *AP-1, NF-kappa-B, and ERK activation thresholds for promotion of neoplastic transformation in the mouse epidermal JB6 model.* Environ Health Perspect, 2002. **110**(9): p. 865-70.
- 120. Wang, X. and Y. Lin, *Tumor necrosis factor and cancer, buddies or foes?* Acta Pharmacol Sin, 2008. **29**(11): p. 1275-88.
- 121. Sliwinska-Mosson, M., et al., *Markers Useful in Monitoring Radiation-Induced Lung Injury in Lung Cancer Patients: A Review.* J Pers Med, 2020. **10**(3).
- 122. Wynn, T.A. and K.M. Vannella, *Macrophages in Tissue Repair, Regeneration, and Fibrosis*. Immunity, 2016. **44**(3): p. 450-462.
- 123. Chung, S.I., et al., *IL-13 is a therapeutic target in radiation lung injury.* Sci Rep, 2016. **6**: p. 39714.
- 124. Hanania, A.N., et al., *Radiation-Induced Lung Injury: Assessment and Management*. Chest, 2019. **156**(1): p. 150-162.
- 125. Chow, E., et al., *Dexamethasone in the prophylaxis of radiation-induced pain flare after palliative radiotherapy for bone metastases: a double-blind, randomised placebo-controlled, phase 3 trial.* Lancet Oncol, 2015. **16**(15): p. 1463-1472.
- 126. Bledsoe, T.J., S.K. Nath, and R.H. Decker, *Radiation Pneumonitis*. Clin Chest Med, 2017. **38**(2): p. 201-208.
- 127. Wang, L.P., et al., *Expression of interleukin-17A in lung tissues of irradiated mice and the influence of dexamethasone*. ScientificWorldJournal, 2014. **2014**: p. 251067.
- 128. Sekine, I., et al., *Retrospective analysis of steroid therapy for radiation-induced lung injury in lung cancer patients*. Radiother Oncol, 2006. **80**(1): p. 93-7.

- 129. Kwok, E. and C.K. Chan, *Corticosteroids and azathioprine do not prevent radiation-induced lung injury.* Can Respir J, 1998. **5**(3): p. 211-4.
- 130. Otani, K., et al., Steroid treatment increases the recurrence of radiation-induced organizing pneumonia after breast-conserving therapy. Cancer Med, 2014. **3**(4): p. 947-53.
- 131. Valkhoff, V.E., M.C.J.M. Sturkenboom, and E.J. Kuipers, *Risk factors for gastrointestinal bleeding associated with low-dose aspirin*. Best Practice & Research Clinical Gastroenterology, 2012. **26**(2): p. 125-140.
- Huang, E.S., et al., *Long-term use of aspirin and the risk of gastrointestinal bleeding*. Am J Med, 2011. **124**(5): p. 426-33.
- 133. Patrono, C., et al., *Clinical pharmacology of platelet cyclooxygenase inhibition*. Circulation, 1985. **72**(6): p. 1177-84.
- 134. Zhang, W.T., et al., *Inhibition of Aspirin-Induced Gastrointestinal Injury: Systematic Review and Network Meta-Analysis.* Front Pharmacol, 2021. **12**: p. 730681.
- 135. Amann, R. and B.A. Peskar, *Anti-inflammatory effects of aspirin and sodium salicylate*. Eur J Pharmacol, 2002. **447**(1): p. 1-9.
- 136. Peng, J., et al., *Aspirin alleviates pulmonary fibrosis through PI3K/AKT/mTOR-mediated autophagy pathway.* Exp Gerontol, 2023. **172**: p. 112085.
- 137. Leonhard, W.N., et al., Salsalate, but not metformin or canagliflozin, slows kidney cyst growth in an adult-onset mouse model of polycystic kidney disease. EBioMedicine, 2019. **47**: p. 436-445.
- 138. Liu, Y., et al., Aspirin alleviates hepatic fibrosis by suppressing hepatic stellate cells activation via the TLR4/NF-κB pathway. Aging (Albany NY), 2020. **12**(7): p. 6058-6066.
- 139. Wang, T., et al., Aspirin targets P4HA2 through inhibiting NF-kappaB and LMCD1-AS1/let-7g to inhibit tumour growth and collagen deposition in hepatocellular carcinoma. EBioMedicine, 2019. **45**: p. 168-180.
- 140. Chavez, E., et al., Effects of acetyl salycilic acid and ibuprofen in chronic liver damage induced by CCl4. J Appl Toxicol, 2012. **32**(1): p. 51-9.
- 141. Broadfield, L.A., et al., *Salicylate enhances the response of prostate cancer to radiotherapy.* Prostate, 2019. **79**(5): p. 489-497.
- 142. O'Brien, A.J., et al., Salicylate activates AMPK and synergizes with metformin to reduce the survival of prostate and lung cancer cells ex vivo through inhibition of de novo lipogenesis. Biochem J, 2015. **469**(2): p. 177-87.
- 143. Demirel, C., et al., *Inhibition of Radiation-Induced Oxidative Damage in the Lung Tissue:*May Acetylsalicylic Acid Have a Positive Role? Inflammation, 2016. **39**(1): p. 158-165.
- 144. Shanmugam, G., S. Rakshit, and K. Sarkar, *HDAC inhibitors: Targets for tumor therapy, immune modulation and lung diseases.* Transl Oncol, 2022. **16**: p. 101312.
- 145. Ceccacci, E. and S. Minucci, *Inhibition of histone deacetylases in cancer therapy: lessons from leukaemia*. Br J Cancer, 2016. **114**(6): p. 605-11.
- 146. Milazzo, G., et al., *Histone Deacetylases (HDACs): Evolution, Specificity, Role in Transcriptional Complexes, and Pharmacological Actionability.* Genes (Basel), 2020. **11**(5).
- 147. Li, Y. and E. Seto, *HDACs and HDAC Inhibitors in Cancer Development and Therapy.* Cold Spring Harb Perspect Med, 2016. **6**(10).
- 148. Chang, C.C., et al., *HDAC2 promotes cell migration/invasion abilities through HIF-1alpha stabilization in human oral squamous cell carcinoma*. J Oral Pathol Med, 2011. **40**(7): p. 567-75.
- 149. Jaguva Vasudevan, A.A., et al., *HDAC5 Expression in Urothelial Carcinoma Cell Lines Inhibits Long-Term Proliferation but Can Promote Epithelial-to-Mesenchymal Transition.* Int J Mol Sci, 2019. **20**(9).

- 150. Yoshikawa, M., et al., *Inhibition of histone deacetylase activity suppresses epithelial-to-mesenchymal transition induced by TGF-beta1 in human renal epithelial cells.* J Am Soc Nephrol, 2007. **18**(1): p. 58-65.
- 151. Wang, Z., et al., Suberoylanilide hydroxamic acid: a potential epigenetic therapeutic agent for lung fibrosis? Eur Respir J, 2009. **34**(1): p. 145-55.
- 152. Travers, J.G., et al., *HDAC Inhibition Reverses Preexisting Diastolic Dysfunction and Blocks Covert Extracellular Matrix Remodeling*. Circulation, 2021. **143**(19): p. 1874-1890.
- 153. Kainthola, A., et al., *Immunological Aspect of Radiation-Induced Pneumonitis, Current Treatment Strategies, and Future Prospects.* Front Immunol, 2017. **8**: p. 506.
- 154. Park, J.K., et al., *Inhibition of histone deacetylase 6 suppresses inflammatory responses and invasiveness of fibroblast-like-synoviocytes in inflammatory arthritis.* Arthritis Res Ther, 2021. **23**(1): p. 177.
- 155. Lyu, X., et al., *HDAC inhibitors as antifibrotic drugs in cardiac and pulmonary fibrosis*. Ther Adv Chronic Dis, 2019. **10**: p. 2040622319862697.
- 156. Smith, B.K., et al., Salsalate (Salicylate) Uncouples Mitochondria, Improves Glucose Homeostasis, and Reduces Liver Lipids Independent of AMPK-beta1. Diabetes, 2016. **65**(11): p. 3352-3361.
- 157. Steinberg, G.R. and D.G. Hardie, *New insights into activation and function of the AMPK*. Nat Rev Mol Cell Biol, 2023. **24**(4): p. 255-272.
- 158. Sun, Y., et al., *Aspirin attenuates liver fibrosis by suppressing TGF-beta1/Smad signaling*. Mol Med Rep, 2022. **25**(5).
- 159. Tsakiridis, E.E., et al., Combined metformin-salicylate treatment provides improved antitumor activity and enhanced radiotherapy response in prostate cancer; drug synergy at clinically relevant doses. Transl Oncol, 2021. **14**(11): p. 101209.
- 160. Dabjan, M.B., et al., A survey of changing trends in modelling radiation lung injury in mice: bringing out the good, the bad, and the uncertain. Lab Invest, 2016. **96**(9): p. 936-49.
- 161. Hong, J.H., et al., Can short-term administration of dexamethasone abrogate radiation-induced acute cytokine gene response in lung and modify subsequent molecular responses? Int J Radiat Oncol Biol Phys, 2001. **51**(2): p. 296-303.
- 162. Ianevski, A., A.K. Giri, and T. Aittokallio, *SynergyFinder 3.0: an interactive analysis and consensus interpretation of multi-drug synergies across multiple samples.* Nucleic Acids Res, 2022. **50**(W1): p. W739-w743.
- 163. Mesci, A., et al., *The Journey of Radiotherapy Dose Escalation in High Risk Prostate Cancer;* Conventional Dose Escalation to Stereotactic Body Radiotherapy (SBRT) Boost Treatments. Clin Genitourin Cancer, 2022. **20**(1): p. e25-e38.
- 164. Roach, M.C., J.D. Bradley, and C.G. Robinson, *Optimizing radiation dose and fractionation for the definitive treatment of locally advanced non-small cell lung cancer.* J Thorac Dis, 2018. **10**(Suppl 21): p. S2465-s2473.
- 165. Sheth, N., et al., Stereotactic Ablative Radiotherapy Fractionation for Hepatocellular Carcinoma in the United States. Cureus, 2020. **12**(6): p. e8675.
- 166. Munshi, A. and R. Ramesh, *Mitogen-activated protein kinases and their role in radiation response*. Genes Cancer, 2013. **4**(9-10): p. 401-8.
- 167. Chang, L., et al., *Emerging roles of radioresistance in prostate cancer metastasis and radiation therapy.* Cancer Metastasis Rev, 2014. **33**(2-3): p. 469-96.
- 168. Huang, R. and P.-K. Zhou, *HIF-1 signaling: A key orchestrator of cancer radioresistance*. Radiation Medicine and Protection, 2020. **1**(1): p. 7-14.
- 169. Sun, J., et al., *UBE2T-regulated H2AX monoubiquitination induces hepatocellular carcinoma radioresistance by facilitating CHK1 activation.* J Exp Clin Cancer Res, 2020. **39**(1): p. 222.

- 170. Weng, Y.S., et al., *Lenvatinib Synergistically Promotes Radiation Therapy in Hepatocellular Carcinoma by Inhibiting Src/STAT3/NF-kappaB-Mediated Epithelial-Mesenchymal Transition and Metastasis*. Int J Radiat Oncol Biol Phys, 2023. **115**(3): p. 719-732.
- 171. Travis, E.L., et al., *Late functional and biochemical changes in mouse lung after irradiation:* differential effects of WR-2721. Radiat Res, 1985. **103**(2): p. 219-31.
- 172. Down, J.D., et al., *Oxygen-dependent protection of radiation lung damage in mice by WR* 2721. Int J Radiat Biol Relat Stud Phys Chem Med, 1984. **46**(5): p. 597-607.
- 173. Puthawala, K., et al., *Inhibition of integrin alpha(v)beta6, an activator of latent transforming growth factor-beta, prevents radiation-induced lung fibrosis*. Am J Respir Crit Care Med, 2008. **177**(1): p. 82-90.
- 174. Hallahan, D.E., L. Geng, and Y. Shyr, Effects of intercellular adhesion molecule 1 (ICAM-1) null mutation on radiation-induced pulmonary fibrosis and respiratory insufficiency in mice.

  J Natl Cancer Inst, 2002. **94**(10): p. 733-41.
- 175. Machtay, M., et al., Systemic polyethylene glycol-modified (PEGylated) superoxide dismutase and catalase mixture attenuates radiation pulmonary fibrosis in the C57/bl6 mouse. Radiother Oncol, 2006. **81**(2): p. 196-205.
- 176. Fox, J. and C.K. Haston, *CXC receptor 1 and 2 and neutrophil elastase inhibitors alter radiation-induced lung disease in the mouse.* Int J Radiat Oncol Biol Phys, 2013. **85**(1): p. 215-22.